INTERNATIONAL DARK-SKY ASSOCIATION
OREGON CHAPTER

TO PRESERVE THE MAGNIFICENT DARK SKIES OF OREGON AND DIMINISH LIGHT POLLUTION FOR THE HEALTH, SAFETY AND WELL-BEING OF ALL LIFE

Oregon Skyglow Measurement Network
Technical Report Edition #7
Data from April 2019 to November 2022
March 6, 2023

Abstract

The Oregon Skyglow Measurement Network, a volunteer-run project of the Oregon Chapter of the International Dark-Sky Association, has two goals - to support the certification of dark sky places and to track any change of skyglow over months and years. The Network currently consists of 44 Sky Quality Meters (SQMs) distributed around Oregon, at sites ranging from light polluted to pristine night sky locations.

The SQMs record the brightness of broadband visible light at night with a 5-minute cadence, continuously. Seven of the SQMs have been running for at least three years, another fifteen meters for one and a half years, the rest for six to twelve months. With the help of 30 volunteers, the dataset now contains over 6 million measurements.

The SQM measurements are processed through two different workflows, consistent with the goals of the project. In the first workflow, support of dark sky place certification, we follow astronomical convention and International Dark-Sky recommendations to include measurements when the sun is at least 18 degrees below the horizon, the moon is at least 10 degrees below the horizon, clouds are absent, and the Milky Way is not overhead. We also implement a static shift to the SQM data to account for the presence of a weatherproof case window and apply a serial adjustment for an apparent aging phenomenon of the SQMs.

The processed data support the continued certification of two existing dark sky places in Oregon as well as the future certification of twelve additional dark sky areas.

In the second workflow, we process the data to track any change of skyglow over time. By necessity this workflow seeks to minimize variation in the night sky brightness measurements due to natural phenomena – the orientation of the Milky Way, time of night, and airglow related to increased solar flux as the current sunspot cycle progresses.

To track change of skyglow over time, we employ the same data filters on the sun, moon, and clouds, along with the weatherproof window static shift and SQM aging adjustment as in the first workflow. Then, instead of discarding measurements when the Milky Way is overhead, we apply a site-specific statistical adjustment to shift the SQM measurements to a galactic latitude of 30 degrees from zenith and to a galactic longitude of 120 degrees. We further adjust the data to 1 AM local time to minimize variation through the night caused by local change of light pollution. We then subtract the brightness attributable to airglow caused by variation in the solar flux over time.

The processed data show increases of 4% to 7% per year for SQM sites in expanding cities in central Oregon. Other peripheral SQM sites show increases of 2% to 4% per year, while remote sites tend to show little to no change in zenith skyglow per year.

A notable seasonal and month-by-month cyclical pattern of skyglow remains in the data after these adjustments. We anticipate that the cyclical pattern remaining is due to a combination of seasonal atmospheric differences and to variable airglow phenomena.

Summary

Outdoor light shining upward brightens the sky at night, which is known as light pollution or skyglow. Light pollution hides the starry night sky and has negative environmental consequences for people and the wild ecosystem. State and Federal organizations measure air, water, and soil pollution, but do not directly measure light pollution. We are running a multi-year project to measure light pollution in Oregon, to bring attention to this environmental issue and to support parks and communities working toward certification as Dark Sky Places.

With support from 30 volunteer individuals and groups, we are currently measuring the absolute level of skyglow directly overhead at 44 sites around Oregon, and also track change of the light pollution over time.

Two sites in Portland, Oregon show the most light pollution. The three most light-polluted sites in central Oregon, which have been running for about 3 years, show an increase of 4% to 7% per year, The long-term sites with the starriest natural skies, furthest from the cities, show little change of light pollution in the overhead night sky.

The measurements show that the two current Dark Sky Places in Oregon, the community of Sunriver, and Prineville Reservoir State Park, retain dark skies. Measurements at sites currently working toward Dark Sky Place certification also meet Dark Sky Place criteria. These locations include Cottonwood Canyon State Park, Wallowa Lake State Park, Black Butte Ranch, Oregon Caves National Monument, the City of Sisters, the Pine Mountain Observatory, and large areas of the Outback of southeastern Oregon. Measurements in the Oregon Outback document pristine night skies overhead and are the starriest night skies in Oregon.

We are expanding the network monthly. We solicit your help to install and maintain additional sites. We would especially like to expand coverage in the Willamette Valley, in the Columbia River Gorge, and along the Oregon Coast.

Background

Light pollution at night has been shown to have a negative effect on people and the larger environment, in addition to being a waste of energy. Light pollution, especially blue light at night, disrupts the circadian rhythm of people and other organisms. The impact on humans includes lack of sleep and probable increase in cancers and other diseases. Various animal species – birds, amphibians, mammals, invertebrates and primates – are adversely impacted by confusion of celestial navigation, misorientation at night, attraction/repulsion to artificial light, impact on predator/prey relationships, effects on timing of breeding, nesting, migration and foraging. Here's a good presentation of this topic by IDA Oregon Board Member, Mary Coolidge, From the Desert to the Coast, the Case for Dark Skies.

State and Federal organizations measure air, water, and soil pollution, but do not directly measure light pollution. In part, to show what is possible, and to bring attention to this environmental issue, the Oregon Chapter of the International Dark-Sky Association (IDA), with support from other groups, is running a multi-year project to measure light pollution in Oregon. We operate a network of continuously recording Sky Quality Meters (SQMs) in Oregon.

Volunteers gather accumulated data every 3 months from the measurement sites. Every six months we update this report to include all data acquired to date, and incorporate data from new stations as well. This report is Edition #7 and incorporates data from several new SQMs. Figure 1 shows the locations of the 44 SQMs as of the date of this report. Appendix A shows a chart of the time ranges of data available from the 37 SQM sites which were recording up to the November 2022 deadline of this report.

Skyglow is literally the glowing sky at night, due to both man-made artificial light and natural light. SQMs measure the brightness of the night sky directly overhead and provide a measure of both light pollution and natural light at night. SQMs are widely used around the world for this kind of survey (Kyba and others, 2015).

Other measurement tools designed to measure skyglow, such as calibrated all-sky cameras (Jechow and others, 2017), provide additional information about skyglow, namely a complete picture of how the skyglow varies across the sky at a given location. Our SQM measurements document the skyglow directly above. Changes of skyglow may be more readily identified by including measurements nearer the horizon. We anticipate augmenting the SQM zenith measurements by all-sky camera data going forward.

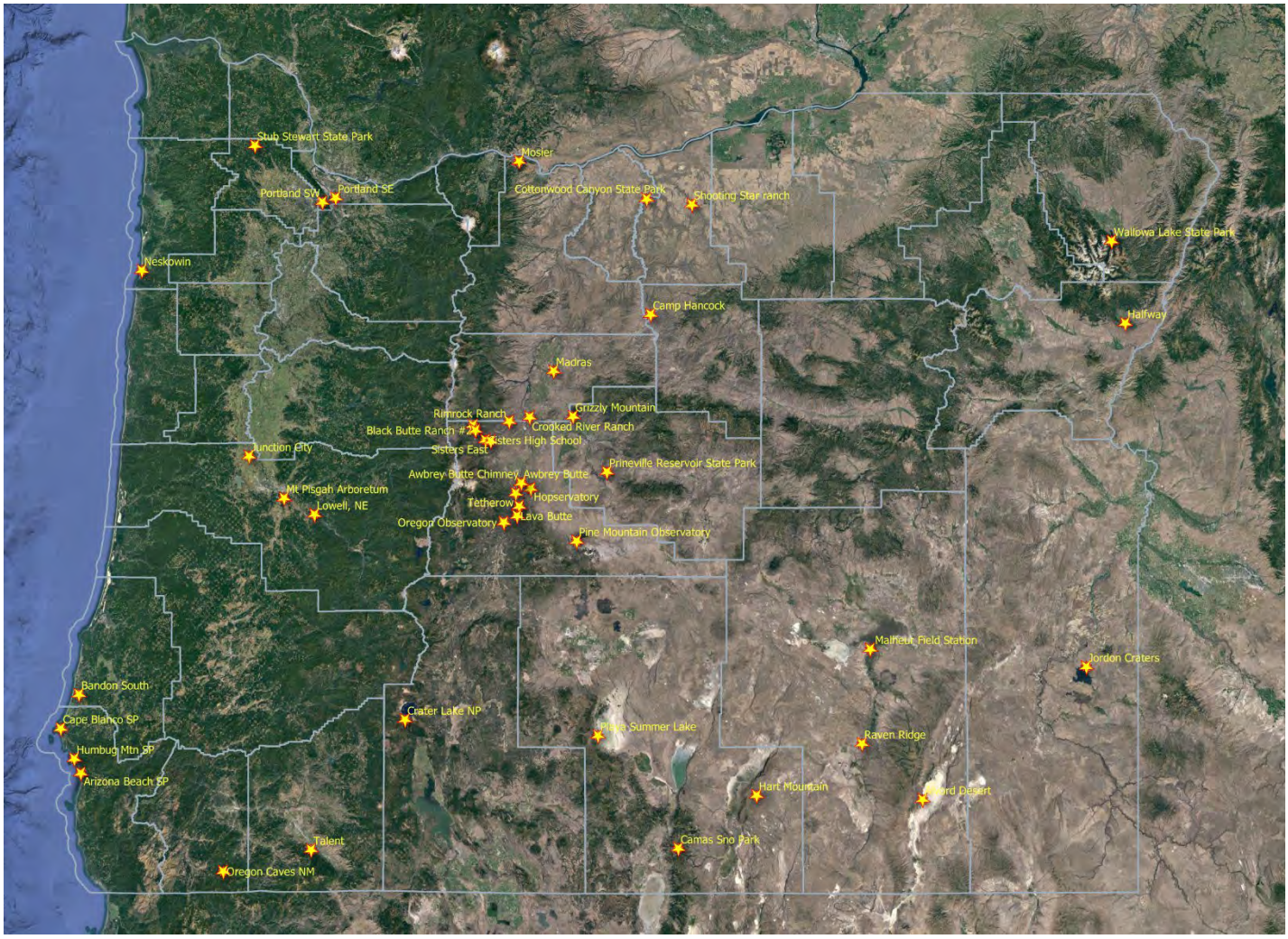

Figure 1. *Yellow stars show the locations of the 44 SQM monitoring sites in Oregon as of the date of this report. The blue outlines demark the counties of Oregon. The background image, from Google Earth, is 450 miles across, from west to east.*

Explanation of Skyglow Measurements

Each SQM is enclosed inside a weatherproof case and is attached to a fixed support, pointed directly upwards. The SQMs are set to record a skyglow measurement every five minutes. Figure 2 shows examples of SQMs installed at various sites in Oregon.

Figure 2. *Examples of SQMs installed at sites in Oregon. The meter resides inside a weatherproof case and points vertically toward the sky.*

Figure 3 shows typical data from five SQMs during the night of August 1-2, 2019, which was a mostly cloud-free night during a new moon period.

Data units in Figure 3 and elsewhere in this report are in a logarithmic scale used by astronomers -- magnitudes per arc second squared (mags/arcsecond^2). This unit of measure, for example, 21.5 mags/arcsecond^2, is like saying that the sky glows as though the light of one 21.5-magnitude star, a very dim star, was spread across each square arcsecond (a very small 2-dimensional area) of sky. Because this scale is logarithmic, small changes in value of mags/arcsecond^2 represent larger changes in a linear brightness scale. We convert the skyglow measurements to a linear scale prior to statistical adjustments for various effects. See Table 1 below for additional information.

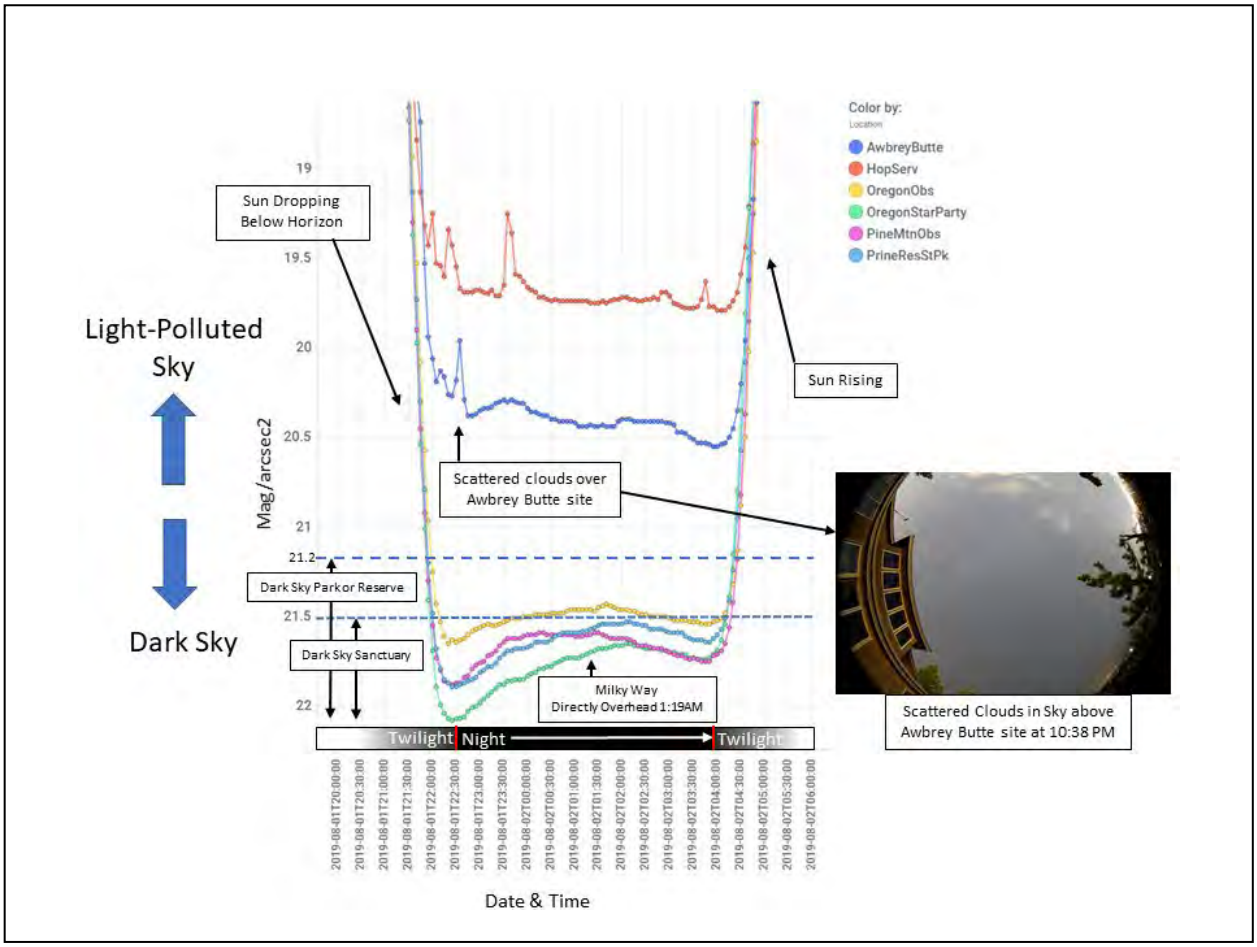

Figure 3. *Typical data from SQMs at six different locations for the same single night of August 1-2, 2019.*

The vertical axis in Figure 3 displays the SQM measurements – larger numbers are toward the bottom and represent measurements of darker sky. The horizontal axis is Date and Time, over the night of August 1-2, 2019, with labels one hour apart. The colored lines show the recorded data from five SQM locations and additional data recorded at a temporary site during the Oregon Star Party at Indian Trail Spring – the green line.

The data in Figure 3 show that the night sky, directly overhead at the Hopservatory and Awbrey Butte sites (the uppermost red and blue lines), are light-polluted compared to the other sites. These two light-polluted sites are located within the light-dome over the city of Bend. The other four sites have darker skies – they are far away from light-polluted cities. The Oregon Star Party site east of Prineville (green line) had the darkest night sky among these six locations on August 1 – 2 and is furthest of all the sites from the Central Oregon cities.

The International Dark-Sky Association (IDA) has a program to recognize areas that are still mostly unaffected by light pollution. Three categories of such dark sky places are known as Dark Sky Parks, Reserves and Sanctuaries. As shown by the horizontal dashed lines, Figure 3, a Dark Sky Park or Reserve must have SQM readings of at least 21.2 mags/arcsecond^2. Dark Sky Sanctuaries must meet a more strict night sky darkness of at least 21.5 mags/arcsecond^2. The data suggest that all four of the darkest Central Oregon SQM locations in Figure 3 may meet the stricter criterion. In fact, Prineville Reservoir State Park is now certified as the first Dark Sky Park in Oregon. Note that other significant criteria must also be met to obtain status as a Dark Sky Park, Dark Sky Reserve or Dark Sky Sanctuary.

Figure 3 shows that the sky overhead at the four dark sites brightens as the Milky Way rises directly overhead, and then darkens as the Milky Way begins descending through the early morning hours. The effect of the Milky Way brightening in the data for the two sites under the City of Bend light dome (Awbrey Butte and Hopservatory), is not obvious because the Milky Way is washed out by the light-polluted skies at those two sites. Instead, we see a gradual darkening through the night hours, which we presume is due to some outdoor lights in the City, being dimmed or turned off, and fewer car headlights as most people are sleeping.

Project Goals & Data Processing Steps

This project has two main Goals: 1) to support certification of Dark Sky Places and 2) to document the level of light pollution and to track its change over time. Processing of the SQM data differs according to these goals, as described below.

Under Goal #1, the skyglow data support local efforts to nominate sites under IDA's International Dark Sky Place Program. So far, these Oregon data have been instrumental in helping to certify the community of Sunriver as a Dark Sky Development of Distinction (Aug 2020) and Prineville Reservoir State Park as the first Dark Sky Park in Oregon (May 2021). Nighttime measurements are currently underway at eight other potential Dark Sky Parks in Oregon -- at these State Parks - Cottonwood Canyon, Wallowa Lake, Cape Blanco, Humbug Mountain, Arizona Beach – and at Oregon Caves National Monument, Pine Mountain Observatory and Newberry National Volcanic Monument.

Volunteers are also measuring skyglow at two possible future Dark Sky Communities in Oregon – at Black Butte Ranch and the City of Sisters. The skyglow data processed by IDA Oregon from six sites in southeastern Oregon were submitted to IDA by the Oregon Outback Dark Sky Network in support of certification of a Dark Sky Sanctuary in that large area.

Under Goal #2, we want to document changes in light pollution over a five-year period at each site. As scientific measurements, the skyglow data will inform responsible local officials of the level of the light pollution problem, ideally leading to change for healthier and safer communities. IDA has identified five principles of responsible outdoor lighting which, when followed, will reduce light pollution.

Processing of the SQM data for Goals #1 and #2 begins with the same first steps, and then diverges in subsequent steps to accommodate each of the two project goals.

Goal #1 - We process the SQM data suitable for Dark Sky Place certification along these steps:

1) Eliminate data influenced by the sun, moon and clouds
2) Adjust data for SQM hardware conditions – presence of the weather proof case and aging of the SQM
3) Exclude any data values greater than 22.0 magnitudes per arc second squared
4) Minimize influence of the brightness of the Milky Way – filter out data acquired when the Milky Way is overhead

Goal #2 - We process data for the level of light pollution and detection of long-term change of skyglow due to artificial sources, along these steps:

1) Same as for Goal #1
2) Same as for Goal #1
3) Same as for Goal #1
4) Minimize Milky Way influence by adjusting the data to a Milky Way position at a specific galactic latitude (30 degrees off the zenith) and galactic longitude (120 degrees)
5) Minimize the influence of time of night by adjusting data to 1AM local standard time
6) Adjust the skyglow data for increased airglow due to an increase in solar activity as we approach the next sunspot maximum

7) Understand variation due to local seasonal effects and minimize those which vary year-to-year and season-to-season
    a. Consider snow cover - use satellite data to eliminate nights when snow cover was present
    b. Consider atmospheric character - particulates, humidity

The processing of the SQM data toward each goal diverges at step 4, the handling of the effect of the Milky Way. For Goal #1, processing for Dark Sky Place certification, we exclude data samples acquired with the Milky Way overhead, which is consistent with IDA advice to not include the Milky Way in any SQM readings. Also, for Goal #1, consistent with IDA advice, we include data from all seasons without adjustment, to characterize the annual night sky brightness at a site.

For Goal #2, long-term tracking, instead of discarding the Milk Way data, we choose to normalize the effect of the Milky Way, to minimize seasonal variation and time of night. And further for Goal #2, in step 6 we adjust the data for changes of airglow and in step 7, we seek to understand and to minimize seasonal and other long-term variations that may also bias the skyglow trends over time.

Goals #1 and #2

Processing Step 1 – Eliminate data influenced by the Sun, Moon and Clouds

Eliminating the effects of sunlight and moonlight is straightforward. To eliminate issues with sunlight, we only consider data recorded after astronomical twilight (dusk) and before the start of astronomical twilight (dawn) – defined as the period during which the Sun is 18 degrees or more below the horizon. To eliminate issues with moonlight, we only consider SQM data recorded when the Moon is 10 degrees or more below the horizon.

Clouds at night significantly affect the brightness of the sky recorded by the SQMs. Figure 4 shows details of SQM data from five sites recorded during the night of August 10-11, 2019, which was a particularly cloudy night across Central Oregon. The data show rapid variation at the 5-minute sampling interval due to changing cloud conditions overhead during that night. The rapid variation over time, caused by clouds is quite different from the smooth track of data acquired during clear nights, as shown in Figure 3.

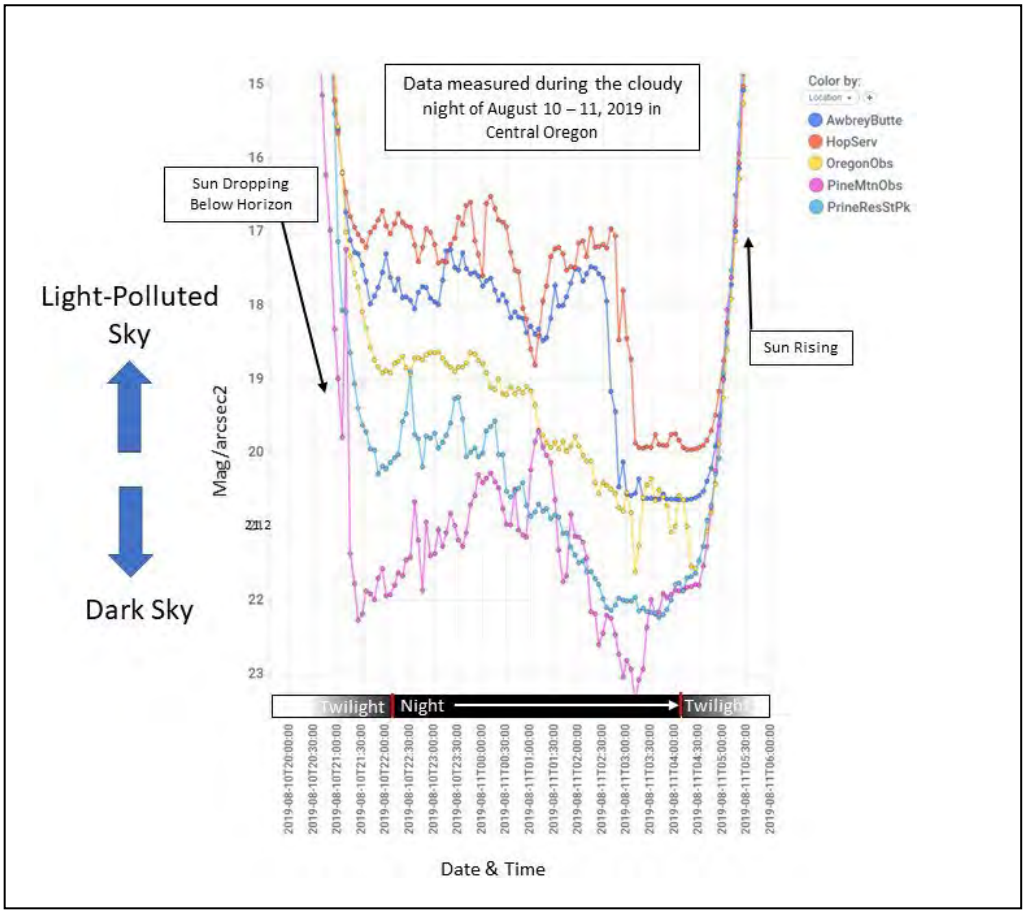

Figure 4. *SQM data recorded during a particularly cloudy night across Central Oregon. The data show rapid variation at the 5-minute sampling interval due to changing cloud conditions overhead during that night.*

To eliminate skyglow measurements taken during cloudy periods, we use an algorithm that measures the "jagginess" of the skyglow data over a 90-minute period. If the skyglow data are relatively smooth over a 90-minute period, we assume that clouds are not present, and we include the center point of that period as a clear sky measurement. This algorithm is based on one used by Grauer and others, 2019, but modified to employ the Residual Standard Error (RSE) as a measure of deviation from a linear fit. See Appendix B for details. We use an RSE cutoff of 20 to exclude cloudy, that is "jaggy", data. Points at the center of each 90-minute segment are excluded if the RSE for that segment is larger than 20, otherwise the point is considered to be measured during clear sky conditions. Note that in a previous report, Edition #4, we used an RSE cutoff of 50, but as explained in Appendix B, we now choose the more conservative cutoff of 20.

The cloud detection algorithm assumes that cloud cover is variable over time. Data acquired under constant cloud cover or in foggy conditions is not caught by the cloud algorithm. We eliminate those data by a different algorithm, described in Appendix B.

Note in Figure 4 that the clouds cause quite bright skyglow readings at the Awbrey Butte and Hopservatory sites, which are light-polluted – the artificial light from the ground reflects downward from the clouds. The inverse occurs at dark sky sites – note that clouds at the Pine Mountain site caused readings much greater than 22 mags/arcsecond^2 in the early morning hours, an unreasonably dark reading for a natural sky – caused by black-appearing clouds blocking the stars. See Appendix C for detailed data plots of this phenomenon and a discussion of the skyglow signature of a site.

Goals #1 and #2

Processing Step 2 - Adjust data for SQM hardware conditions –the weatherproof case and SQM aging

The SQM hardware resides inside a weatherproof case. The top of the case has a clear window that slightly darkens each measurement. Unihedron, the manufacturer, specifies that users should subtract 0.11 magnitudes per arc second squared from the data to account for the presence of this window. Accordingly, we do so.

Recent research (Puschnig and others, 2020) using SQMs from three different locations, documents that as the SQM device and weatherproof enclosure age, there is a darkening effect on measured data, in their case an average of about .04 mags/arcsecond^2 per year. This aging effect increases the skyglow measurements over time, making the sky seem slightly darker than reality. Other researchers (Alarcon and others, 2021) found no evidence of aging of a different photometer, the TESS instrument.

Unihedron (personal communication, 2022) notes that two issues can be involved: 1) development of a translucent film on the blue glass IR filter, which seems related to moisture and 2) yellowing of the plastic case of the semiconductor sensor over time.

To understand this phenomenon better, we obtained two new SQMs and installed them to run in parallel to two SQMs that had been running for several years. The results from our experiment suggest that a darkening effect is present, but a smaller one compared to the estimate from Puschnig and others. Our estimate is .019 mags/arcsecond^2 per year. Accordingly, we subtract values proportional to this assumed aging effect from our data, based on the progressive, serial exposure over time of measurements from each SQM in our network. See details in Appendix D.

Goals #1 and #2

Processing Step 3 - Eliminate out of bounds values

It is widely considered that the darkest clear night sky should not have any zenith brightness values greater than 22 mags/arcsecond^2. Other observations suggest that some night skies reach up to 22.1 or even 22.3 mags/arcsecond^2. At present, we adopt a conservative view and filter out any values greater than 22.0 from our data. See Appendix C for additional comments.

Goal #1

Processing Step 4 - Filter out measurements taken when the Milky Way is overhead

As noted above, when processing the SQM data for Dark Sky Place certification, we exclude data samples acquired with the Milky Way overhead, which is consistent with IDA advice to not include the Milky Way in any SQM readings, to avoid biasing the data. Accordingly, we eliminate any data points acquired when the plane of the Milky Way is within 30 degrees of the zenith. We choose thirty degrees to accommodate the 20-degree FOV (10 degrees half width half maximum) of the SQM, plus 10 more degrees to take a conservative approach.

After Steps 1-4, the processing for Goal #1, for Dark Sky Place measurements, is complete. We have removed the effects of the sun, moon, clouds, weatherproof cover, SQM aging, out of bounds data and presence of the Milky Way. So, we can compare the brightness of the clear night skies at the current sites (Figure 5).

Figure 5 lists the 37 sites for which we had data as of the November 2022 deadline for this report. This Edition of the report includes data from Crater Lake National Park for the first time. The sites are organized in Figure 5 by the median value of the site's SQM data – the highest amount of light pollution on the top to the least on the bottom. The sites on the very bottom, beginning with Hart Mountain, have essentially pristine night skies overhead. As we acquire additional data over time, the exact order of the sites may change.

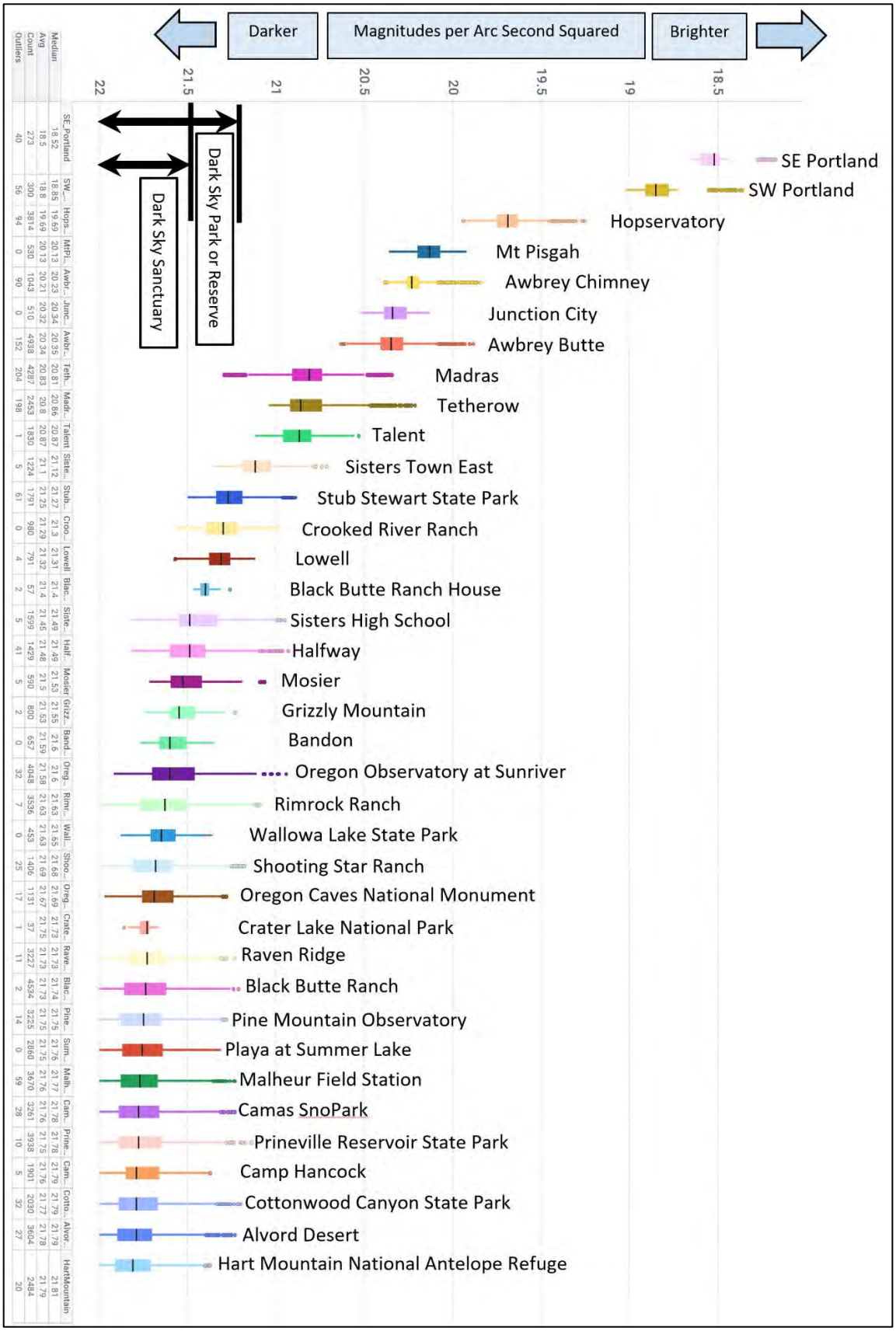

Figure 5. *Box plot showing the clear sky measurements of the 37 sites with data as of the November 2022 deadline for this report. IDA's cutoffs for Dark Sky Places are shown in the upper left. Many of our measurement sites qualify for dark sky place certification. The vertical black line in each box marks the median value. The horizontal size of the box marks the central 50% of data. Table 1 provides the summary statistics at each site.*

Table 1 summarizes the average brightness of the night sky in Figure 5 for each site in the logarithmic mags/arcsecond^2 scale. The "X Brighter" column in Table 1 on the far right shows how much brighter, on a linear scale, each site is compared to Hart Mountain, the darkest night sky site in our data set to date. The clear night skies in and near the cities of central Oregon are 3x to 7x brighter, that is, 3x to 7x more light-polluted, than the pristine night skies at Hart Mountain. Clear night skies at the two sites in the city of Portland, at the top of Table 1, are about 20x brighter than the clear night skies at Hart Mountain.

	Median (mag/arc second squared)	Median (microCandelas/ meter squared)	X Brighter
Southeast Portland	18.52	4221.08	20.70
Southwest Portland	18.85	3114.75	15.28
Hopservatory	19.69	1436.89	7.05
Mount Pisgah Arboretum	20.13	958.13	4.70
Awbrey Chimney	20.23	873.82	4.29
Junction City	20.34	789.63	3.87
Awbrey Butte	20.35	782.39	3.84
Tetherow	20.81	512.18	2.51
Madras	20.86	489.13	2.40
Talent	20.87	484.65	2.38
Sisters Town East	21.12	384.97	1.89
Stub Stewart State Park	21.27	335.29	1.64
Crooked River Ranch	21.30	326.15	1.60
Lowell	21.31	323.16	1.58
Black Butte Ranch House	21.40	297.46	1.46
Sisters High School	21.49	273.79	1.34
Halfway	21.49	273.79	1.34
Mosier	21.53	263.89	1.29
Grizzly Mountain	21.55	259.07	1.27
Bandon	21.60	247.41	1.21
Oregon Observatory	21.60	247.41	1.21
Rimrock Ranch	21.63	240.67	1.18
Wallowa Lake State Park	21.65	236.28	1.16
Shooting Star	21.68	229.84	1.13
Oregon Caves NM	21.69	227.73	1.12
Crater Lake NP	21.73	219.49	1.08
Raven Ridge	21.73	219.49	1.08
Black Butte Ranch	21.74	217.48	1.07
Pine Mountain Observatory	21.75	215.49	1.06
Playa at Summer Lake	21.76	213.51	1.05
Malheur Field Station	21.77	211.56	1.04
Camp Hancock	21.78	209.62	1.03
Prineville Reservoir State Park	21.78	209.62	1.03
Camas SnoPark	21.79	207.69	1.02
Cottonwood Canyon State Park	21.79	207.69	1.02
Alvord Desert	21.79	207.69	1.02
Hart Mountain	21.81	203.90	1.00

Table 1. *Summary of SQM* ***clear night data*** *at each location. The clear night skies in Portland, OR are about 20x brighter than at Hart Mountain. The median values in the first data column are in the logarithmic units of* ***mags/arcsecond²****. The second data column lists the median values after conversion to a linear brightness scale. The "X Brighter" column shows how much brighter is the clear night sky at each site on the linear scale compared to the current darkest site – Hart Mountain. (See this link for information about converting from the logarithmic* ***mags/arcsecond²*** *scale to candelas.)*

Skyglow from Cloudy Nights – the Second Part of the Signature

The previous section summarized the clear night data from each measurement site. We also want to characterize each site's measurements during cloudy conditions. We achieve that by selecting the "jaggy" data – namely points that have a RSE value greater than the cutoff of 20.

Table 2 summarizes the statistics for these measurements taken during cloudy conditions. The "X Brighter" column in Table 2 shows that under clouds, the night sky in Portland, Oregon is up to 150x brighter than the sky under cloudy conditions at Hart Mountain. Clouds near cities reflect light pollution back down to the surface environment causing very bright night sky readings. By contrast, clouds at a dark sky site like Hart Mountain appear black because there is no artificial light pollution coming from the ground to light them up. Additionally, the clouds block out starlight, so pristine night sky sites like Hart Mountain are particularly dark when the sky is overcast.

We can consider the skyglow at Hart Mountain to be the natural case, and the skyglow over cities – those sites near the top of Table 2 - to be quite un-natural. The impact on the wild ecosystem of light pollution in cloudy conditions within and near cities is likely significant.

Location	Median (mag/arc second squared)	Median (microCandelas/ meter squared)	X Brighter
Southeast Portland	16.69	22773.18	154.17
Southwest Portland	17.11	15467.63	104.71
Hopservatory	18.81	3231.65	21.88
Mount Pisgah Arboretum	18.93	2893.50	19.59
Awbrey Chimney	19.27	2115.55	14.32
Junction City	19.18	2298.39	15.56
Awbrey Butte	19.5	1711.68	11.59
Tetherow	19.87	1217.37	8.24
Madras	19.96	1120.53	7.59
Talent	20.14	949.34	6.43
Sisters Town East	20.7	566.79	3.84
Stub Stewart State Park	21.34	314.36	2.13
Crooked River Ranch	21.03	418.24	2.83
Lowell	20.4	747.18	5.06
Black Butte Ranch House	21.48	276.33	1.87
Sisters High School	21.12	384.97	2.61
Halfway	20.97	442.00	2.99
Mosier	21.12	384.97	2.61
Grizzly Mountain	21.52	266.33	1.80
Bandon	21.21	354.34	2.40
Oregon Observatory	20.99	433.93	2.94
Rimrock Ranch	21.68	229.84	1.56
Wallowa Lake State Park	21.82	202.03	1.37
Shooting Star	21.87	192.94	1.31
Oregon Caves NM	21.93	182.57	1.24
Crater Lake NP	21.93	182.57	1.24
Raven Ridge	22.12	153.26	1.04
Black Butte Ranch	21.75	215.49	1.46
Pine Mountain Observatory	22.12	153.26	1.04
Playa at Summer Lake	22.05	163.46	1.11
Malheur Field Station	22.11	154.68	1.05
Camp Hancock	22.13	151.85	1.03
Prineville Reservoir State Park	21.8	205.79	1.39
Camas SnoPark	21.9	187.68	1.27
Cottonwood Canyon State Park	21.96	177.59	1.20
Alvord Desert	22.11	154.68	1.05
Hart Mountain	22.16	147.71	1.00

Table 2. *Summary of SQM* ***cloudy night data*** *at each location. The sites are listed in the same order as in Table 1. The cloudy night skies in Portland, Oregon are up to 150x brighter than cloudy nights at Hart Mountain. The median values in the second data column are in the logarithmic units of* ***mags/arcsecond^2****. These data have been adjusted for the age of each SQM and filtered to remove data acquired when the Milk Way is within 30 degrees of zenith. Values higher than 22.0 mags/arc second squared are included because they record the fact that clouds will block the stars and are representative of cloudy conditions. The third column lists the median values after conversion to a linear brightness scale. The "X Brighter" column shows how much brighter on the linear scale is the cloudy night sky at each site compared to the current darkest site – Hart Mountain.*

Goal #2 – Determine long term change of light pollution

Processing Step 4 - Adjust Clear Sky SQM Data for the Position of the Milky Way

When the Milky Way is overhead, the SQM will record a brighter night sky. For Goal #2, instead of eliminating those measurements as we did for Goal #1, we keep those data and adjust out that effect in processing. We first convert the data from the logarithmic scale (mags/arc second squared) to linear (microcandelas per meter squared), then adjust the SQM data for the galactic latitude, then adjust that data for the galactic longitude. By this method, we minimize the seasonal nature of the Milky Way pattern and also avoid loss of data. This process is described in Appendix E.

Processing Step 5 - Adjust data to 1AM local standard time to minimize the influence of time of night

As the night progresses, our skyglow measurements show that the night sky grows progressively darker, especially for light polluted sites. Because we have already adjusted the data for the position of the Milky Way, we expect that the darkening through the evening hours is due to outdoor lights being turned off and fewer car headlights about, as most people are sleeping instead of driving around. To minimize this effect, we statistically adjust the data in the linear space (microcandelas per meter squared) at each site to 1AM local standard time. As with the adjustments for position of the Milky Way, this adjustment to 1AM is an effort to minimize variation that might otherwise obscure or bias any long-term trends in the skyglow data. See details and figures in Appendix F.

Previously, in this report series, we experimented with a different "time of night" adjustment – namely we only included data from 10:30PM local standard time to 4:30AM local standard time, which is the time range of the summer nights in our latitude range. That filtering was an effort to overcome the difference in time of darkness during winter versus summer nights. In our northern hemisphere winter, we experience much longer evening hours of darkness, versus the summer months. That is, darkness in the winter begins much earlier in the evening. In Edition #5, we experimentally applied that filtering to the data, which had already been adjusted to 1AM. There was no benefit to that truncation of data and in fact, the seasonal trends became noisier. Therefore, we do not truncate the data by time of night.

Discussion – Impact on seasonal trends of each progressive adjustment to the skyglow data

Figure 6 (taken from Edition #6 of this report) summarizes the seasonal variation in the skyglow data for four dark sky sites, along with the progressive impact of adjustments for galactic latitude, galactic longitude and time of night. The horizontal axis of Figure 6 shows the months of the year. The vertical axis is the skyglow data at each site and at each progressive level of data adjustment, averaged by month. Data points are the average at each month from each site for 1.5 to 3 years of recording time.

Figure 6 shows that, prior to any adjustment for the galactic position and time of night (the brown dots and lines), the skyglow data for these dark sky sites show a dramatic seasonal pattern of darker in springtime (March-April-May) and brighter in late autumn and early winter (Oct-Nov-Dec). This pattern is consistent with the fact that the portion of the Milky Way crossing the zenith in March is in Auriga, which is significantly darker than the portion of the Milky Way crossing zenith in November in much brighter Cygnus. After the adjustment for galactic latitude (the red dots and lines in Figure 6), the seasonal pattern is greatly reduced. Calculations in Appendix G show that the reduction for the dark sky sites drops on average to 46% of the original variation.

The impact of including the galactic longitude adjustment is lesser (purple dots and lines), and amounts to another 14% reduction. The impact on the seasonal pattern of including the time adjustment to

1AM is not clear (blue dots and lines), but overall tends to be slightly beneficial, just 1%. See the tables of data in Appendix G.

As we might expect, the adjustment for galactic position has little impact on the seasonal pattern of the light-polluted sites – after all, the Milky Way is largely invisible due to the light pollution at those locations. Moreover, the seasonal pattern is different for those sites too. See Appendix G for additional figures and discussion.

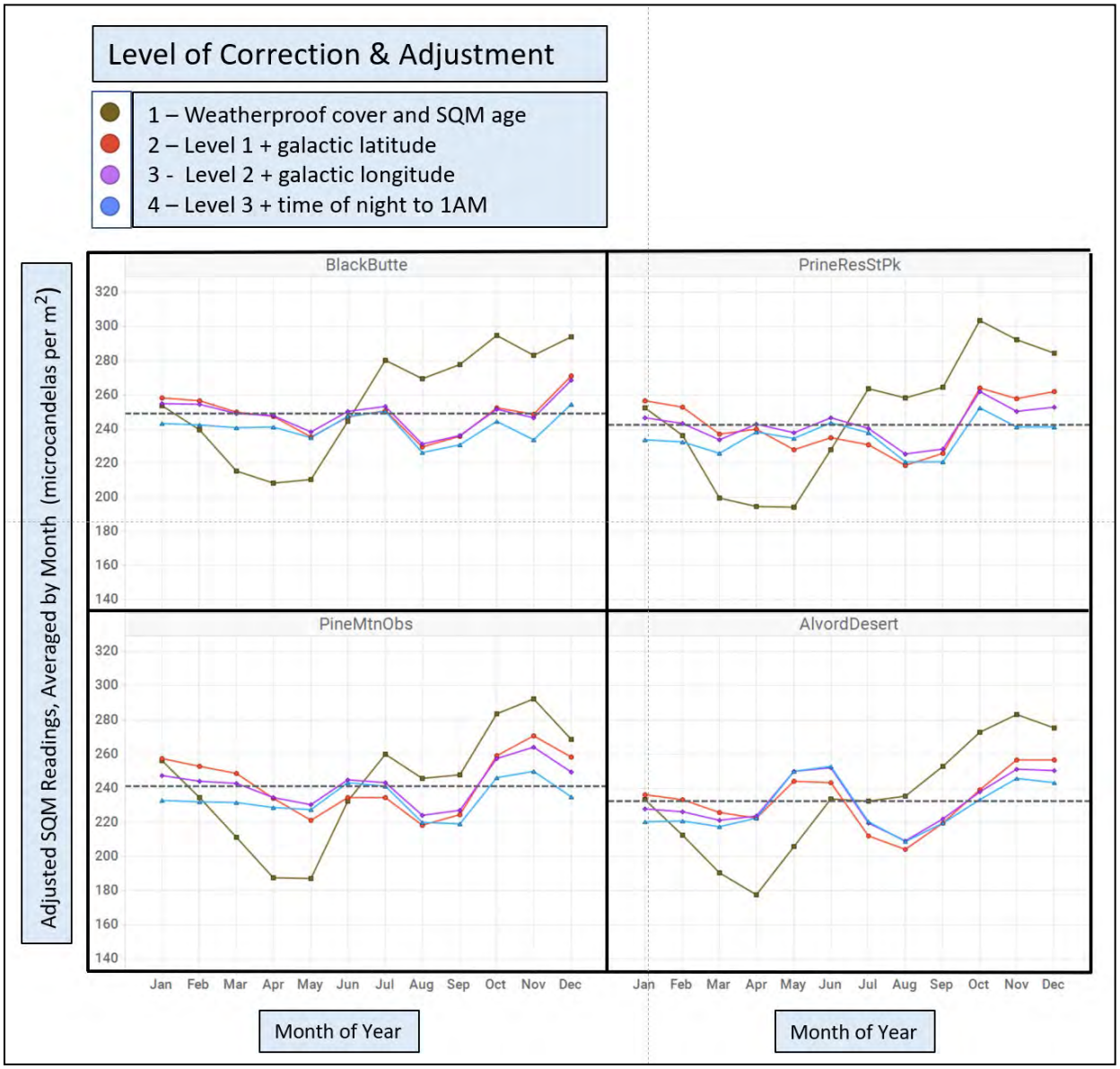

Figure 6. The average monthly SQM data for four dark sky sites after the progressive impact of adjustments for galactic latitude, galactic longitude and time of night. See explanation in text. Also see Appendix G for a plot of all of the sites, tables of data and additional discussion.

Goal #2

Processing Step 6 – Adjust SQM data for increase of airglow due to increase of solar flux

Another factor to consider in zenith skyglow trends over long periods is variations of airglow, the light emitted from the atmosphere itself due to the impact of space weather on Earth (Grauer and others, 2019; Grauer & Grauer, 2021). Airglow is known to vary on a wide range of time scales, from rapid

variation in minutes across one night, to strong, years-long changes correlated to the 11-year solar sunspot cycle.

There are several known causes of airglow variation, including (1) the solar flux input to the earth's atmosphere which arrives in about 7 minutes from the sun at the speed of light, (2) impact of the solar wind's magnetic field, which arrives from the sun in about 4.5 days and (3) its interaction with the earth's magnetic field. In the following, we adjust our skyglow data for variations in (1) the solar flux, which can play a significant role in estimates of skyglow change per year.

The sun is currently rising out of a solar sunspot minimum, toward a predicted sunspot maximum in July 2025. So, space weather may cause our SQM data to read brighter since our SQM project began in mid-2019, by increased airglow, independently of any changes in light pollution from the ground.

Accordingly, we have estimated the increase of airglow since the beginning of our SQM project, and adjusted the SQM data of our long-term sites. Figure 7 shows the estimated airglow contribution to the clear night sky (yellow dots) and the SQM data for the Prineville Reservoir State Park site (red dots). We subtract the estimated airglow, sample-by-sample from the corresponding clear night sky measurements of the SQM. The process of adjustment for airglow is described in Appendix H.

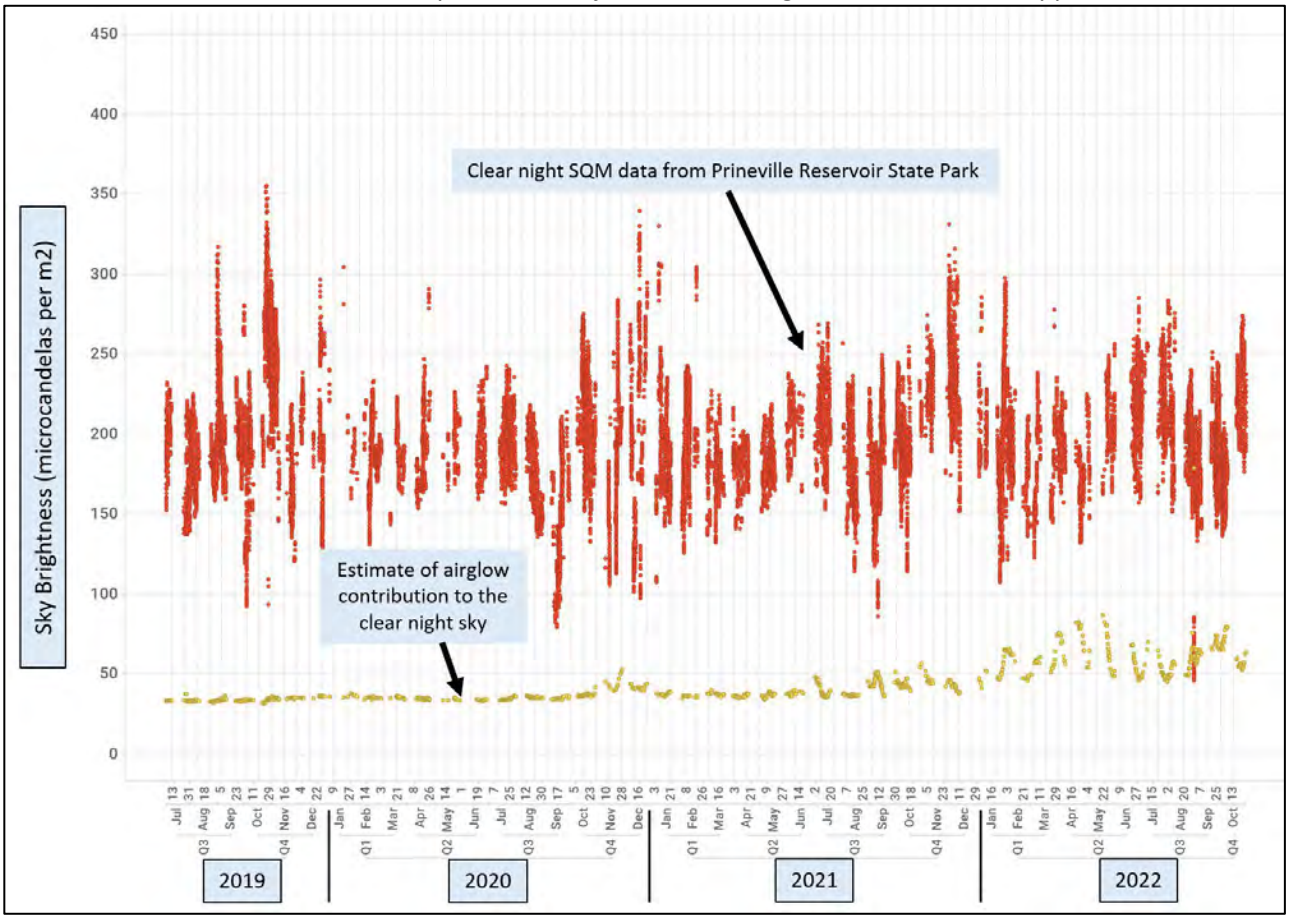

Figure 7. SQM data from Prineville Reservoir State Park shown in red, after adjustment for weatherproof cover, age, galactic latitude, galactic longitude, time of night and airglow. The estimated airglow is shown in yellow for each SQM data point, based on airglow data from Krisciunas and others, 2007. See Appendix H. Note the increase in estimated airglow (yellow dots) since September 2021.

Large zig-zag brightness changes of the clear night sky, from month to month, are still present in the data even after the airglow adjustment for solar flux (Figure 8, which is from Edition 6 of this report). Several phenomena may contribute to this pattern:

1) It is likely that seasonal atmospheric character, probably water content and particulate content, contribute to seasonal variation at each site.

2) Grauer and Grauer, 2021 show data for increased airglow over periods of days, unrelated to solar flux, with amplitudes of brightness change on the order of the changes shown in Figure 8 – about 50 to 100 microcandelas per meter squared. While we have adjusted the current data for variations in solar flux (see Appendix H), we have not to date explored airglow effects caused by interaction of the magnetic fields of the earth and solar wind. One characteristic of airglow effects is their simultaneous impact over a large region. It's worth noting that the Black Butte, Prineville Reservoir and Pine Mountain sites shown in Figure 8 are 30 to 40 miles apart, and that the Alvord Desert site is about 170 miles from the other 3 sites.

At present, the causes of the zig-zag pattern, typified by Figure 8, is not resolved.

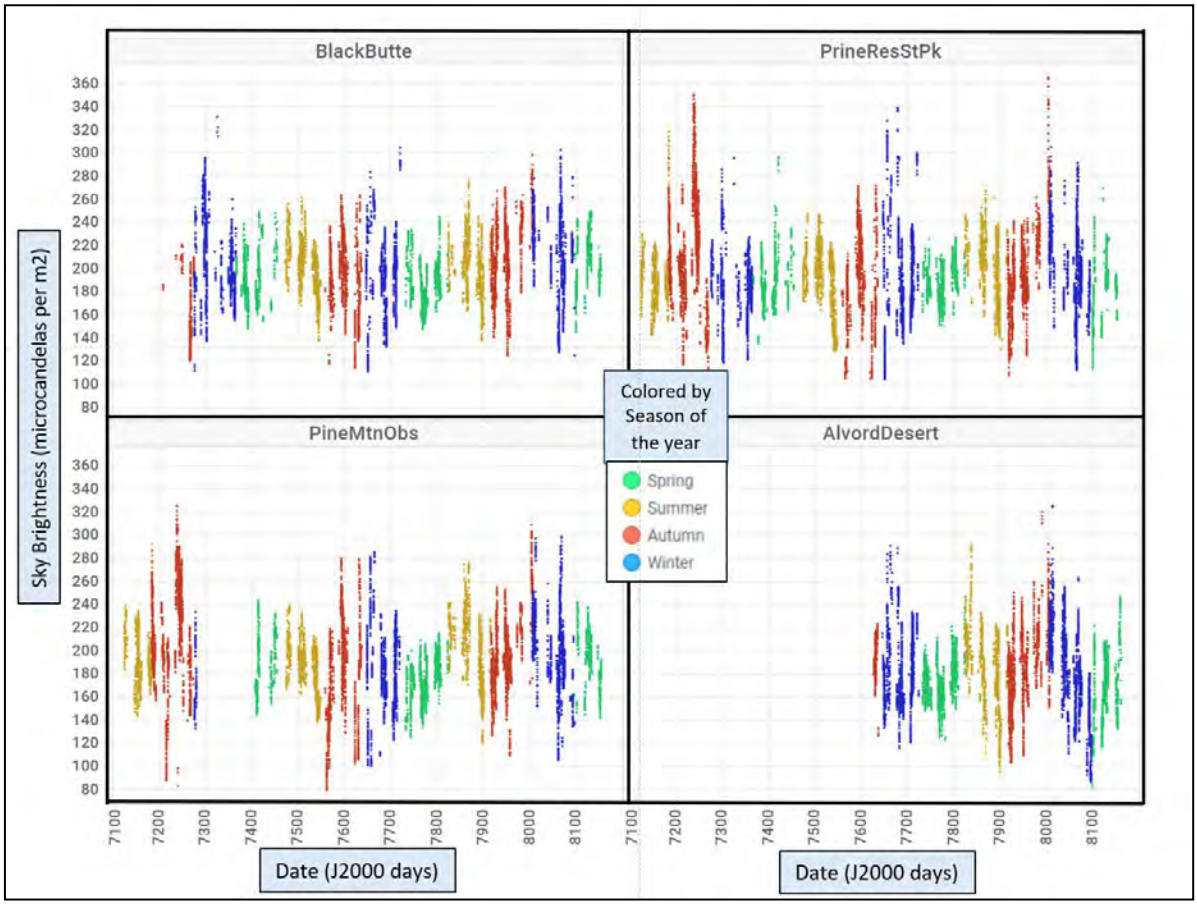

Figure 8. The clear night sky data for four dark sky sites over several years of time, after adjustment for galactic latitude, galactic longitude, time of night and solar flux. Each cluster of vertically-smeared points were acquired during a new moon period. The data points are colored by season of the year.

Goal #2

Processing Step 7 - Minimize other seasonal effects in the data

Other seasonal effects that will affect skyglow include snow cover in winter and variations in character of the atmosphere such as the particulate concentration and absolute humidity.

Previously, in Edition #4 of this report series, we eliminated any nights with local snow cover on the ground, and found that the effect was surprisingly minimal on the long-term trend.

Atmospheric particulates increase in late summer, largely due to forest fire activity. There is also a trend of increased particulates since the beginning of our SQM study, which will likely contribute to increased skyglow, although complex competing influences are present (Cinzano and Falchi, 2012; Kocifaj and Komar, 2016).

In the high desert environment of most of our SQM sites, the relative humidity tends to be higher in the winter than in summer, but the colder winter air will hold less water, so we really need to know the absolute humidity. And ideally not just on the ground, but along the atmospheric path.

We don't attempt any adjustment of the skyglow data for atmospheric effects at present. As we expand the SQM network into more non-arid regions of Oregon, with different seasonal atmospheric properties, we expect to better understand these effects.

Changes of Skyglow over Time

After processing the SQM data for Goal #2, (namely through weatherproof cover, age, galactic latitude, galactic longitude, time of night and solar flux/airglow), we plot the adjusted data over the time since we began recording data. Figure 9 shows the adjusted clear night sky data for the 22 sites for which we have at least a year and a half of data, plotted over time. The solid line across each data subset in Figure 9 is a linear regression fit to the sky brightness recorded over time.

The data in Figure 9 appear as individual points – one per month – because we have averaged the data by month to minimize bias that may be introduced by the large differences in numbers of samples acquired each month (see Appendix I.) Some months of data are missing from individual sites due to failure of batteries and in the case of Pine Mountain Observatory, due to a winter storm, which blew the SQM mounting pole off the zenith direction.

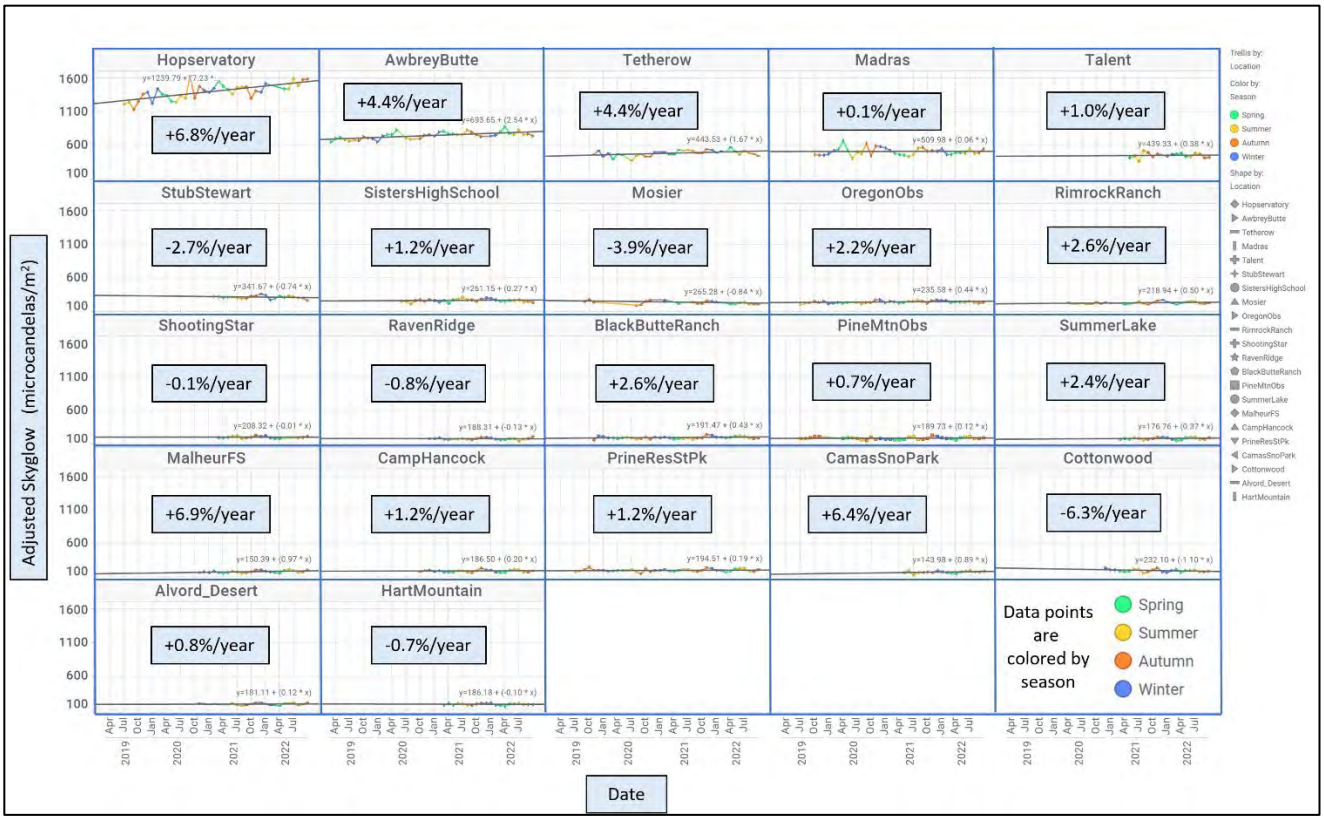

Figure 9. The adjusted clear sky data for the sites with at least 1.5 years of data, plotted over time. The black line across each data subset is a linear regression fit. The percentage changes of skyglow are shown for each site. The data are adjusted according to Goal #2 as described in the text. See Appendix I for an enlarged plot from each individual site.

Note that the points in Figure 9 are colored by season of the year. For the dark sky sites, the adjusted skyglow during the autumn tends to be brighter than during the summer, which is another way of looking at the same seasonal pattern shown in Figure 6. See Appendix I for enlarged plots for each site and a clearer view of this pattern.

Table 3 summarizes four parameters to consider in studying the change of sky brightness over time at the long-term sites:

a) The Slope of the long-term regression lines from Figure 9,
b) The Percentage change over time at each site,
c) The R-squared statistic from the linear regression, and
d) The Residual Standard Error of the regression fit.

The dark sky sites with a moderate slope of regression line (for example, Malheur Field Station) express a large percentage change because of the small values involved. This phenomenon is a known issue with the calculation of percentage values. At any rate, the data are clear that the sky brightness has been increasing at the Malheur Field Station. We are unaware of any reason for that increase.

The increase of 4% to 7% per year in the light-polluted sites in central Oregon (first three sites of top row of Figure 9) seems due to the increase in population of that area over the past few years along with ineffective enforcement of the existing lighting ordinances.

Location	Slope of Long Term Regression	Pct Change Per Year	R Squared	Residual Standard Error
Hopservatory	7.23	6.8	49.06	86.5
AwbreyButte	2.54	4.4	42.10	39.7
Tetherow	1.67	4.4	17.62	38.6
Madras	0.06	0.1	0.01	57.4
Talent	0.38	1	0.33	38.1
StubStewart	-0.74	-2.7	4.15	22.7
SistersHighSchool	0.27	1.2	1.21	21.3
Mosier	-0.84	-3.9	16.86	22.3
OregonObs	0.44	2.2	8.80	16.9
RimrockRanch	0.5	2.6	5.77	18.5
ShootingStar	-0.01	-0.1	0.00	15.7
RavenRidge	-0.13	-0.8	0.29	16.2
BlackButteRanch	0.43	2.6	7.46	16.0
PineMtnObs	0.12	0.7	0.61	17.5
SummerLake	0.37	2.4	2.25	15.0
MalheurFS	0.97	6.9	17.57	15.2
CampHancock	0.2	1.2	0.69	17.7
PrineResStPk	0.19	1.2	1.41	18.8
CamasSnoPark	0.89	6.4	7.52	17.2
Cottonwood	-1.1	-6.3	11.64	21.1
Alvord_Desert	0.12	0.8	0.26	16.6
HartMountain	-0.1	-0.7	0.18	14.8

Table 3. *Four parameters to consider for the summary of skyglow change over time at each long-term site. See text for explanation.*

We note that the Mosier site shows a 4% per year decrease in skyglow. We are not aware of any local changes to explain that decrease. That site has a history of missing data and as the histogram in Appendix I shows, much of the Mosier data is from the Autumn with little from the Winter and Spring. We suspect a bias due to incomplete seasonal data may be at the root of the apparent decrease of skyglow at that site.

The large increase (6.4%) of skyglow at the Camas Sno Park may be related to moving the SQM to a nearby, but different location, before the last data download. It will be worthwhile to separate that site into before-and-after-move data sets going forward.

The Cottonwood site shows a strong decrease in skyglow (-6.3%), which may be due to lighting improvements over time, as that site works toward Dark Sky Park certification.

The R-squared statistic is traditionally interpreted as the percentage of variance explained by the regression equation. The Hopservatory site shows a strong increase in brightness over time, and as shown in the 3rd column of Table 3, the linear regression is said to account for 49% of that increase. The dark sky sites have very little zenith sky brightness change over time, and therefore show dramatically small R-squared values.

The Residual Standard Error (RSE) is a better statistic to assess the goodness of fit of the regression equations. On that basis (Table 3, fourth column), we interpret that the dark sky sites have a much better fit to the linear regression than do the light-polluted sites. In fact, the Hopservatory site, the most light-polluted among these 22 sites, shows the largest RSE, and the most scatter of data, despite having the largest R-squared value.

In summary, we recognize various sky brightness trends in our data. Going forward, we continue to acquire additional data and will follow up at several sites to better understand the origin of the trends.

At the darker sites, changes of skyglow will be more evident near the horizon. This calls for an additional measuring system, such as a calibrated all-sky camera. This could be either a tripod-mounted system used at key sites during cloud-free, new moon conditions or an all-weather camera, always operating, acquiring images and periodically calibrated to further understand seasonal patterns and other issues that may become evident.

Acknowledgements

IDA Oregon acknowledges and thanks the representatives at the public and private SQM sites for their continued support on this project -- the Hopservatory, Tetherow, Madras, the Oregon Observatory at Sunriver, Black Butte Ranch, Prineville Reservoir State Park, the Pine Mountain Observatory, Rimrock Ranch, Sisters High School, Astronomy Club of City of Sisters, Crooked River Ranch, Grizzly Mountain, Camp Hancock, the Malheur Field Station, Raven Ridge, Southern Oregon Travel, Oregon Outback Dark Sky Network, Stub Stewart State Park, Shooting Star Ranch, Summer Lake, Summit Prairie, Alvord Desert, Hart Mountain National Antelope Refuge, Halfway, Cottonwood Canyon State Park, Wallowa Lake State Park, Oregon Caves National Monument, Bandon, Mt Pisgah Arboretum, Lowell, Junction City, Southeast and Southwest Portland and Crater Lake National Park.

We also appreciate the ongoing support of the Rose City Astronomers, the Sisters High School Astronomy Club and the City of Sisters Astronomy Club.

We also acknowledge the free-to-nonprofit availability and use of Tibco's exceptional Spotfire and Statistica software which have been critical to our analyses of the SQM data.

Project Contacts:

Bill Kowalik **bill.kowalik@darksky.org**

Mike McKeag **michael.mckeag@darksky.org**

References

Alarcon, M.R., Serra-Ricart, M., Lemes-Perera, S. and Mallorquin, M., 2021, Natural Night Sky Brightness during Solar Minimum, The Astronomical Journal, 162:25.

Cinzano, P., Falchi, F., 2012, The Propagation of Light Pollution in the Atmosphere, Monthly Notices of the Royal Astronomical Society, Vol 427, Issue 4, pp 3337-3357.

Coolidge, M., 2021, From the Desert to the Coast, the Case for Dark Skies, video presentation to the Cape Perpetua Collaborative, Oregon.

Grauer, A.D., Grauer P.A., Davies, N. and Davies G., 2019, Impact of Space Weather on the Natural Night Sky, Publications of the Astronomical Society of the Pacific.

Grauer, A.D., Grauer P.A, 2021, Linking Solar Minimum, Space Weather, and Night Sky Brightness, Nature Portfolio, Scientific Reports, 11:23893.

IDA, International Dark Sky Places Program.

Jechow, A, Kollath, Z, Ribas, SJ, Spoelstra H, Hölker, F and Kyba, CCM, 2017, Imaging and Mapping the Impact of Clouds on Skyglow with All-Sky Photometry, Scientific Reports.

Kocifaj, M., and Komar, L, 2016, A Role of Aerosol Particles in Forming Urban Skyglow and Skyglow from Distant Cities, Monthly Notices of the Royal Astronomical Society, Vol 458, Issue 1, pp 438-448.

Krisciunas, K., 1997, Optical Night-Sky Brightness at Mauna Kea over the Course of a Complete Sunspot Cycle, Journal of the Astronomical Society of the Pacific, 109, pp 1181-1188.

Krisciunas, K., Semler, D.R, Richards, J., Schwarz, H.E., Zuntzeff, N.B., Vera, S., and Sanhueza, P., 2007, Optical Sky Brightness at Cerro Tololo Inter-American Observatory from 1992 to 2006, Publications of the Astronomical Society of the Pacific, 119, pp 687-696.

Kyba, C., Tong, K., Bennie, J. et al., 2015, Worldwide Variations in Artificial Skyglow. Sci Rep 5, 8409.

Puschnig, J., Posch, T. and Uttenthaler, S., 2013, Night Sky Photometry and Spectroscopy Performed at the Vienna University Observatory.

Puschnig, J., Naslund, M., Schwope, A., and Wallner, S., 2020, Correcting Sky Quality Meter measurements for Aging Effects Using Twilight as Calibrator, MNRAS, 000, pp 1-6.

Schnitt, S., Ruhtz, T., Fischer, J., Holker, F. and Kyba, C.C.M., 2013, Temperature Stability of the Sky Quality Meter, Sensors (Basel), 13 (9), pp 12166-12174.

Sky Quality Meters, Unihedron.

Unihedron, 2022, Personal Communication.

Appendix A – Time duration of data from each SQM site

Figure A1 show the data coverage over time of each SQM site as of this Edition (#7) of the report. The chart is color-coded by the season of the year. Data gaps are caused by battery failure, structural support failure of the SQM mounting, or adverse weather conditions that prevented timely access. There are 22 sites with at least 1.5 years of data coverage. The long-range trend for those 22 sites is analyzed elsewhere in this report.

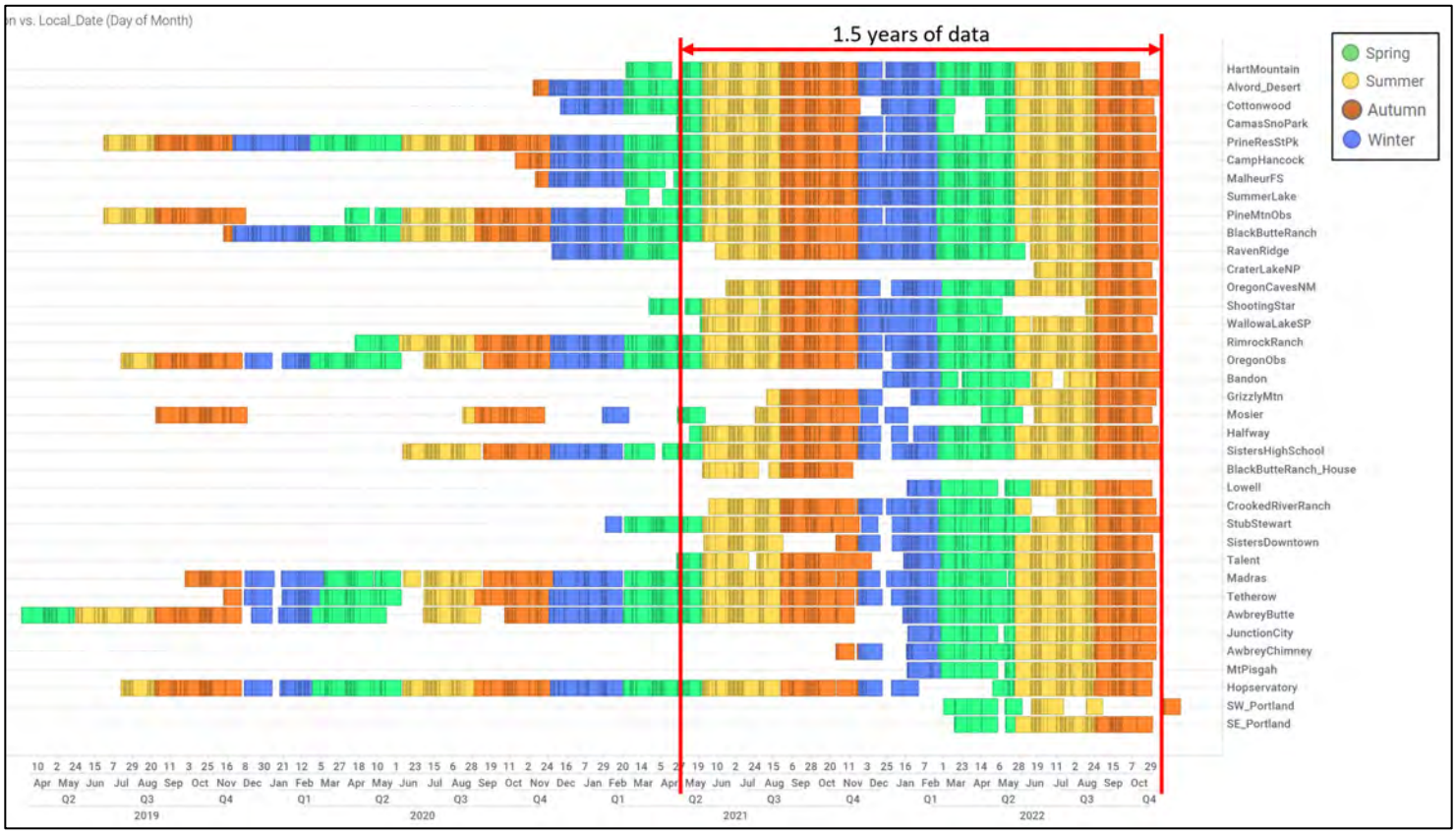

Figure A1. Time range of data available from the 37 SQMs as of the November 2022 deadline for this report. The plot is colored by seasons of the year. The red lines mark 1.5 years of data coverage. Sites with more than 1.5 years of coverage are analyzed for long term trends elsewhere in this report.

Appendix B - Cloud Removal Algorithm

To eliminate skyglow measurements taken during cloudy periods, we use an algorithm that measures the "jagginess" of the skyglow data over a 90-minute period. If the skyglow data are relatively smooth over a 90-minute period, we assume that clouds are not present, and we include the center point of that period as a clear sky measurement. Figure B1 shows a diagrammatic explanation. Figure B2 shows data examples.

This algorithm is based on one used by Grauer and others, 2019, but modified to employ the Residual Standard Error (RSE) as a measure of deviation from a linear fit. This algorithm is now implemented in Unihedron's UDM software, under the processing option "Tools/.dat to Sun-Moon-MW-Clouds."

We use a RSE cutoff of 20 to exclude cloudy, that is "jaggy", data. Points at the center of each 90-minute segment are excluded if the RSE for that segment is larger than 20, otherwise the point is considered to be measured during clear sky conditions.

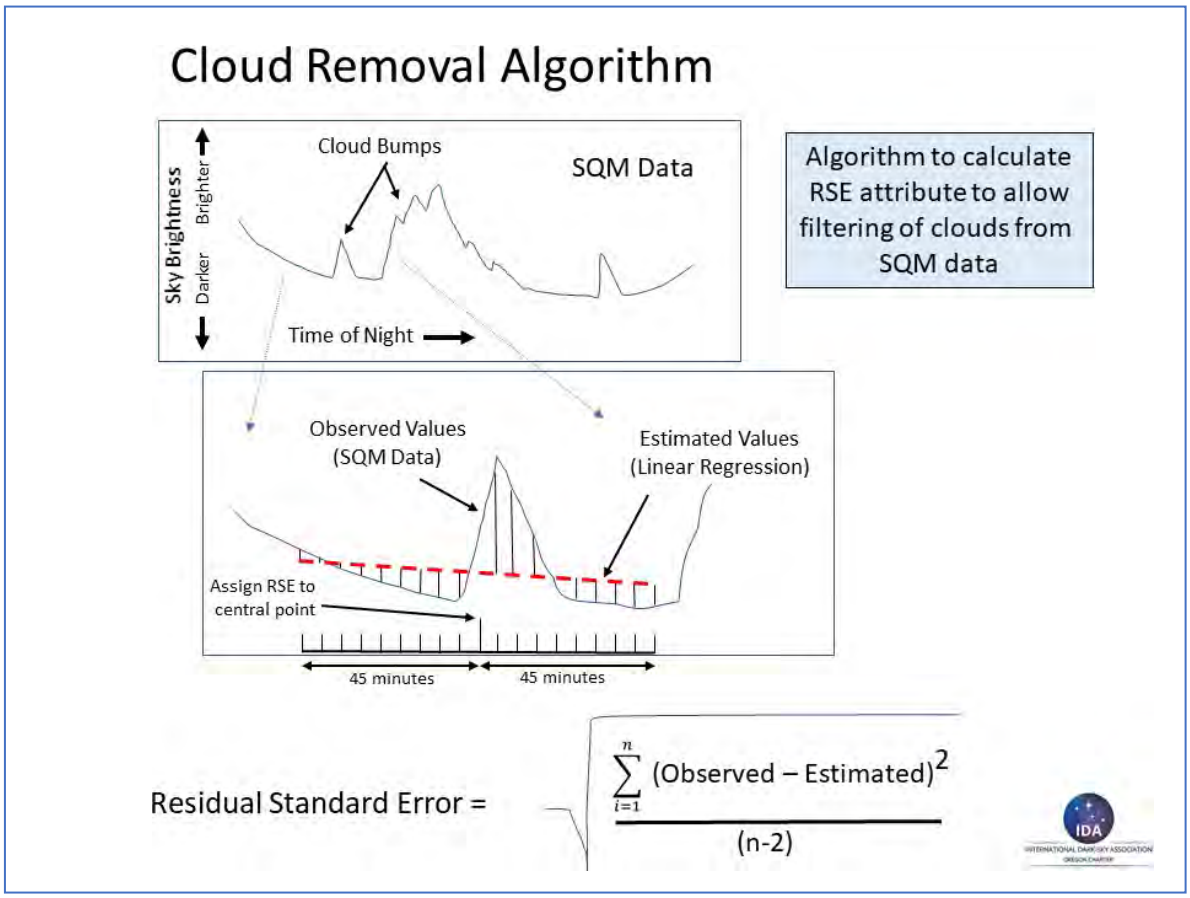

Figure B1. Diagrammatic explanation of the calculation of residual standard error which is used as the statistic to gauge the presence of clouds at each data point. We fit a linear regression to a sliding 90-minute interval of SQM data and assign the residual standard error to the center point of the time interval.

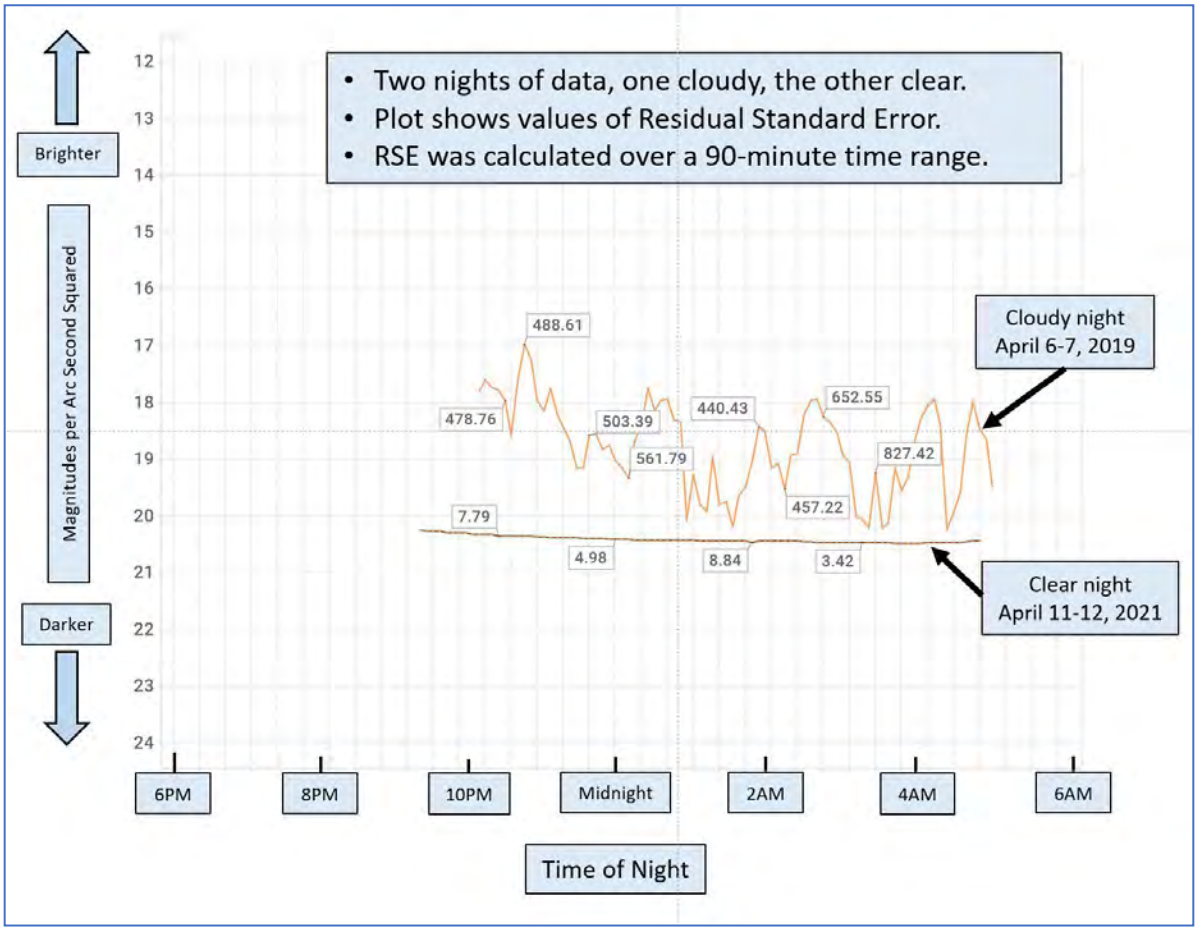

Figure B2. Data from two different nights, one cloudy, the other clear. The residual standard error values are shown at several point along the profiles. The clear night data has much smaller RSE values compared to data acquired during the cloudy night.

Filtering out cloudy data samples requires a choice of a cutoff RSE value. Previously we used a cutoff value of 50, but after studying density plots of RSE data (Figure B3), we chose a more conservative RSE value of 20. Figure B3 shows that a cluster of data points lies below the RSE value of 20. We take this as a natural clustering of cloud-free data, and accordingly use the RSE value of 20 to separate clear from cloudy data samples.

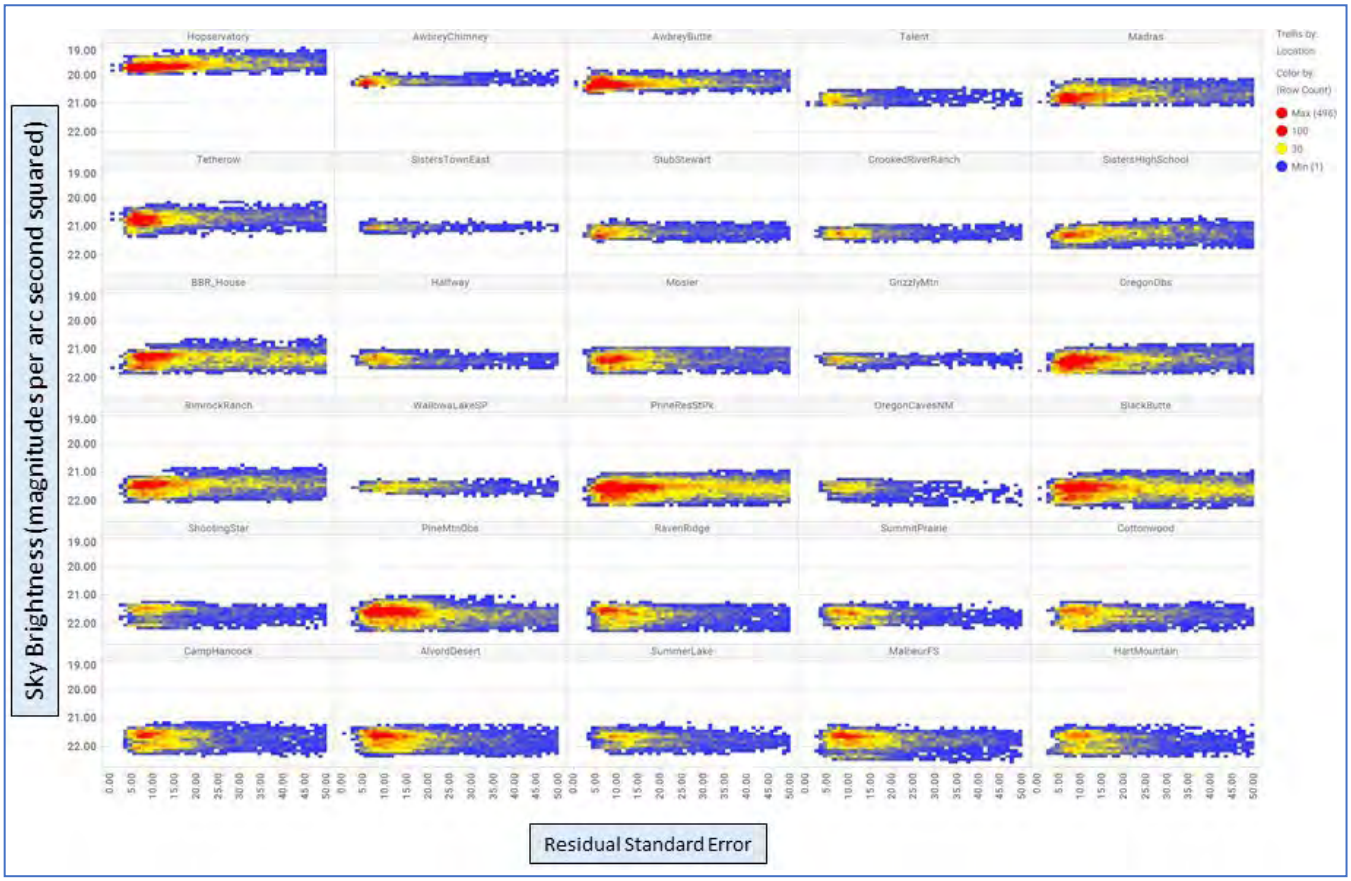

Figure B3. Density plot of residual standard error values versus sky brightness for all 30 SQM sites as of Edition #5 of this report. All of the sites show a cluster of values at the short end of the RSE scale. We choose a cutoff value of 20 going forward, to include those clustered values as clear sky data points.

The cloud removal algorithm effectively filters out SQM measurements acquired when cloud conditions vary during the 90-minute time span. However, it fails to remove cloudy data from periods of uniform overcast or fog – see Appendix C, Figure C4 for examples. In previous editions of this report, we manually deleted those sparse points outside the high-density data zone at each site. In this Edition #7 of the report series, we employ an automatic spatial filter to remove those points.

The spatial filter operates in the density plot domain as in Figure C4. Figure B4 shows an enlarged segment of the density plot domain. The Y-axis of the domain is magnitudes per arc second squared, binned by .05 magnitudes per arc second squared. The X-axis of the domain is time-since-1500-hours, binned by 5 minutes of time. The algorithm (Figure B4) uses an empirically-derived spatial operator, 7 bins tall by 3 bins wide. The operator is taller than wide because the patterns of interest tend to be horizontal in the density plot domain.

At each point of the density plot grid (Figure B4), the algorithm sums the number of measurements under the operator and applies the sum to the central point. If the sum is smaller than a cutoff value, then the central point is considered sparse and is eliminated from consideration. We use a cutoff of 25 for most of the sites, but iteratively customize the cutoff to smaller values for sites with fewer data points to date.

This algorithm removes sparse points outside of the high-density region of data. We assume that constant clouds and fog will cause measurements to be outside the high-density region of data at each site. The possibility exists of such data overlapping the high-density data, in which case we do not eliminate it. See additional comments and compare Figures C4 and C5 in Appendix C.

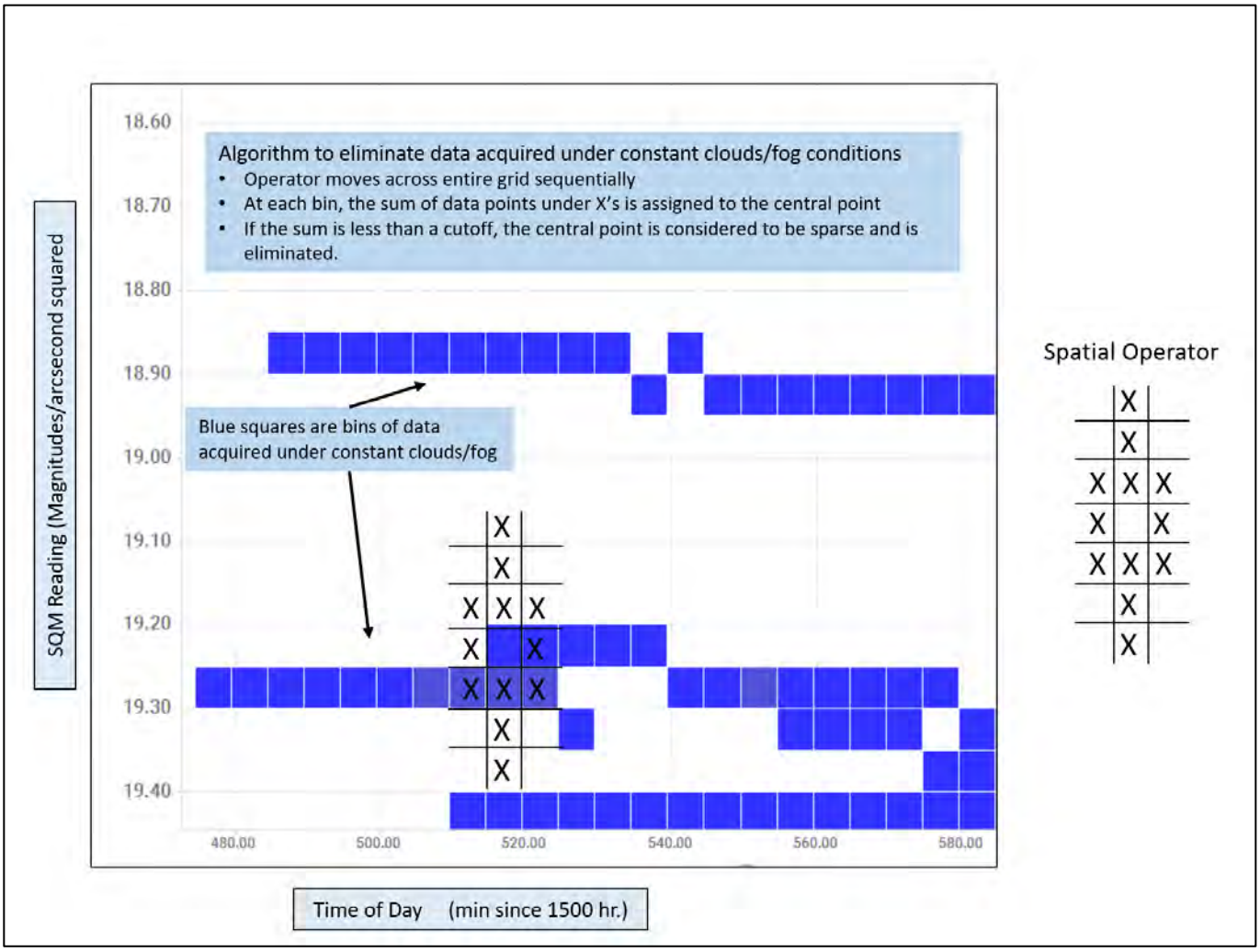

Figure B4. Algorithm to eliminate data acquired under constant clouds/fog conditions. The operator moves across the entire grid sequentially. At each bin of the grid, the sum of data points under the X's is assigned to the central point. If the sum is less than a cutoff, the central point is considered to be sparse and is eliminated. See Appendix C, Figures C4 and C5, for the results of applying this filter.

Appendix C - Skyglow Signature of a Site

Skyglow data acquired over months and years provides a cumulative signature, which is characteristic of the amount of light pollution at each measurement site. We summarize two main features of that signature: (1) the brightness of the clear night sky and (2) the brightness of the night sky during cloudy conditions.

Measurements of the darkness of the **clear night sky** are useful to satisfy Dark Sky Place criteria and for comparison between sites without the complication of variable cloud cover. The darkness of the night sky **during cloudy conditions** provides an enhanced measure of the environmental impact of light pollution. At light polluted sites, the clouds are lit up from below and cast much more light downward into the environment, compared to sites without light pollution -- where clouds overhead appear black and compound the natural darkness.

Figure C1 shows the SQM measurements acquired at the Awbrey Butte neighborhood of the City of Bend, from July 2019 to September 2020. The vertical axis is the SQM brightness reading. The horizontal axis is local time of the night, in minutes since 3PM of the previous daytime. Data are from all of the nights, whether clear nights or cloudy nights, and only if the Sun is at least 18 degrees below the horizon, and the Moon is at least 10 degrees below the horizon.

Figure C1 is a density plot. The color of each small square in the plot is proportional to the percentage of measurements that fall into that position. Each small square includes one or more of the SQM measurements. The colors are scaled independently for each site. See Puschnig and others (2013) for another example of a density plot of SQM data.

The red and yellow trend in the plot across the darkest sky measurements at the bottom of the plot identifies the very frequent measurements over the time period. We call that red trend the “Most Common Clear Dark Sky Night” or MCC for short. The large sparse, scattered area of blue and yellow color above the red trend represents SQM measurements taken under cloudy skies at night. Both features of the density plot, the dense red trend and the sparse blue pattern above, and other subtleties present, represent the skyglow signature of the site.

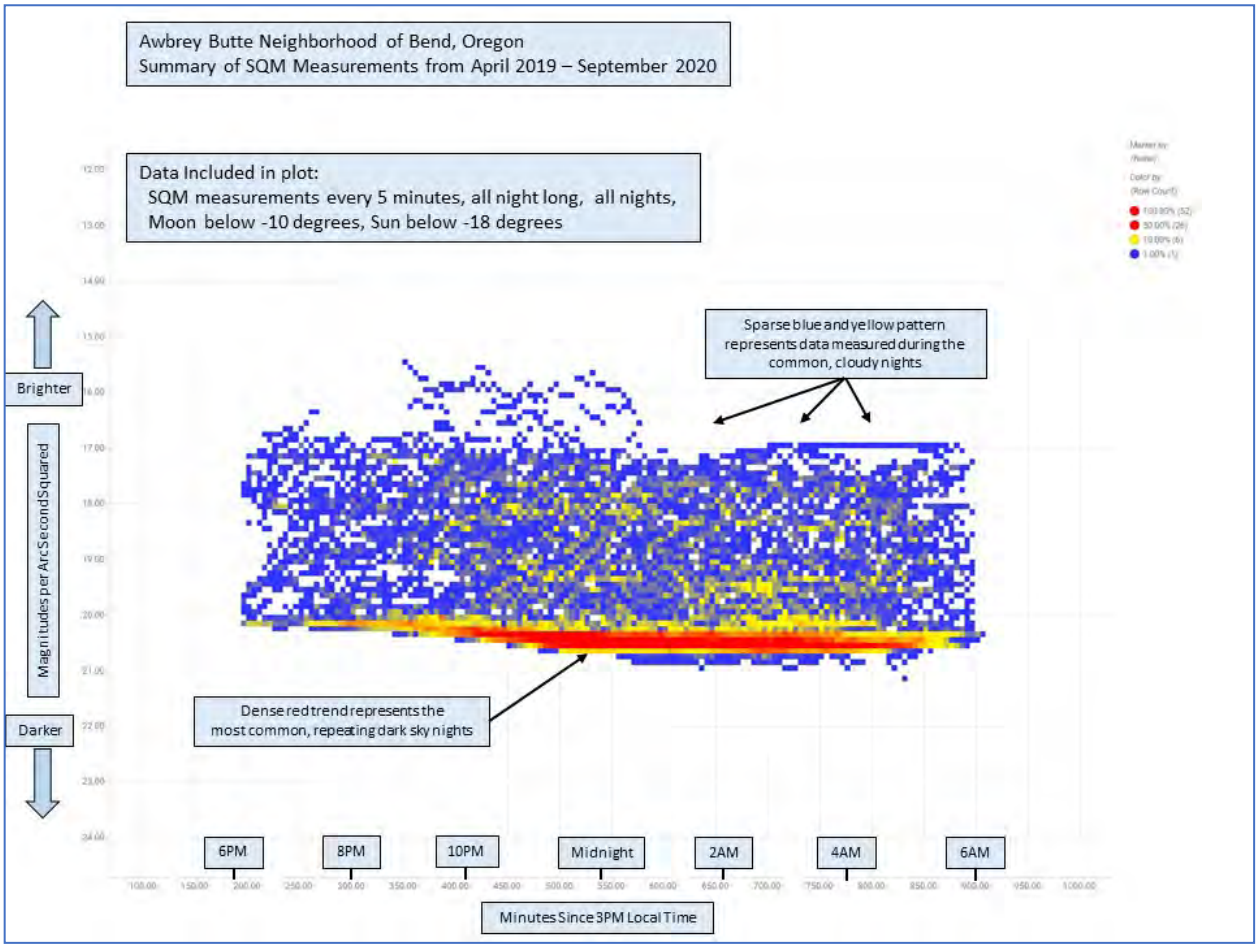

Figure C1. *Density plot of SQM data from the Awbrey Butte Neighborhood site. Each small square represents the percentage of 5-minute SQM samples that fall into that zone. We take the dense red trend across the bottom of the data as the Most Common Clear Dark Sky Nights (MCC). The sparse blue and yellow pattern at brighter skyglow values are due to measurements under cloudy skies at night.*

Figure C2 shows an SQM signature density plot with an entirely different character – from the Pine Mountain Observatory (PMO) site which has very little light pollution overhead. The red and yellow streak of MCC at this site is positioned between 21 and 22 mags/arcsecond^2, and is about 4x darker than the Awbrey Butte site (20 – 21 mags/arcsecond^2). Moreover, the sparse blue pattern of clouds is entirely below the red streak, instead of above it.

This signature is characteristic of dark sky sites -- there is very little light pollution coming from the ground at the PMO site, so any clouds overhead are not lit up from below – instead, the clouds appear black and block the starlight. Because the clouds appear black, the data from cloudy nights plot below the clear night MCC red streak on the plot.

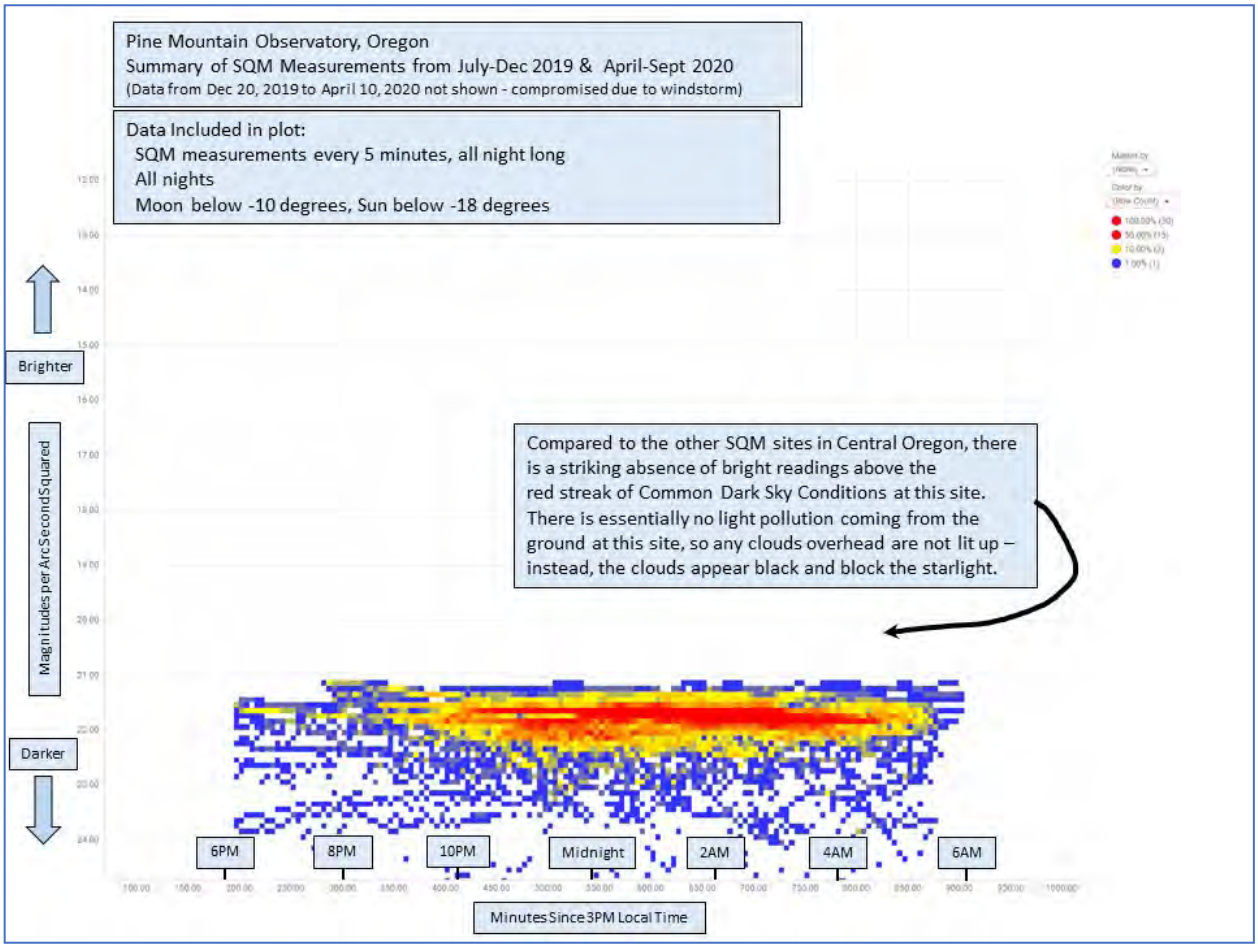

Figure C2. *Density plot of SQM data from the Pine Mountain Observatory site. Note the absence of bright readings above the red and yellow streak of MCC at this site. See explanation in the figure and in the text.*

Figure C3 summarizes the density plots for all of the SQM sites in the Oregon SQM Network which have been recording up to November 2022. The plots are arranged from top left to bottom right, from most light-polluted to least light-polluted. Some sites have been recording for shorter periods, so they show more sparse density plots. Appendix A summarizes the data available over time for each site.

Notice that the red streak in each successive plot of Figure C3 falls lower, toward darker readings. In that progressions, there is a trend for cloudy conditions – the sparse blue points – to fall above the red streak for the light-polluted sites, and to fall below the red streak for the darker sky sites. Anomalies are present in that pattern, which require further work to understand. For example, (a) the Stub Stewart and Mt Pisgah sites show a pattern of sparse darker readings below the red streak, and (b) the Cottonwood Canyon site shows readings above the red streak.

In the first years of this project, we considered that the characteristic red and yellow streak of our initial sites in Oregon, which were in the relatively dry, high desert environment of central and eastern Oregon, might not appear in other climatic areas of Oregon. However, we note that the two sites in Portland, and the Mt Pisgah, Junction City and Lowell sites in the Willamette Valley, the Bandon site on the Oregon coast and the Oregon Caves site in the southwest mountains, which all have a non-arid, Mediterranean climate, also show the high-density pattern.

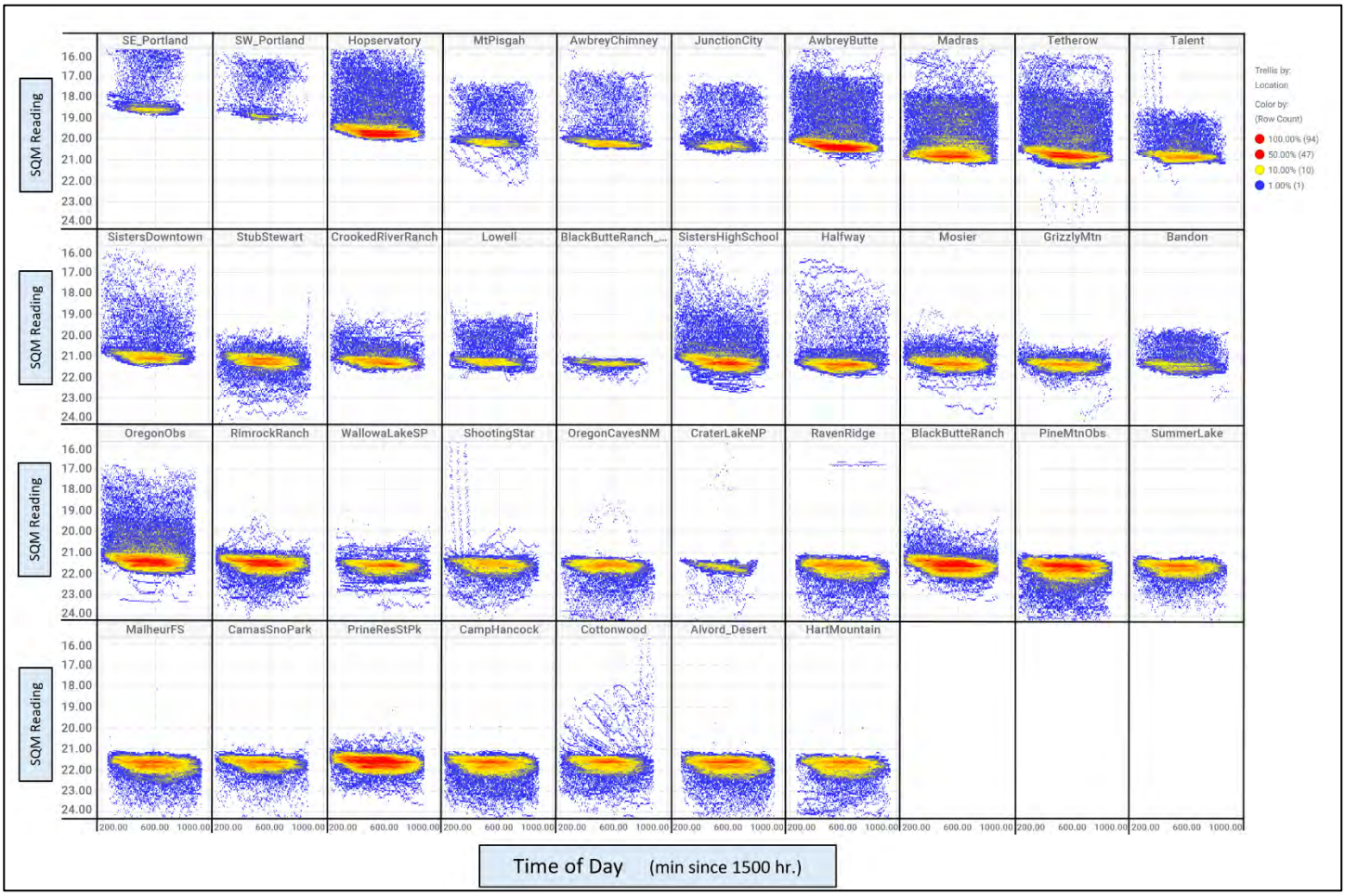

Figure C3. *Density plots of SQM data from the 37 sites with data available to November 2022.*

Figure C4 shows the data for all of the sites after "jaggy" data – cloudy data – removal by the algorithm described in Appendix B and after deleting data higher than 22.0 magnitudes/arc second squared. Note that the algorithm failed to remove cloudy data from periods of uniform overcast or fog – there are smooth blue lines above and below the high-density points at many of the sites in Figure C4, especially for the more light-polluted sites near the top of the Figure.

In previous editions of this report, we manually deleted those points above and below the high-density red/yellow zones at each site. In this Edition #7 of the report series, we employed an automatic spatial filter, described in Appendix B, to remove the sparse points which passed through the cloud filter. The cleaned, cloud-free data are shown in Figure C5.

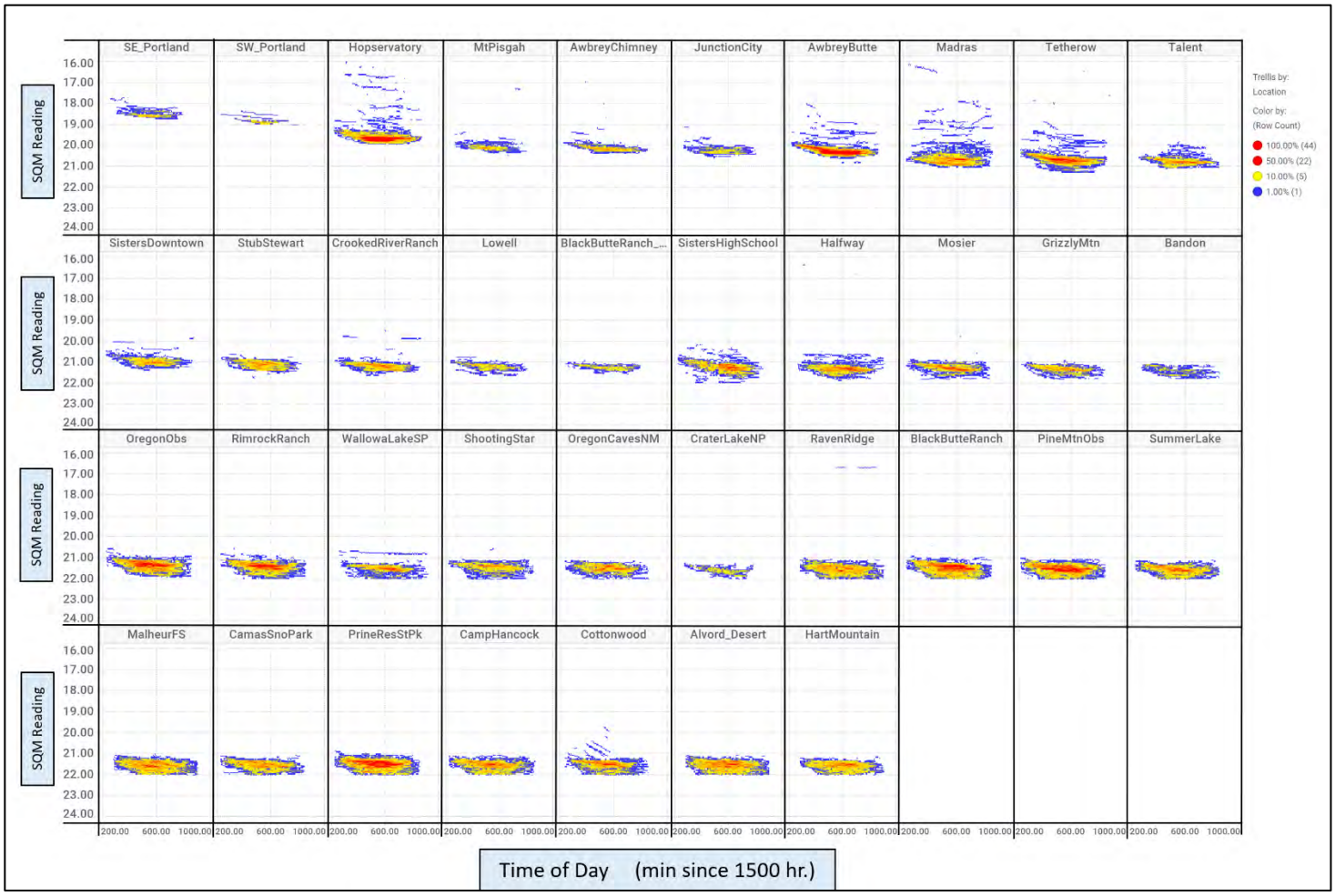

Figure C4. *Density plots of SQM data from all 37 sites after application of the cloud removal algorithm. The algorithm fails to remove cloud cover that is consistent over time – the blue points above and below the high-density zones.*

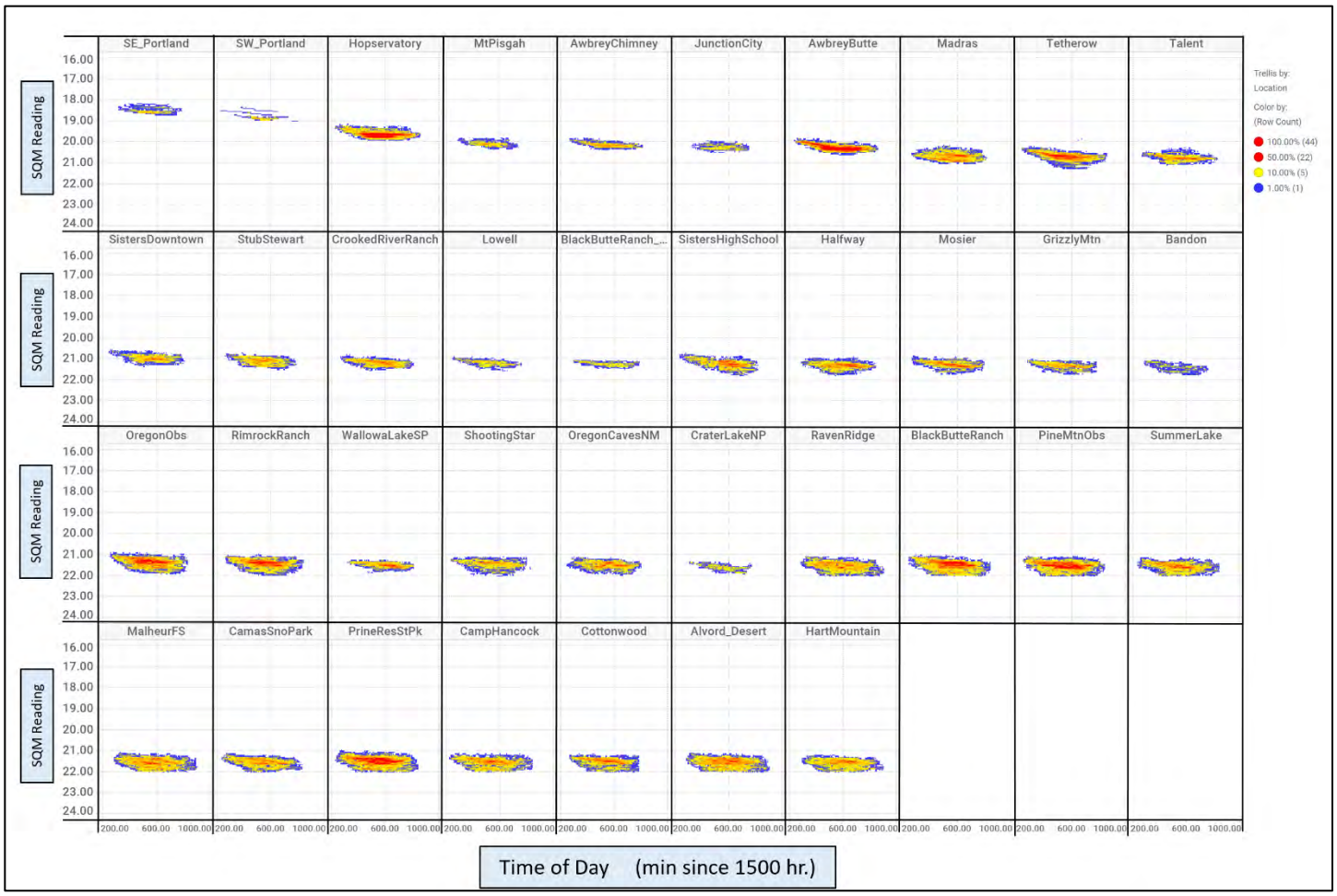

Figure C5. *Density plots of SQM data from all 37 sites after automatic cleaning of the smoothly-varying cloudy data. Because the SW_Portland site has so little data to date, we did not apply the cleaning to that site's data.*

Note that for some of the darker sites, for example, the Alvord Desert site, the density plots have a flat base in Figure C5, indicating that our data cutoff above 22.0 magnitudes/arc second squared is not appropriate. In other words, some clear nights at the darker sites record values in excess of 22.0. We plan to consider that issue in the next edition of this report series.

Appendix D – Darkening over time with aging of SQMs

Recent research (Puschnig and others, 2020) documents that as the SQM device and weather proof enclosure age, that there is a darkening effect on measured data, in their case an average of about .04 mags/arcsecond^2 per year. This aging will darken the skyglow measurements over time.

Unihedron (personal communication, 2022) notes that two issues can be involved: 1) development of a translucent film on the blue glass IR filter, which seems related to moisture and 2) yellowing of the plastic case of the semiconductor sensor over time.

Also, Unihedron (personal communication, 2022) notes that SQMs manufactured before late 2013 used a plastic rectangular lens plate on the meter (not the weatherproof housing) that could yellow with age. SQMs manufactured after late 2013 use a glass plate which is not subject to aging. The SQMs used in our project date from 2019 onward.

To understand this phenomenon better, we obtained two new SQMs and installed them to run in parallel to two SQMs, which had been running for about three years. We installed one at a light polluted site (Awbrey Butte) and the other at a dark sky site (Prineville Reservoir State Park). Both ran in parallel for several weeks.

Figure D1. New and old SQMs running in parallel at two different sites, with the goal of assessing aging phenomena of the SQM unit. Awbrey Butte site on the left, Prineville Reservoir State Park on the right.

Figure D2 shows the results of this experiment.

Figure D2. Box plot comparing data recorded by the two sets of parallel-running SQMs. In both cases, the older SQMs recorded slightly darker skies on average.

Table D1 summarizes the statistics of this experiment.

SQM	SQM ID	Install Date	End of Test Date	SQM Exposure (days)	SQM Exposure (Years)	Difference of Exposure (years)	Count	Average	Median	Msas Difference of Average	Msas difference per Exposure Year
Awbrey Butte Old SQM	A5055IWP	13-Mar-19	2022-02-20	1075	2.9452		819	20.404090	20.44		
Awbrey Butte New SQM	ABSCDE1J	22-Jan-22	2022-02-20	29	0.0795	2.8658	814	20.351351	20.38	0.052739	0.018403188
Prineville Old SQM	AK06E3YZ	30-Jun-19	12-Feb-22	958	2.6247		366	21.766366	21.81		
Prineville New SQM	ABSCDQTV	30-Jan-22	12-Feb-22	13	0.0356	2.5890	373	21.715764	21.76	0.050602	0.019544688
										Mean	**0.018973938**

Table D1. The older SQM in each case recorded an average value .05 magnitudes per arc second squared darker than the new SQM in parallel. This amounts on average to .019 per year of exposure.

Distributed over the time range of exposure difference, we estimate a darkening of about .019 magnitudes per arc second squared per year of exposure. Accordingly, we subtract values proportional to this assumed aging effect progressively from our data, based on the serial exposure time of each data point of each SQM in our network.

Puschnig and others 2020 had three SQM sites at widely different locations, ranging from about 48 to 60 degrees North latitude. They noted aging proportional to the latitude of exposure, with less darkening at higher latitudes, related to the amount of sunlight exposure at each site. Figure D3 plots the Puschnig and others aging data versus latitude. Given that data, the Oregon SQMs at about 44 degrees north latitude should have a darkening at about .06. Instead, we find a darkening of less than .02.

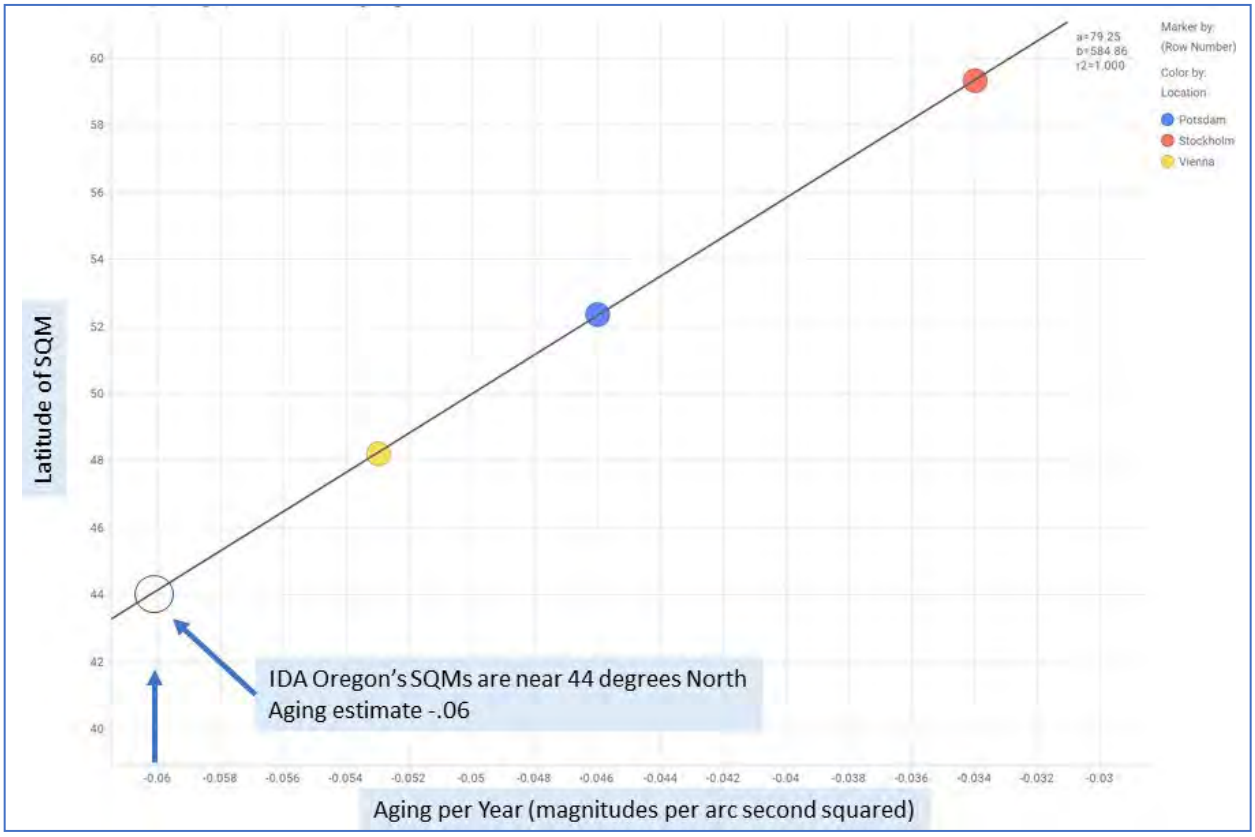

Figure D3. Data on aging of SQMs from Puschnig and others, 2020. There is a strong relationship of latitude on the rate of aging. Based on the three SQMs in their data set (colored dots) the Oregon SQMs should have an aging rate of about .06 per year. Our current experimental data suggest a smaller aging rate of slightly less than .02 per year.

Our parallel SQM experiment only involved two pairs of SQMs. Additional experimental data along with re-calibration of older SQMs should shed additional light on this. It could be that our observations of older SQMs recording darker values are not caused by darkening, but by some other calibration issue. We currently attribute the difference to aging of the older SQM. We have implemented the approximately .02 per year aging adjustment in our data processing in this report.

Appendix E - Adjustment for Brightness of the Milky Way

When the Milky Way is overhead, the SQM will record a brighter night sky. Instead of eliminating those measurements as we did for Goal #1 (measurements in support of Dark Sky Places), we instead keep those data and normalize out that effect in processing toward Goal #2. By this method, we minimize the seasonal nature of the Milky Way pattern, and also avoid loss of data.

In the following, "galactic latitude" refers to the angle between the zenith at an SQM site and the center of the highest arc of the Milky Way in the night sky. A galactic latitude of zero signifies that the SQM is pointed directly into the Milky Way overhead. "Galactic longitude" measures the radial angle along the Milky Way.

The left side of Figure E1 shows a plot of the SQM measurements (after conversion to the linear candelas scale) from the clear sky data on the vertical axis versus the galactic latitude of the SQM pointing direction. These data are for two dark sky sites, Black Butte Ranch and Prineville Reservoir State Park. The data is colored by season of the year.

The black line through the data on the left side of Figure E1 is a 4^{th} order polynomial fit to the data, which shows a broad maximum of SQM-measured brightness near galactic latitudes around zero. We measured a brighter sky when the Milky Way was overhead.

The polynomial fit allows an adjustment for galactic latitude, which is shown on the right side of Figure E1. After adjustment, the polynomial fit to the data is now horizontal. We adjusted the data to a galactic latitude of 30 degrees, which is midway between the high and low of the original data across the range of galactic latitude. The most dramatic effect of this adjustment is that the measurements during the spring (green points) shift upward (brighter), while measurements during the autumn (red points) shift downward (darker).

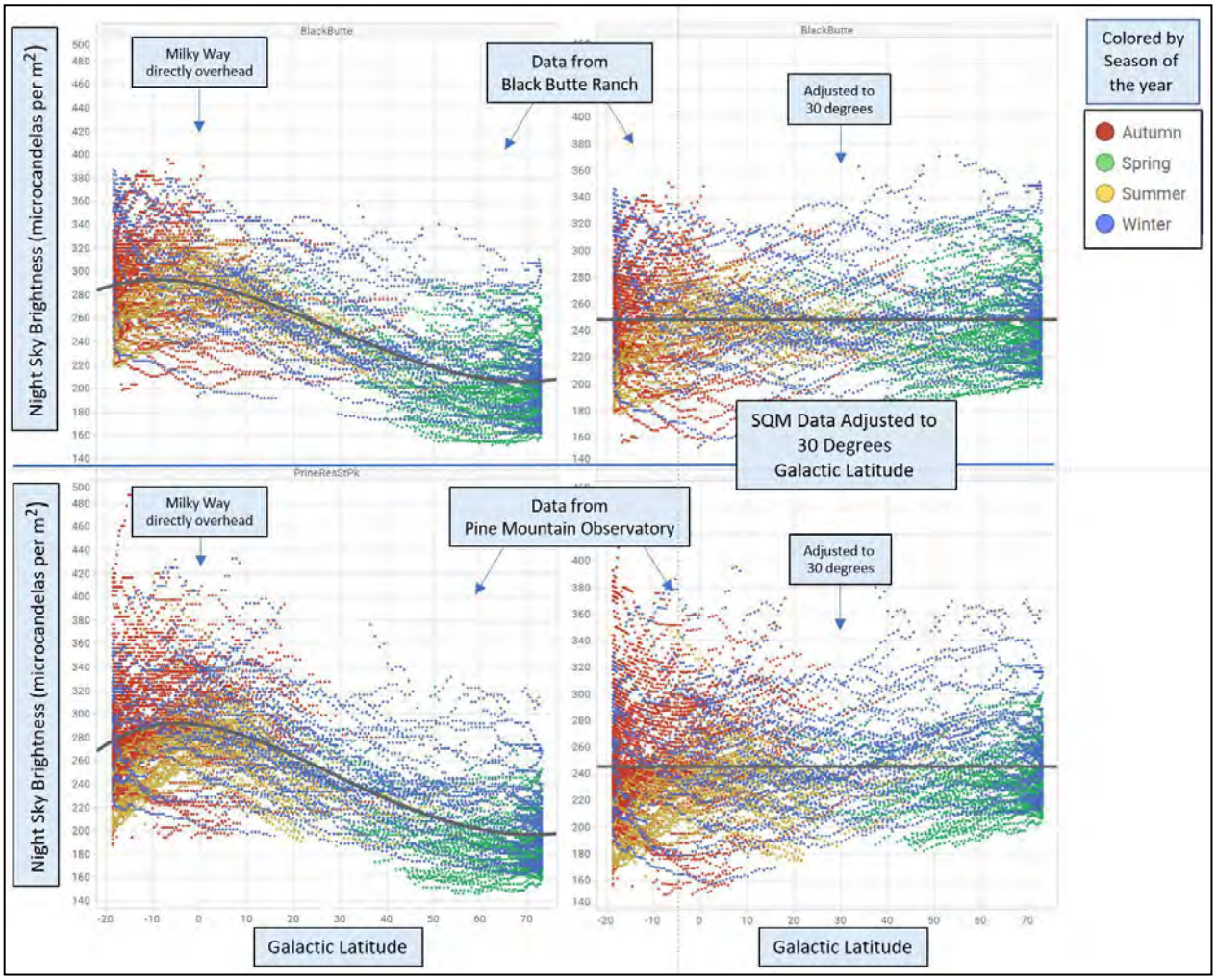

*Figure E1. Adjustment of SQM data for the position of the Milky Way – galactic latitude – in the sky for two dark sky sites -- the Black Butte Ranch and Prineville Reservoir State Park sites. The left part shows the original data, the right part shows the data after adjustment for galactic latitude. The black line through the data in each case is a 4th order polynomial fit. The points are colored by the season of the year. The adjustment **lowers** (makes darker) the Autumn data, while **raising** (makes brighter) the Spring data. Winter is defined as Dec-Jan- Feb, Spring as Mar-Apr-May, Summer as Jun-Jul-Aug and Autumn as Sep-Oct-Nov.*

Because the Milky Way varies in brightness along its arc, we explored the potential of reducing the seasonal variation in the SQM data by adjusting it for galactic longitude. We apply a linear regression fit of the galactic latitude adjusted data to galactic longitude and adjust the result to 120 degrees galactic longitude. Figure E2 shows the galactic longitude adjustment for the same two sites as shown in Figure E1. The adjustment for galactic longitude slightly lowers the autumn and winter data, and slightly raises the spring and summer data.

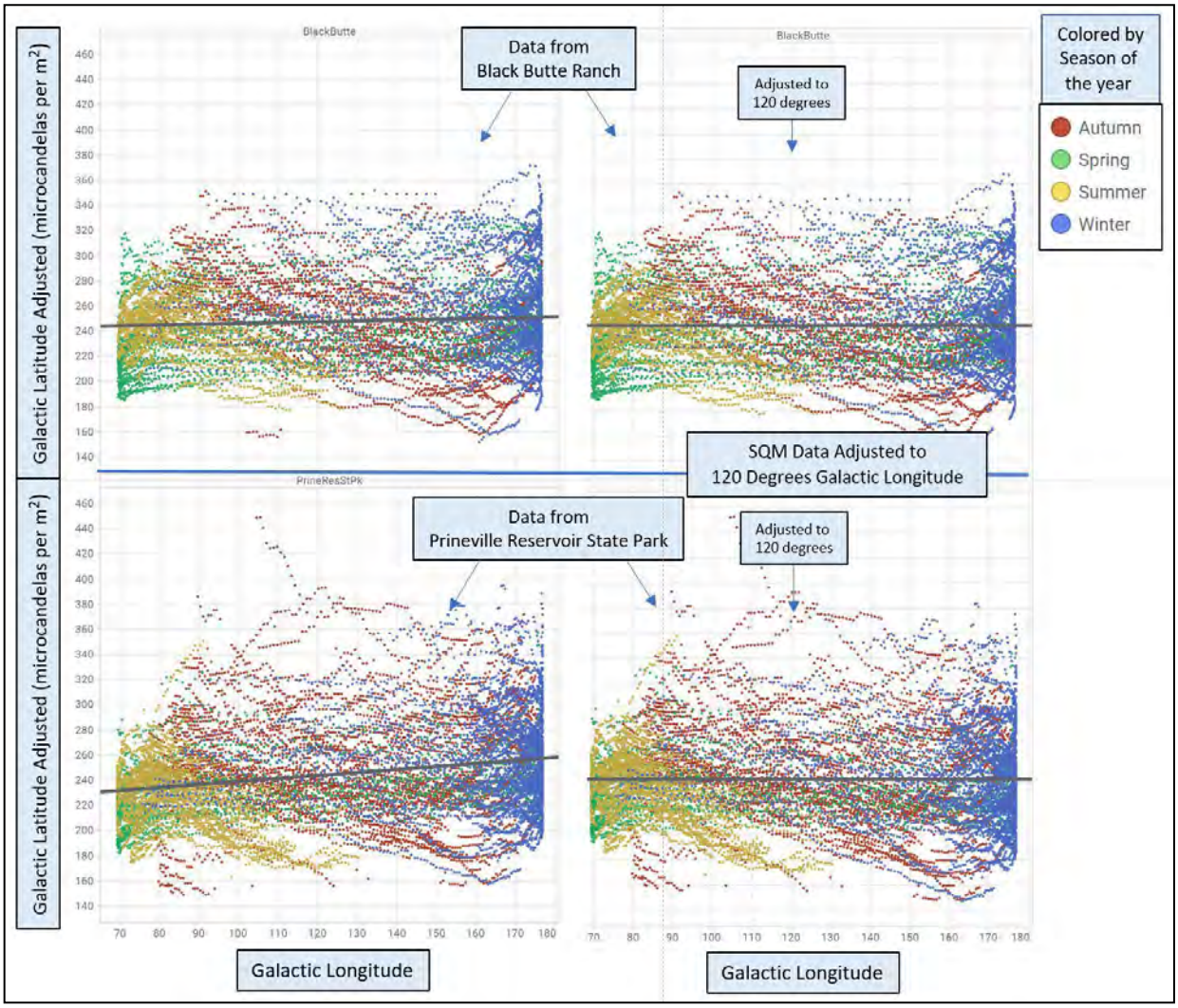

Figure E2. Adjustment of SQM data for the position of the Milky Way – galactic longitude – in the sky for two dark sky sites -- the Black Butte Ranch and Prineville Reservoir State Park sites. The left part shows the data after adjustment for galactic latitude, while the right part shows the data after subsequent adjustment for galactic longitude. The black line through the data in each case is a linear regression fit. The points are colored by the season of the year. The adjustment generally ***raises*** *(makes brighter) the spring and summer data, while* ***lowering*** *(makes darker) the autumn and winter data.*

Appendix F - Adjust data to 1AM local standard time to minimize the influence of time of night

As the night progresses, our skyglow measurements show that the night sky grows progressively darker, especially for light polluted sites. Because we have already adjusted the data for the position of the Milky Way, we expect that the darkening is due to outdoor lights being turned off and fewer car headlights about, as most people are sleeping instead of driving around. To minimize this effect, we statistically adjust the data at each site to 1AM local standard time. As with the adjustments for position of the Milky Way, this adjustment to 1AM is an effort to minimize variation that might otherwise obscure or bias any long-term trends in the skyglow data.

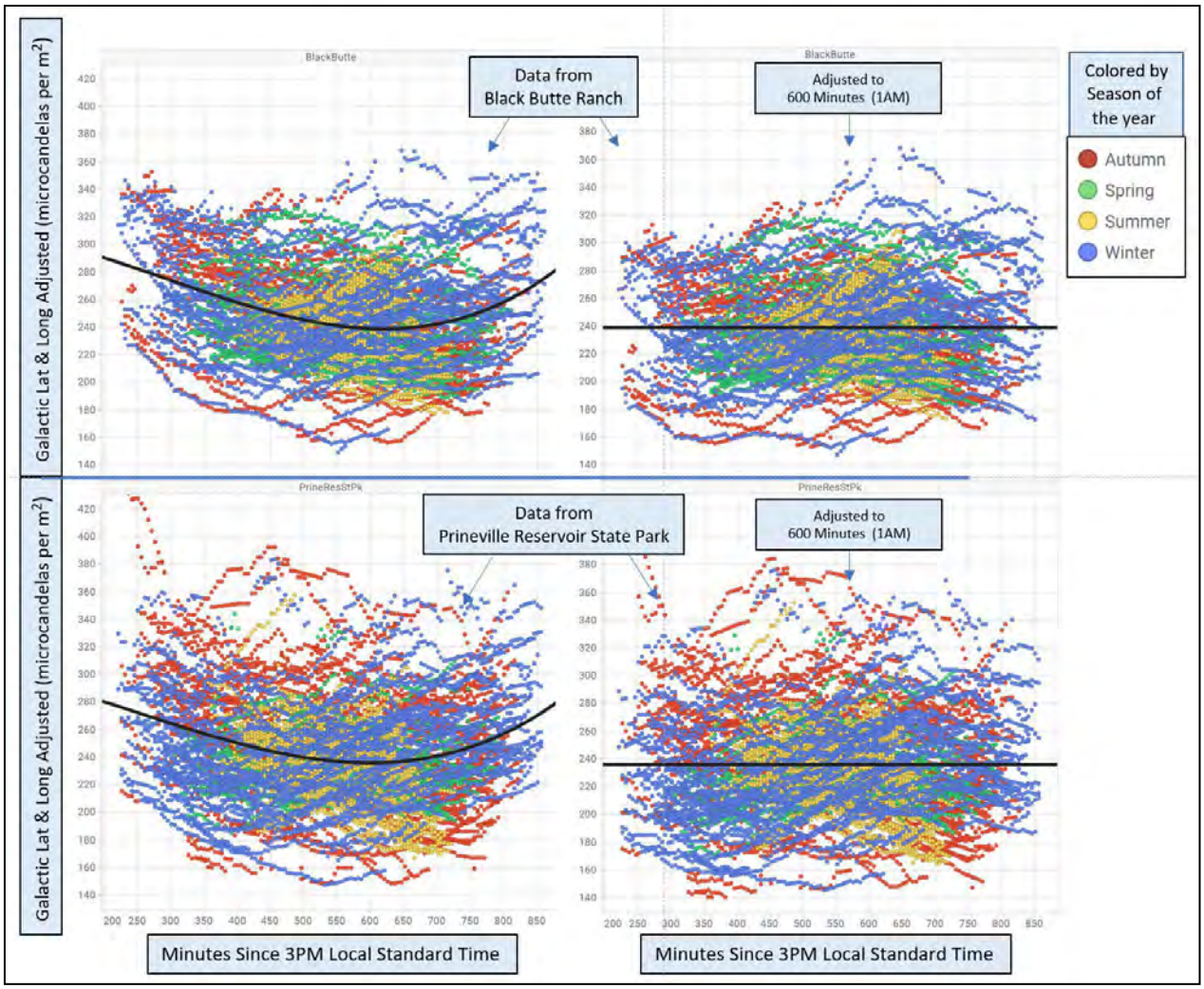

Figure F1. Adjustment of data to 1AM local time at two dark sky sites, Black Butte Ranch and Prineville Reservoir State Park. The data have already been adjusted for galactic latitude and galactic longitude. This correction uses a 3rd order polynomial fit to adjust data to 1AM local time and seeks to minimize variation across the night. The left side of images are before the local time adjustment, the right half afterwards. 1AM local time is at 600-minutes-since-3PM local standard time.

Previously, in Edition #5 of this report series, we applied a different "time of night" adjustment – namely we only included data from 10:30PM local standard time to 4:30AM local standard time, which is the time range of the summer nights in our latitude range. That filtering was an effort to overcome the difference in time of darkness during winter versus summer nights. In our northern hemisphere winter, we experience much longer evening hours of darkness, versus the summer months. That is, darkness in the winter begins much earlier in the evening. As a final level of

adjustment to the skyglow data, we experimentally applied that filtering to the data which had already been adjusted to 1AM.

The left side of Figure F2 shows data for the light-polluted Hopservatory site, prior to adjustment for the position of the Milky Way and time of night. At the beginning of the evening in the autumn and winter (red and blue dots), the skyglow is quite bright, we expect due to most outdoor lights being on and people driving about with car headlights lights on. As the evening hours pass, the light pollution and skyglow decrease. The right side of Figure F2 shows the same data after adjustment for the position of the Milky Way and time of night (1AM). A linear regression line through the data is horizontal, so we conclude that filtering out the early evening and late morning data to match the summer time hours (yellow dots) is likely inappropriate and counter-productive, given the loss of associated data points. We instead employ the adjustment to 1AM, without discarding the early evening and morning data.

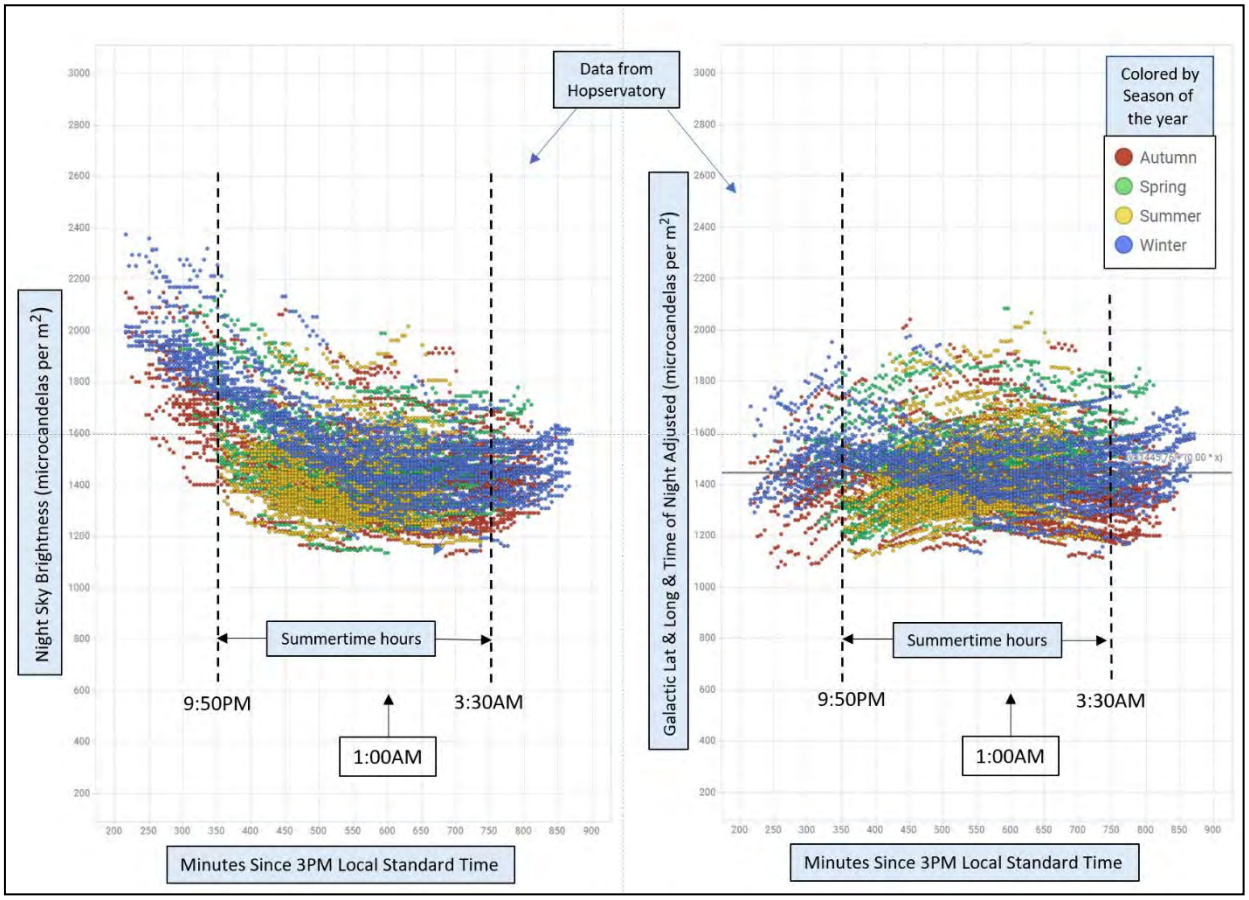

Figure F1. Clear sky data acquired at the Hopservatory, a light polluted site. There is a pronounced drop in sky brightness from the early evening toward 1AM. Points are colored by season of the year. See text above for discussion.

Appendix G – Assessment of minimizing the seasonal pattern in the SQM data

As described in the main body of the report, we notice a strong seasonal pattern to the brightness of the clear night sky in the SQM data. This appendix summarizes our efforts to minimize the seasonal pattern in an effort to improve the definition of the long-term trend at each site. These data are from Edition 6 of this report series.

For example, Figure G1 summarizes the seasonal variation in the skyglow data for four dark sky sites, along with the progressive impact of adjustments for galactic latitude, galactic longitude and time of night. The vertical axis is the skyglow data at each site and at each level of data adjustment, averaged by month. Data points are the average at each month from each site for one and a half to three years of recording time.

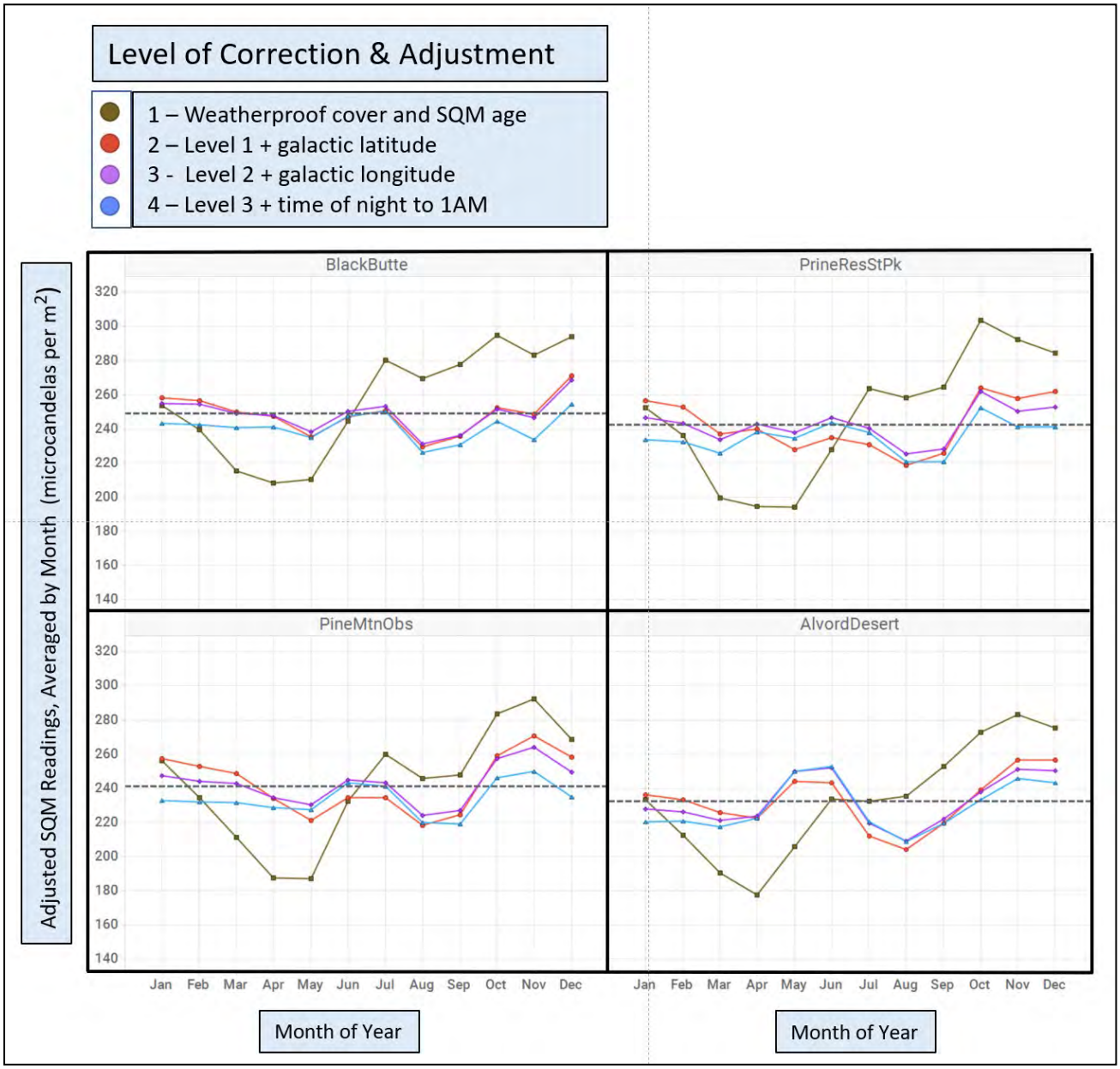

Figure G1. The average monthly SQM data for four dark sky sites after the progressive impact of adjustments for galactic latitude, galactic longitude and time of night. The dashed horizontal line marks the average value across months and adjustments for each site. See explanation in text.

Figure G1 shows that, prior to any adjustment for the galactic position and time of night, the skyglow data for these dark sky sites show a dramatic seasonal pattern of darker in springtime (March-April-May) and brighter in late autumn and early winter (Oct-Nov-Dec) – the brown dots and lines. This pattern is consistent with the fact that the portion of the Milky Way crossing the zenith in March is in Auriga, which is significantly darker than the portion of the Milky Way crossing zenith in November in much brighter Cygnus. After the adjustment for galactic latitude (the red dots and lines in Figure G1), the seasonal pattern is greatly reduced.

The impact of including the galactic longitude adjustment is lesser (purple dots and lines). The impact on the seasonal pattern of including the time adjustment to 1AM is not clear (blue dots and lines), but overall tends to be positive as shown in Table G1 below.

Figure G2 summarizes the seasonal variation in the skyglow data for four light-polluted sites, along with the progressive impact of adjustments for galactic latitude, galactic longitude and time of night. As we might expect, the adjustment for galactic position has little impact on the seasonal pattern of the light-polluted sites – after all, the Milky Way is largely invisible due to the light pollution at those locations.

The Tetherow site has some expression of the darker Mar-Apr-May period and brighter Oct-Nov-Dec characteristic of the dark sky sites (Figure G1) – Tetherow has the darkest skies of these four sites (See Figure 5 in the main report).

Moreover, the darkest night sky for the other three light-polluted sites in Figure G2 is not in the springtime, but occurs during the summer – May-Jun-July.

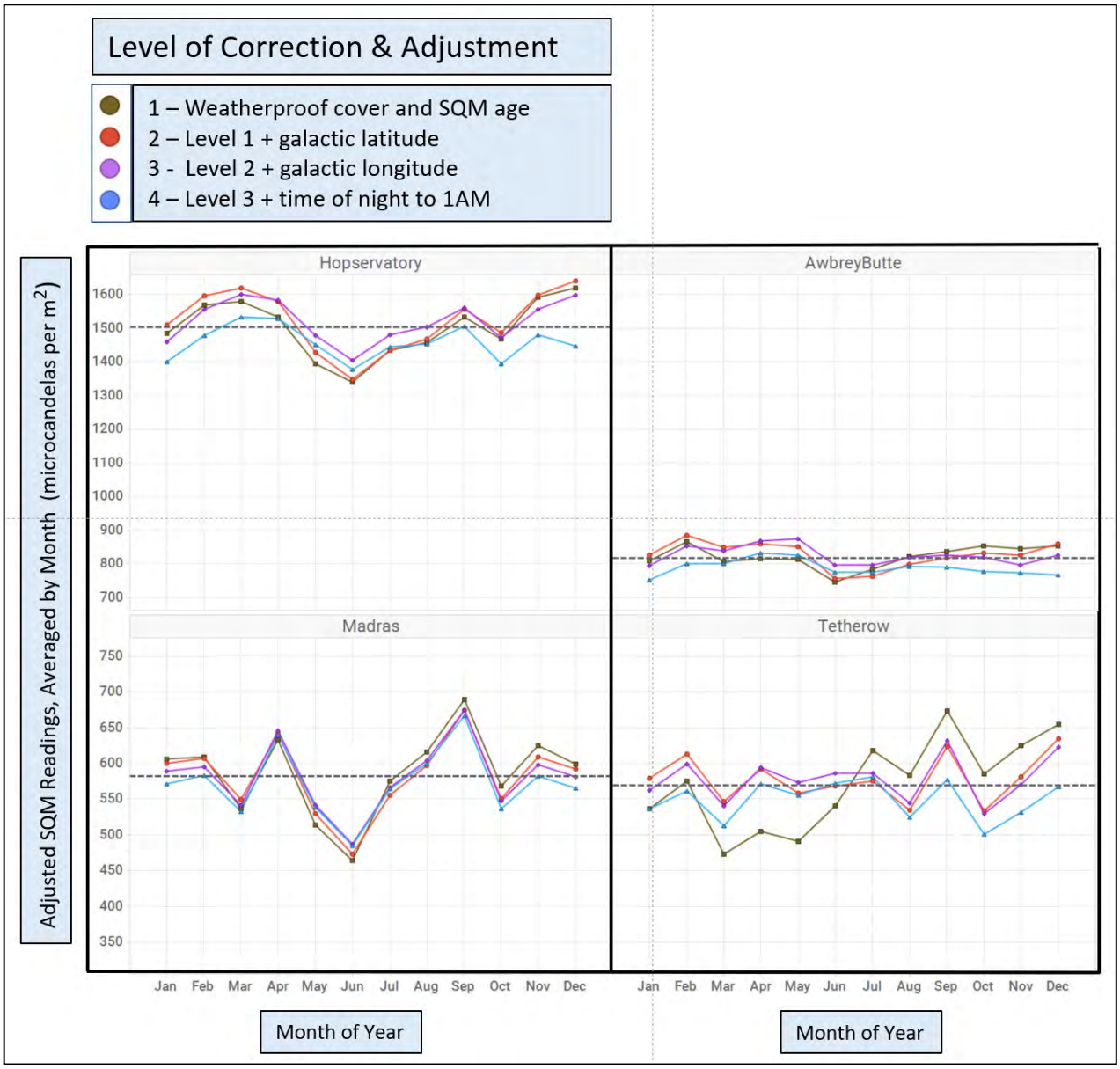

Figure G2. The seasonal variation for four light-polluted sites after the progressive impact of adjustments for galactic latitude, galactic longitude and time of night. The dashed horizontal line marks the average value across months and adjustments for each site. See explanation in text.

For completeness, Figure G3 summarizes the seasonal variation in the skyglow data for all of the 15 long-term sites, along with the progressive impact of the adjustments. The sites with the strongest light pollution are in the upper left and progress to lesser light pollution to the lower right.

As described above, the Level 1 to Level 4 adjustments reduce the season variation for the dark sky sites. However, Figure G3 shows that a noticeable seasonal pattern remains in the data after these adjustments, whether at dark sky or light polluted sites.

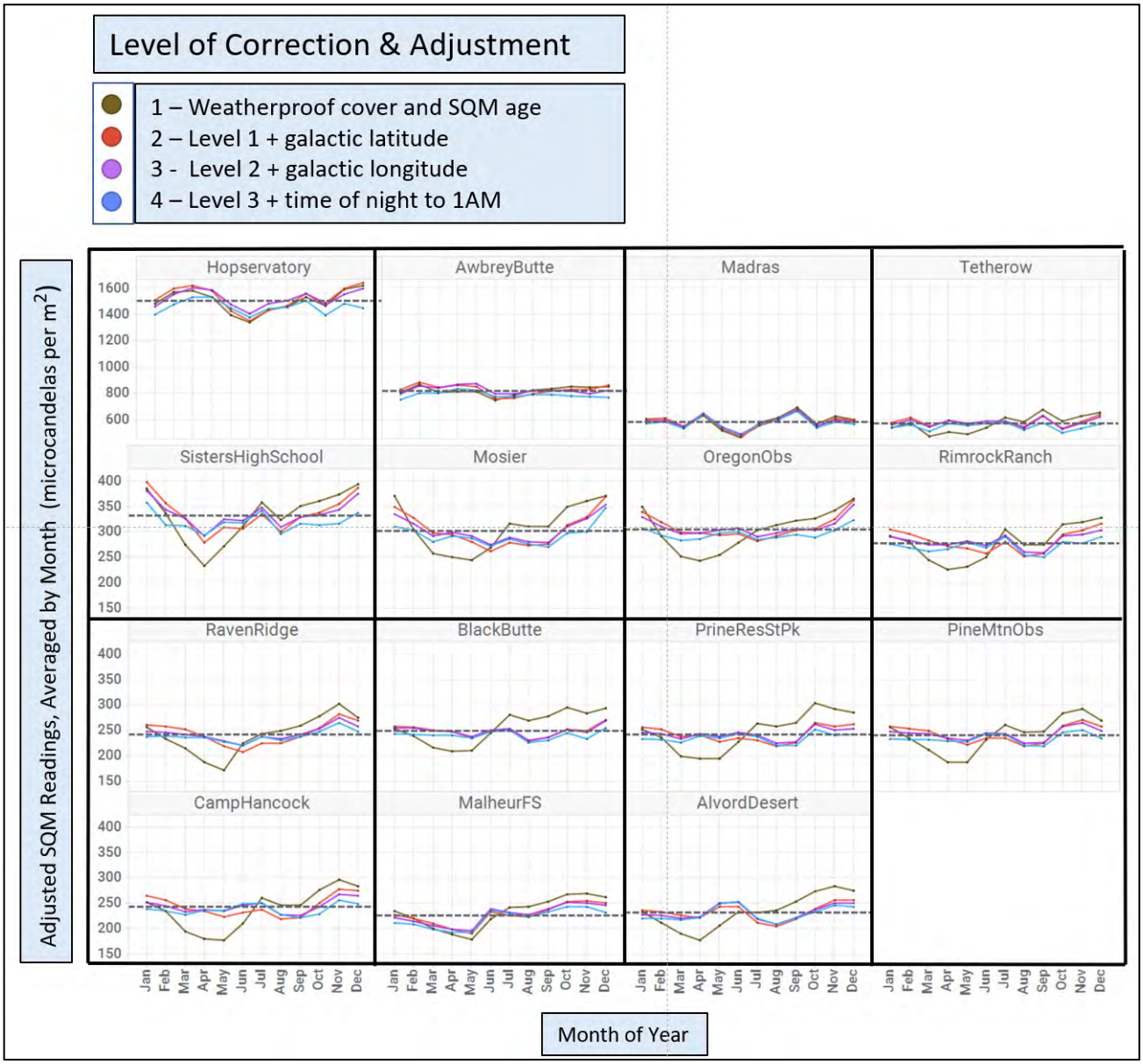

Figure G3. The seasonal variation for all 15 long term sites after the progressive impact of adjustments for galactic latitude, galactic longitude and time of night. The dashed horizontal line marks the average value across months and adjustments for each site. See explanation in text. Data are from Edition #6 of this report series.

Table G1 summarizes numerically the data shown graphically in Figures G1, G2 and G3. The values in Table G1 are the sums of the absolute value of the vertical deviations (i.e., along the sky brightness axis) from average of all values at each site. In other words, the data in Table G1 represents the area between the grand mean (dashed line in Figures G1, G2 and G3) and each curve.

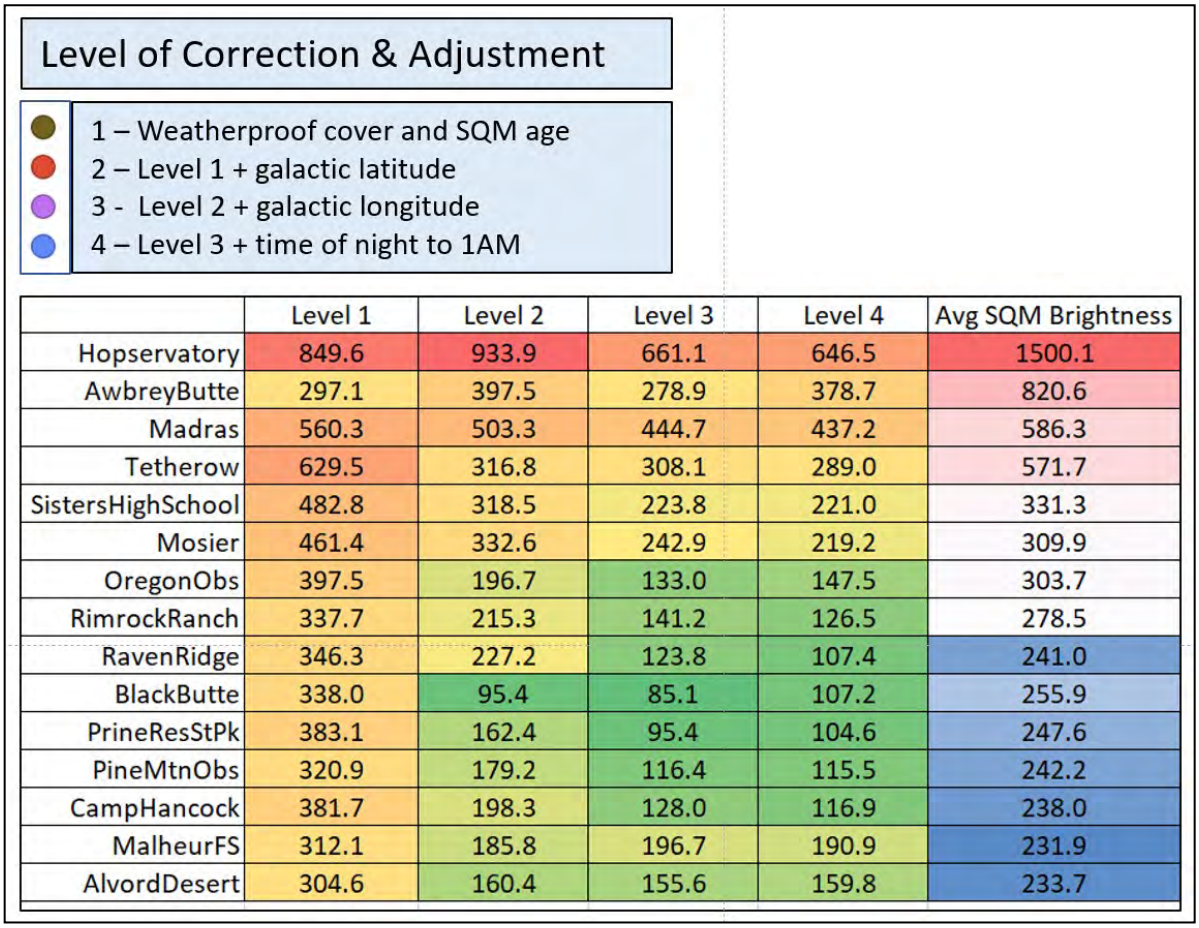

	Level 1	Level 2	Level 3	Level 4	Avg SQM Brightness
Hopservatory	849.6	933.9	661.1	646.5	1500.1
AwbreyButte	297.1	397.5	278.9	378.7	820.6
Madras	560.3	503.3	444.7	437.2	586.3
Tetherow	629.5	316.8	308.1	289.0	571.7
SistersHighSchool	482.8	318.5	223.8	221.0	331.3
Mosier	461.4	332.6	242.9	219.2	309.9
OregonObs	397.5	196.7	133.0	147.5	303.7
RimrockRanch	337.7	215.3	141.2	126.5	278.5
RavenRidge	346.3	227.2	123.8	107.4	241.0
BlackButte	338.0	95.4	85.1	107.2	255.9
PrineResStPk	383.1	162.4	95.4	104.6	247.6
PineMtnObs	320.9	179.2	116.4	115.5	242.2
CampHancock	381.7	198.3	128.0	116.9	238.0
MalheurFS	312.1	185.8	196.7	190.9	231.9
AlvordDesert	304.6	160.4	155.6	159.8	233.7

Table G1. Four different levels of increasing adjustment to minimize seasonal trends. See text for explanation.

Table G1 lists the numeric data from the graphical display in Figure G3. Column 1 lists the long term SQM site locations, in the order of increasing night sky darkness from the Goal #1 process (see Figure 5 or Table 1 of main report).

Columns 2 – 5 of Table G1 show the sums of absolute value of deviations from the mean at the four levels of adjustment. Smaller values are better. The values are color coded according to size. Red color represents the strongest deviation from its grand mean (Hopservatory site). Progressive color scale through orange, yellow and green show lesser deviations. A change of color away from red (i.e., toward green) across the columns indicates a lessening of the seasonal pattern due to the progressive adjustments. The last column on the right summarizes the average clear night sky brightness of the sites, color coded from red (light polluted) to blue (dark sky sites).

Table G2 shows the same data as Table G1, except it shows percentages of the value versus Level 1 for each SQM site, instead of the absolute values.

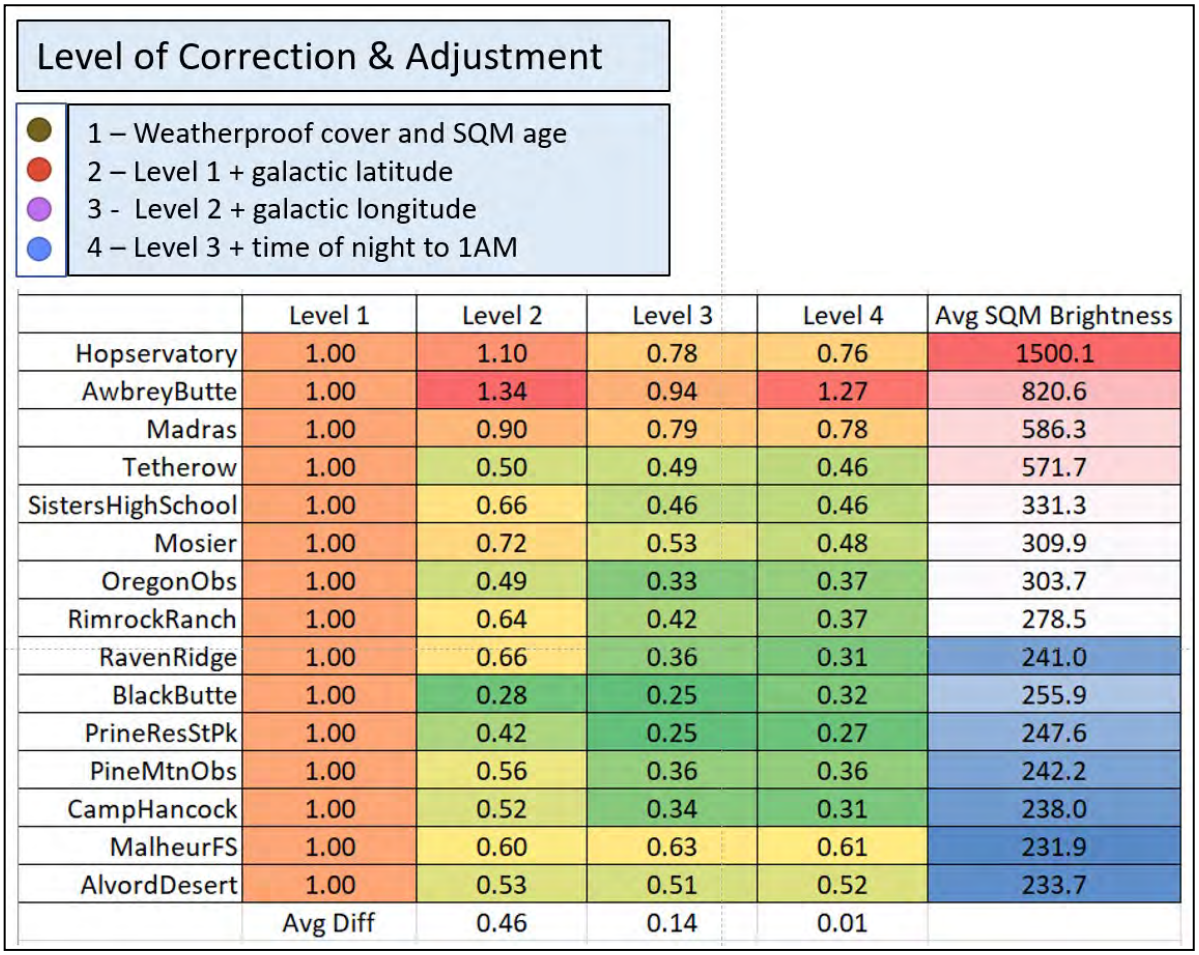

	Level 1	Level 2	Level 3	Level 4	Avg SQM Brightness
Hopservatory	1.00	1.10	0.78	0.76	1500.1
AwbreyButte	1.00	1.34	0.94	1.27	820.6
Madras	1.00	0.90	0.79	0.78	586.3
Tetherow	1.00	0.50	0.49	0.46	571.7
SistersHighSchool	1.00	0.66	0.46	0.46	331.3
Mosier	1.00	0.72	0.53	0.48	309.9
OregonObs	1.00	0.49	0.33	0.37	303.7
RimrockRanch	1.00	0.64	0.42	0.37	278.5
RavenRidge	1.00	0.66	0.36	0.31	241.0
BlackButte	1.00	0.28	0.25	0.32	255.9
PrineResStPk	1.00	0.42	0.25	0.27	247.6
PineMtnObs	1.00	0.56	0.36	0.36	242.2
CampHancock	1.00	0.52	0.34	0.31	238.0
MalheurFS	1.00	0.60	0.63	0.61	231.9
AlvordDesert	1.00	0.53	0.51	0.52	233.7
	Avg Diff	0.46	0.14	0.01	

Table G2. Same data as Table G1, except showing percentages of the value in Level 1 for each SQM site.

In Table G2, the bottom row, “Avg Diff” is the average difference versus the previous Level of adjustment for the 10 darkest sky sites. For those darker sky sites, the adjustment for galactic latitude reduces the season variation on average down to 46% of the original variation. The galactic longitude adjustment reduces the seasonal variation another 14%. The time of night adjustment reduces the variation on average only 1%.

So, it is clear from these analyses that adjustments from Level 1 to Level 4 help to reduce the seasonal pattern. However, much seasonal pattern is still present in the data afterwards. For example, Figure G4 shows that there is significant variation in each night/week/month’s data at each site, compared to the variation over years of time.

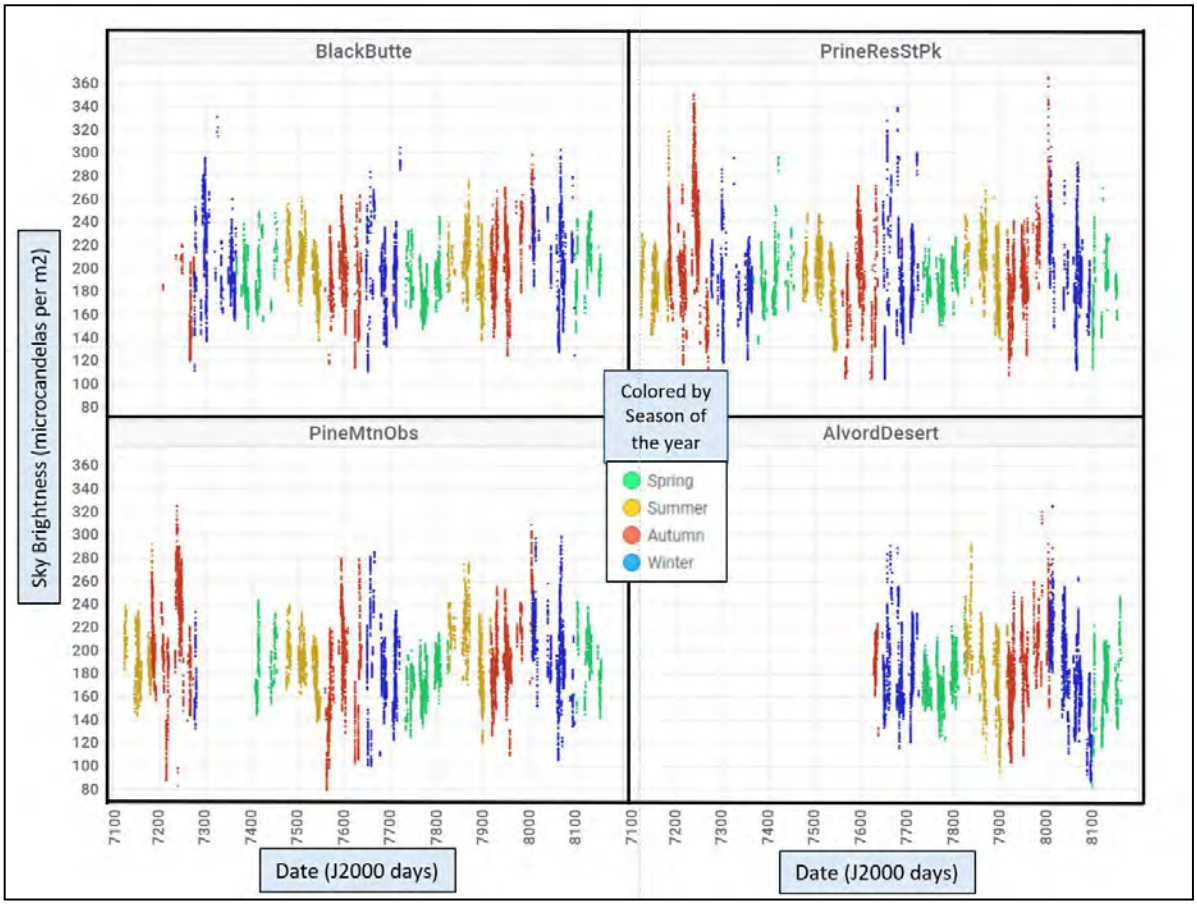

Figure G4. The clear night sky data for four dark sky sites over several years of time, after adjustment for galactic latitude, galactic longitude, time of night and solar flux. Each cluster of vertically-smeared points were acquired during a new moon period. The data points are colored by season of the year.

The plots in Figure G4 show that strong zig-zag patterns remain in the data, with consistent trends from month-to-month at each of these sites. Several phenomena may contribute to this pattern:

3) It is likely that atmospheric character, especially water content and particulate content contribute to seasonal variation at each site.

4) Grauer and Grauer, 2021 show data for increased airglow over periods of days, unrelated to solar flux, with amplitudes of brightness change on the order of the changes shown in Figure G4 – about 50 to 100 microcandelas per meter squared. While we have adjusted the current data for variations in solar flux (see Appendix H), we have not to date explored airglow effects caused by interaction of the magnetic fields of the earth and sun. One characteristic of airglow effects is their simultaneous impact over a large region. It's worth noting that the Black Butte, Prineville Reservoir and Pine Mountain sites are 30 to 40 miles apart, and that the Alvord Desert site is about 170 miles from the other 3 sites.

At present, the causes of the zig-zag pattern, typified by Figure G4, is unresolved.

Appendix H – Adjustment for airglow related to solar flux

Another factor to consider in zenith skyglow trends over long periods is variations of airglow, the light emitted from the atmosphere itself due to the impact of space weather on Earth (Grauer and others, 2019; Grauer & Grauer, 2021). Airglow is known to vary on a wide range of time scales, from rapid variation in minutes and across one night, to strong, years-long changes correlated to the 11-year solar sunspot cycle. We focus on an estimate of the long-term change of airglow.

The sun is currently rising out of a solar sunspot minimum, toward a predicted sunspot maximum in July 2025 (Figure H1). So, space weather may cause our SQM data to read brighter since our SQM project began in mid-2019, by increased airglow, independently of any changes in light pollution from the ground.

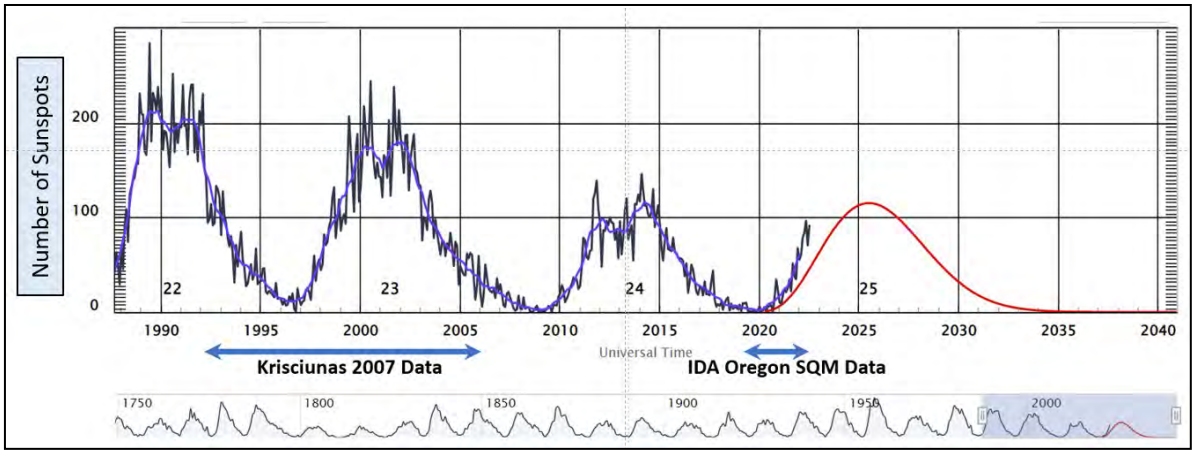

Figure H1. Solar cycle progression from NASA's Space Weather Prediction Center. The current time span of SQM data is shown by the horizontal arrow in the lower right. The time span of data used by Krisciunas, 2007 is shown by the arrow in the lower left. (Figure is from https://www.swpc.noaa.gov/products/solar-cycle-progression)

Krisciunas and others, 2007 showed that visible light measured at the zenith is correlated to the 10.7cm radio flux (Figure H2).

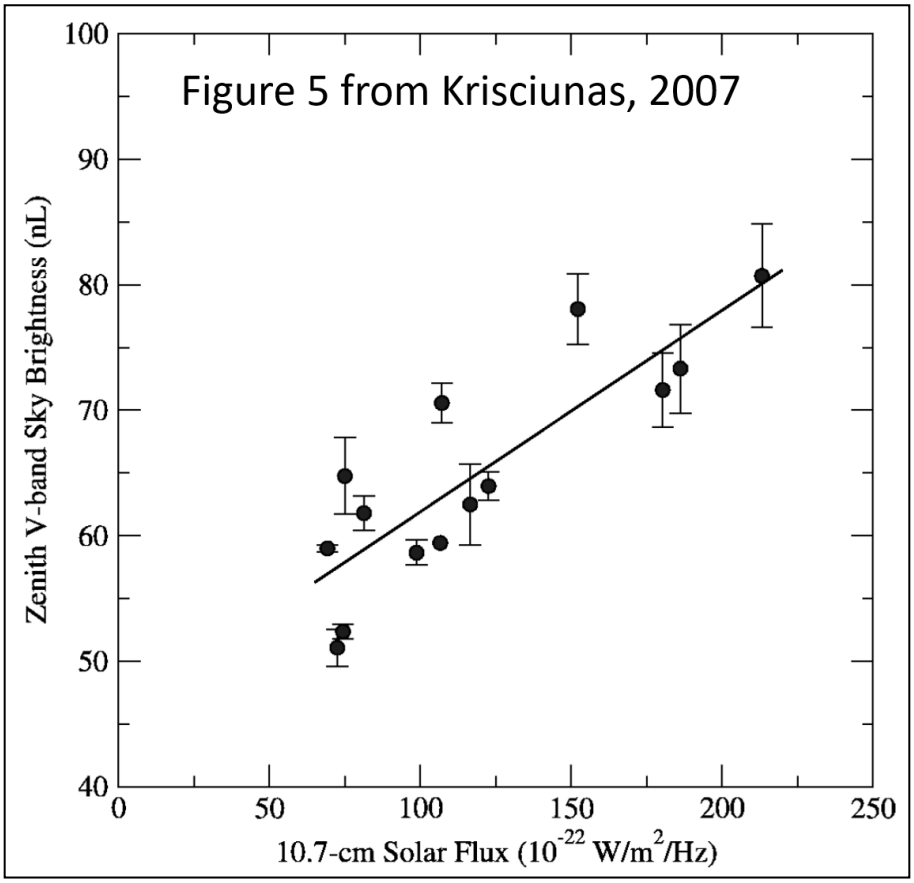

Figure H2. Relationship between V-band zenith sky brightness and 10.7-cm solar flux measured at Cerro Tololo Observatory in Chile, during 1992-2006 (Figure 5 from Krisciunas and others, 2007).

We use the relationship shown in Figure H2 and the hourly solar flux data from the Canadian Solar Radio Monitoring Program to estimate the contribution of natural airglow to the visible band zenith sky brightness, and subtract that estimate from our measured SQM data. We use the hourly solar flux measurement which is closest in time to our individual SQM measurements.

A histogram of the selected solar flux measurements (Figure H3) shows that our data fall into the left side of the range of data measured by Krisciunas and others, 2007.

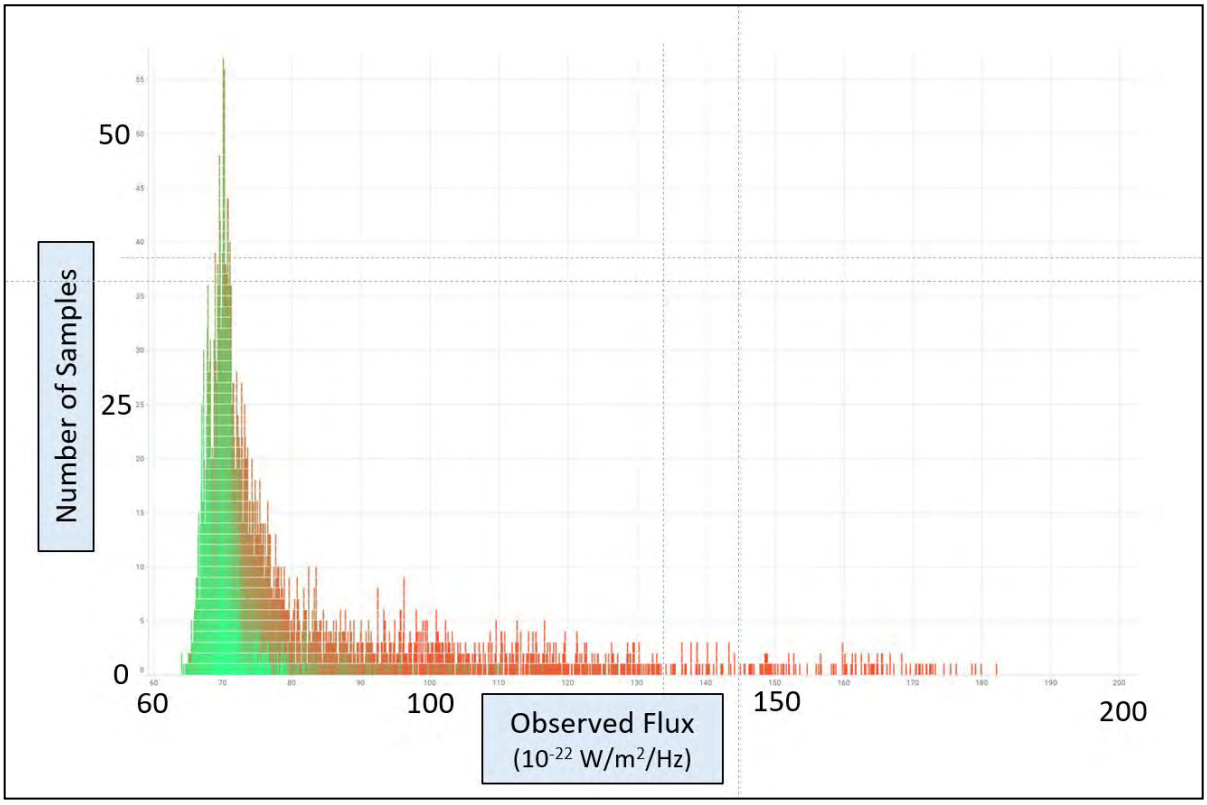

Figure H3. Histogram of solar flux measurements from the hourly Canadian data set for the time of the Oregon SQM project – January 2019 to July 2022. The points in the histogram are colored by the date of acquisition – green nearest to January 2019 and red nearest to July 2022.

A plot of 10.7 cm solar radio flux (Figure H4) shows the changes from the beginning of our SQM data in March 2019 to May 2022. The most dramatic increase occurred since September 2021.

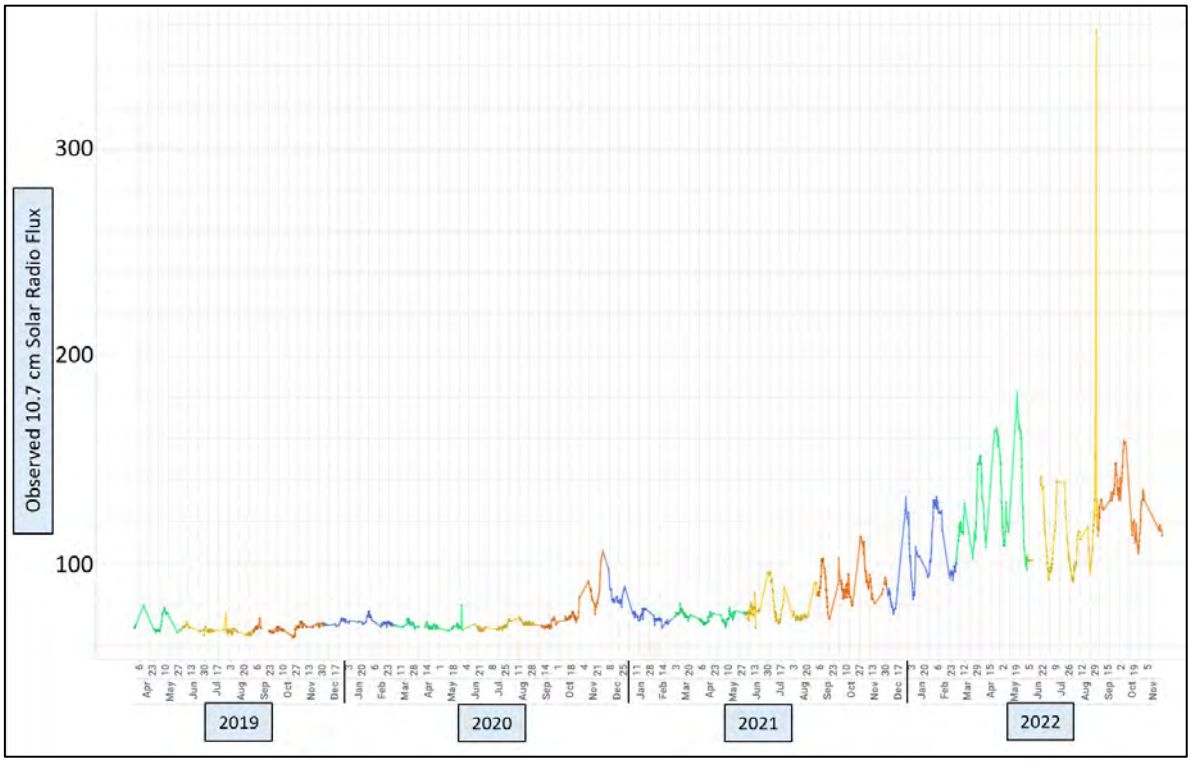

Figure H4. Observed 10.7 cm solar radio flux since the beginning of our SQM project. Out of curiosity, the data points are colored by the season of the year – spring is green, summer is yellow, autumn is red and winter is blue.

To perform the adjustment for airglow, we take the linear equation in Figure H2 as

ZenithV-Band-Brightness = 46. + 0.1575 x SolarFlux,

where SolarFlux is in the units shown in Figure H2, and the ZenithV-Band-Brightness is in units of nanoLamberts. Note that one nanoLambert units is equivalent to 3.18310 microcandelas per meter squared, which is the unit measure of our SQM data, having previously converted the SQM data from magnitudes per arc second squared.

Because we are interested in the change of V-band brightness due to the solar flux, we eliminate the Y-intercept (46.) from the correction – otherwise we would be subtracting the entire brightness of the Cerro Tololo night sky from our Oregon SQM measurements. Figure H5 shows an example of SQM data and the corresponding estimated adjustment for airglow. To adjust for airglow, we subtract the estimated values point by point from the SQM data which has previously been adjusted to Level 4.

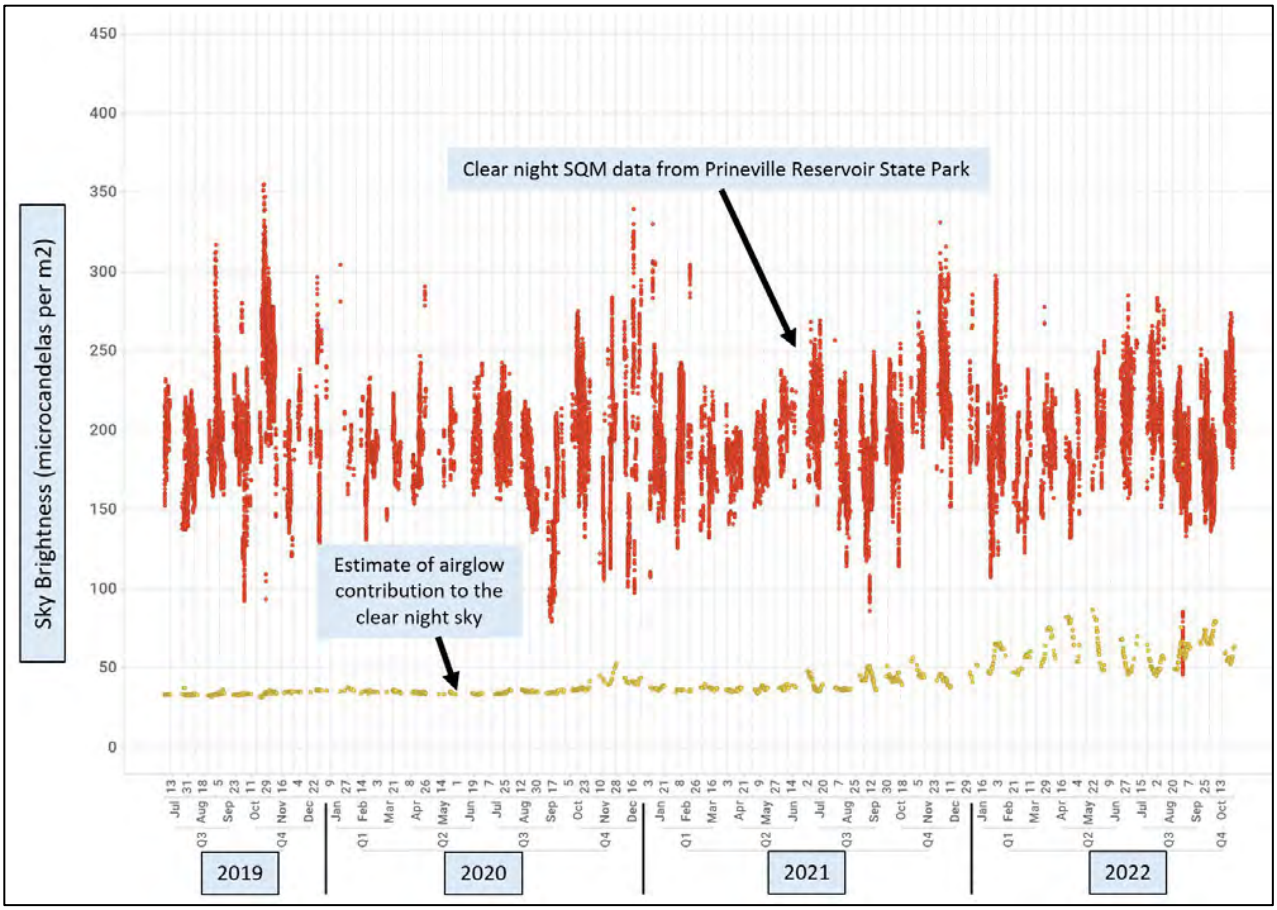

Figure H5. SQM data from Prineville Reservoir State Park shown in red, after adjustment to Level 5 (adjusted for weatherproof cover, age, galactic latitude, galactic longitude, time of night and airglow). Estimated airglow in yellow for each SQM data point, based on the Krisciunas and others, 2007 airglow data. Note the increase in estimated airglow since September 2021.

Appendix I – Long-term trends of our SQM data

Previously in this report series, we fitted linear regression equations to all of the clear sky data points. As we have progressed in data capture, it has become clear that some months express many more data points than others (Figure I1). And given the seasonal nature of our data, those months can exert an undue bias on the long-term trends.

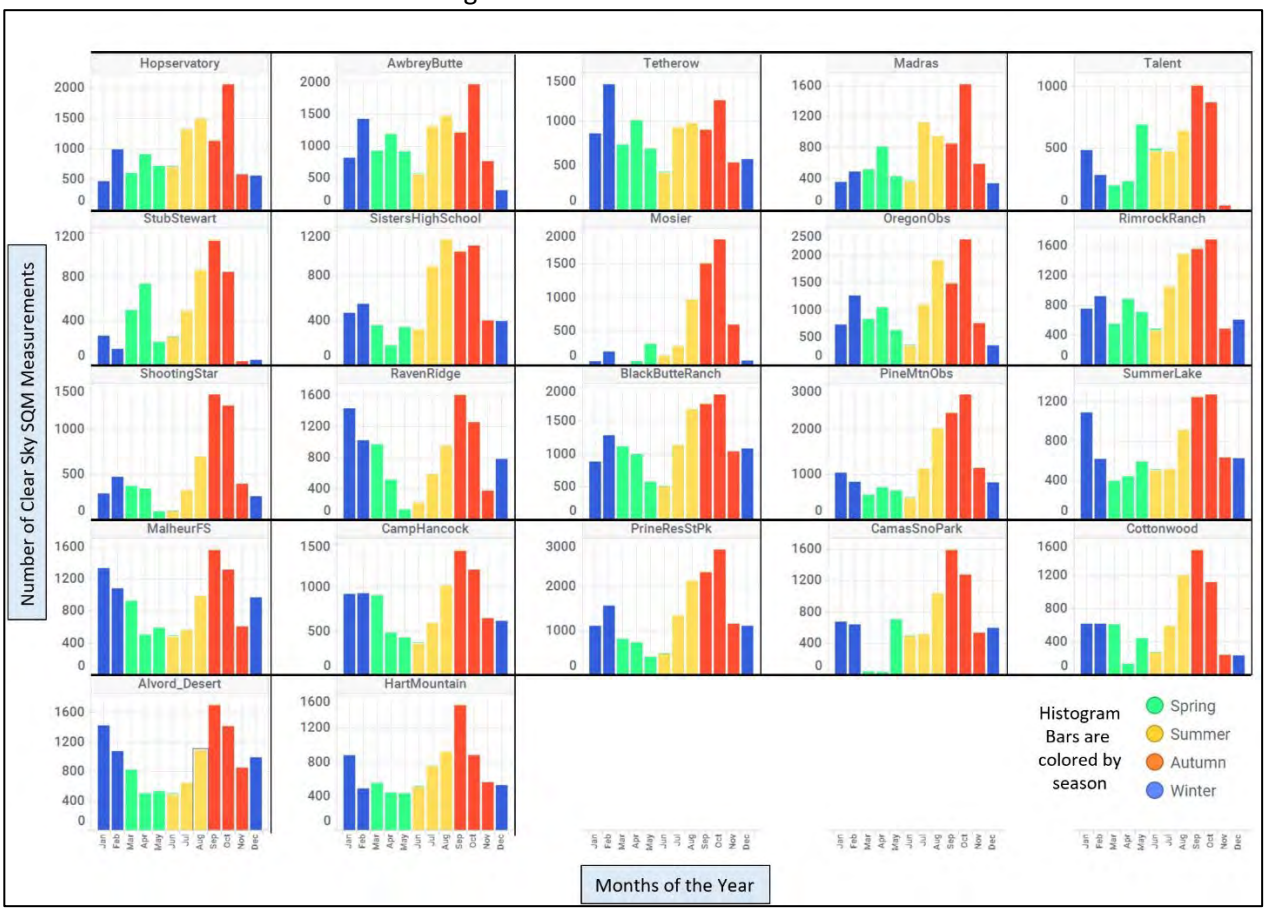

Figure I1. Histograms of clear sky data by month from each of the long term SQM sites. Note that October at many sites has 6x more measurements than does June. The long-term trends will be biased by this dichotomy. The histogram bars are colored by the season of the year.

To minimize this bias, we now use the mean of each month to better characterize the trend, instead of using all the individual data points. Table 3 of the main report summarizes our best estimates of the long-term trends of skyglow change after adjustment.

The following figures show an enlarged view of the long-term data at each of the 22 sites. These are the same plots that are shown in small scale in Figure 9 in the main body of this report

Hopservatory

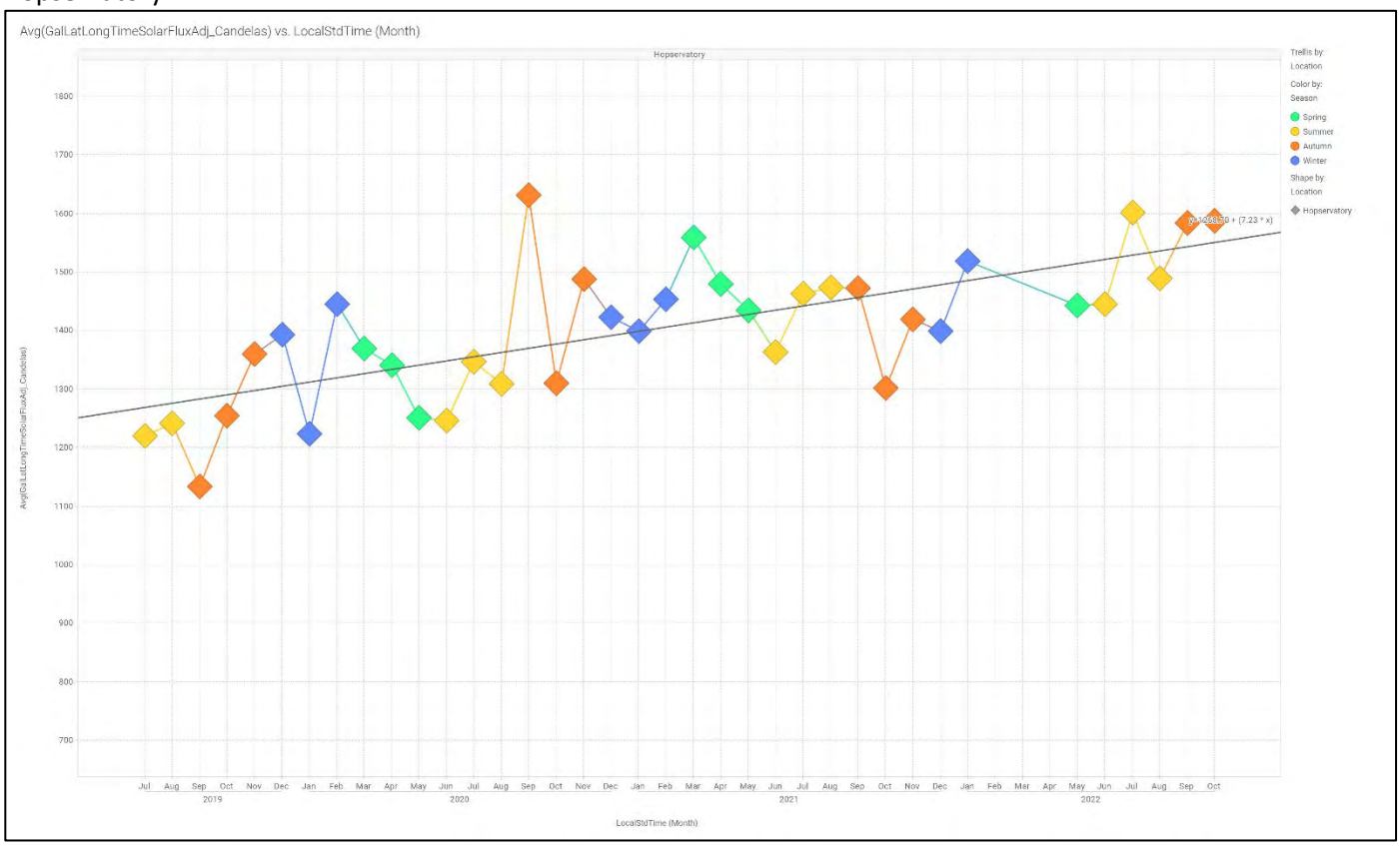

Awbrey Butte

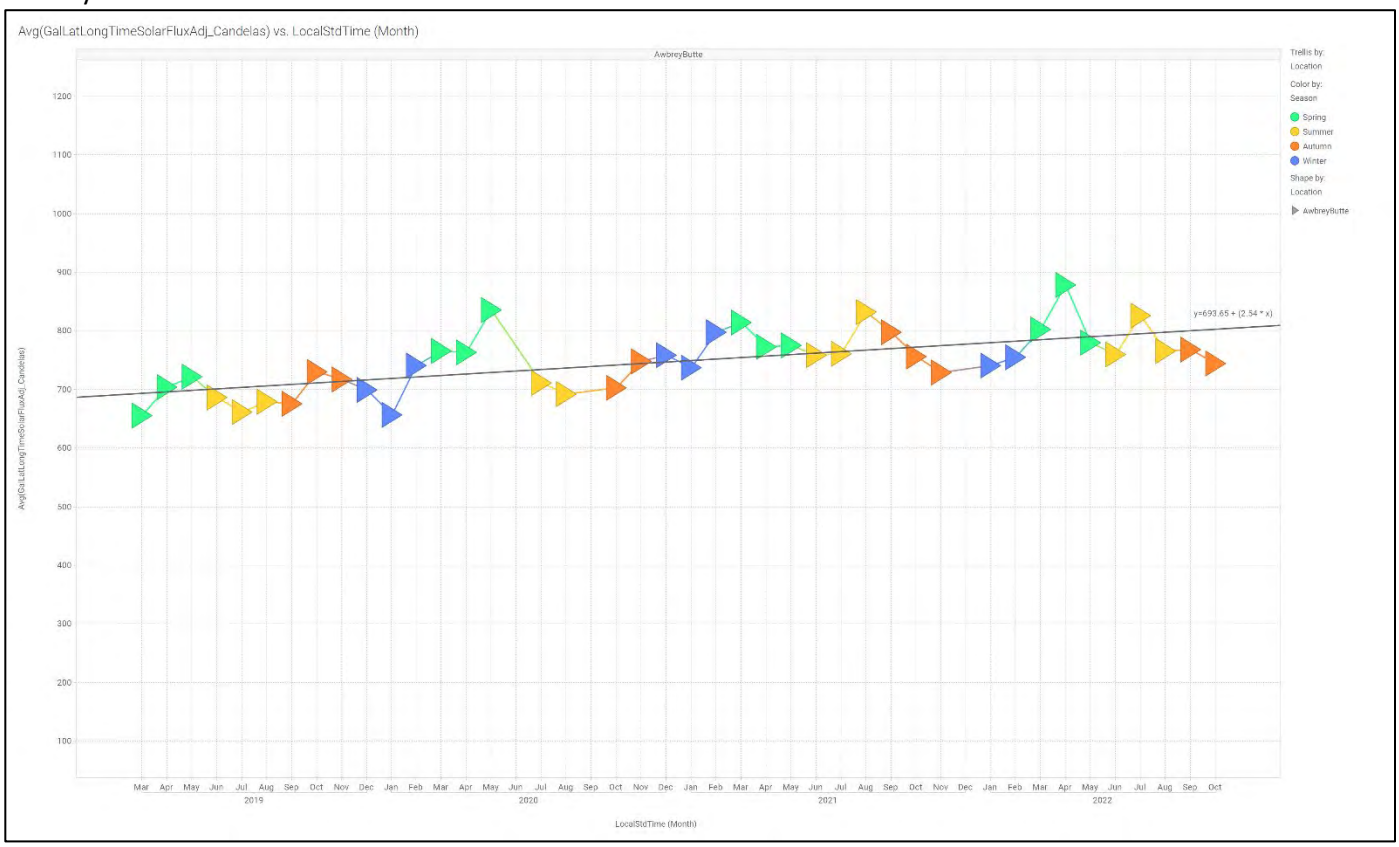

Tetherow

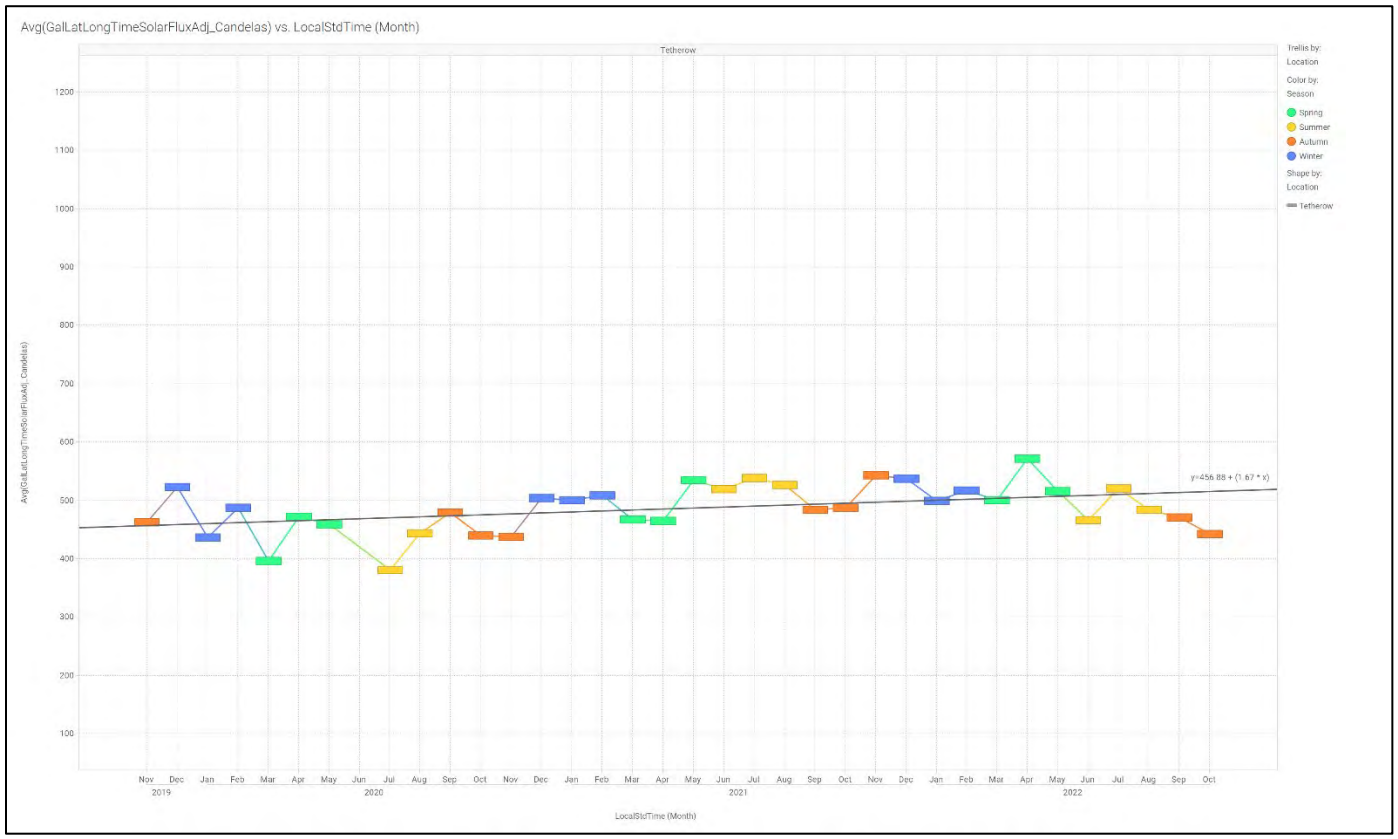

Madras

Talent

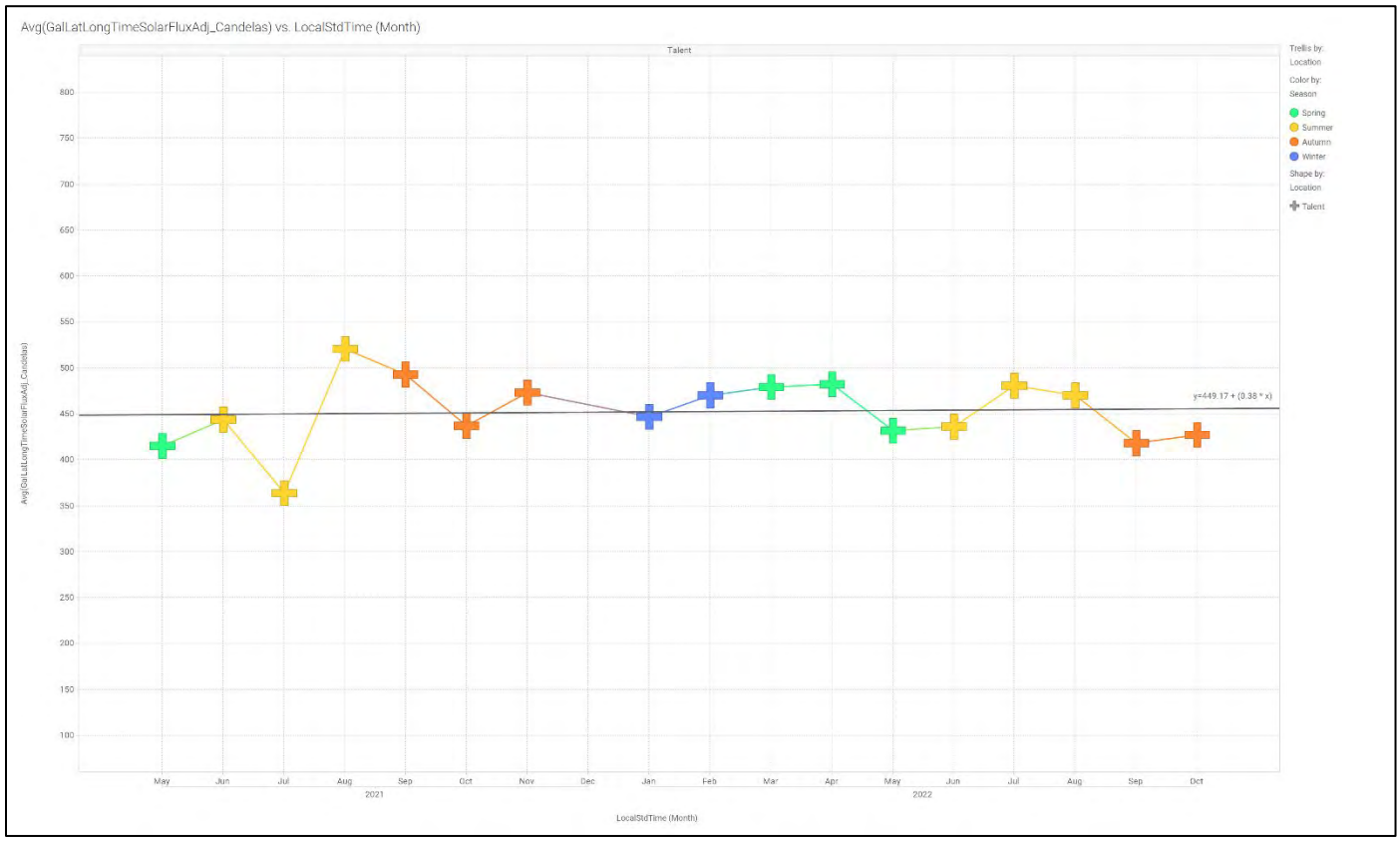

StubStewart

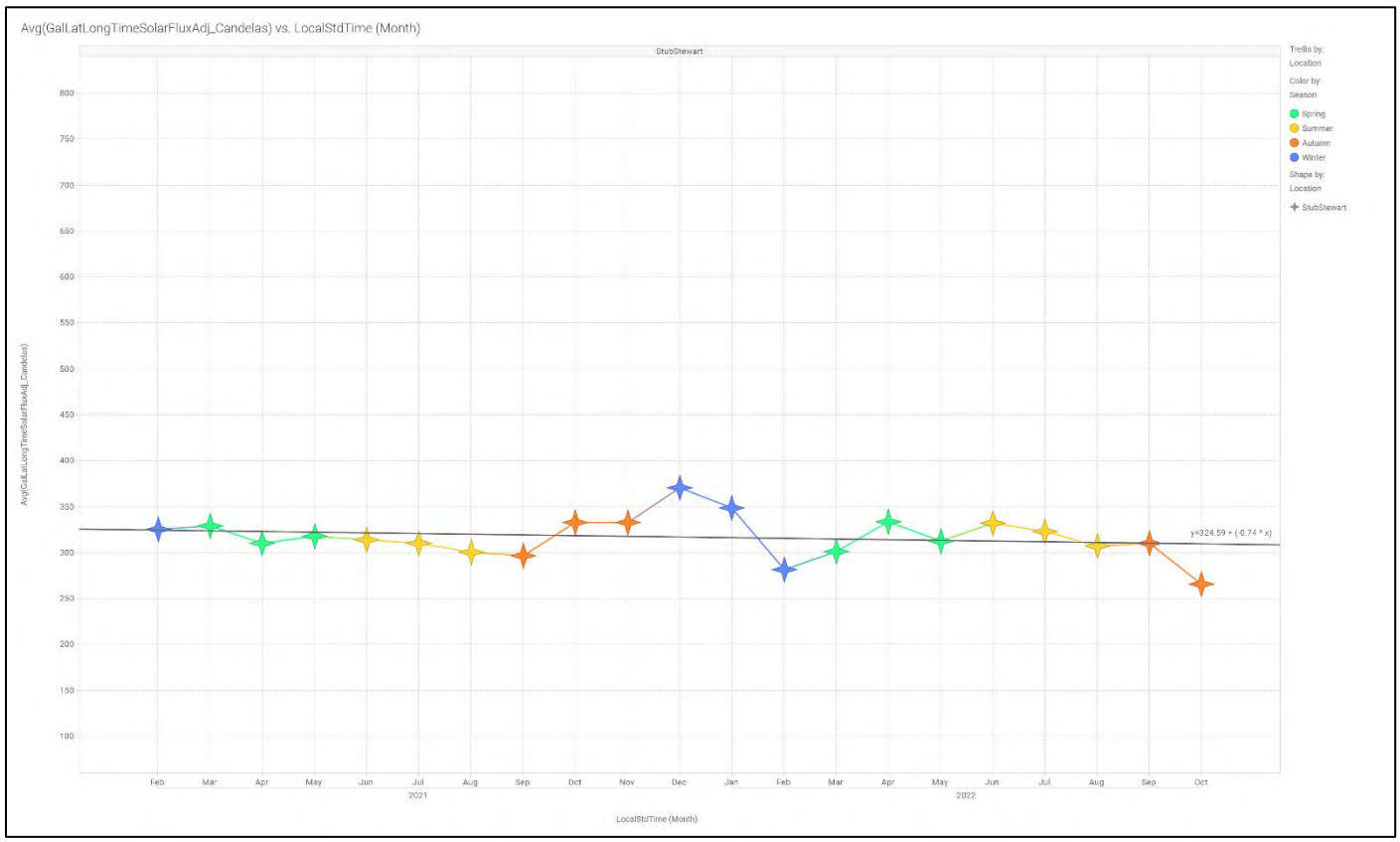

Sisters High School

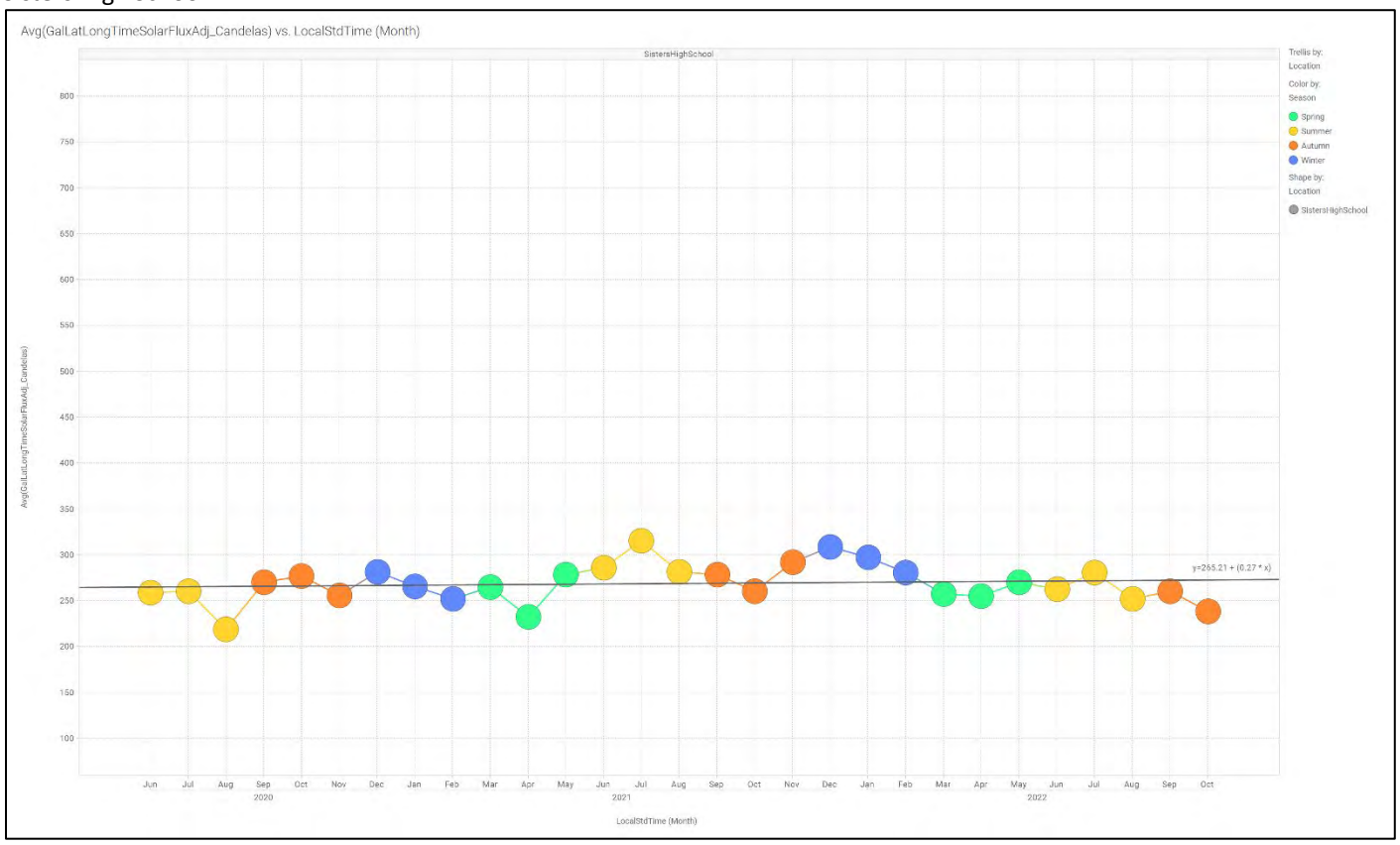

Mosier

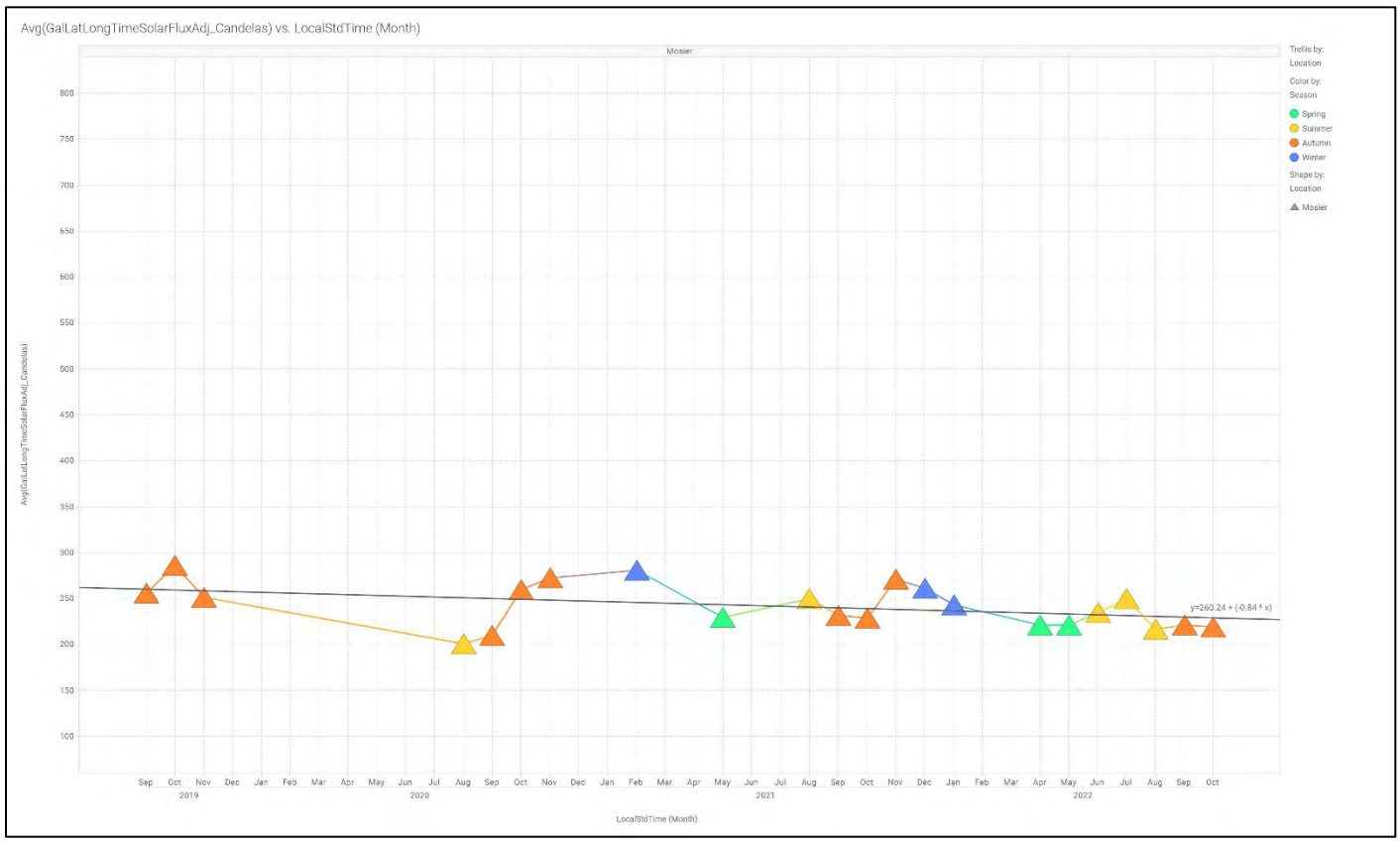

OregonObs

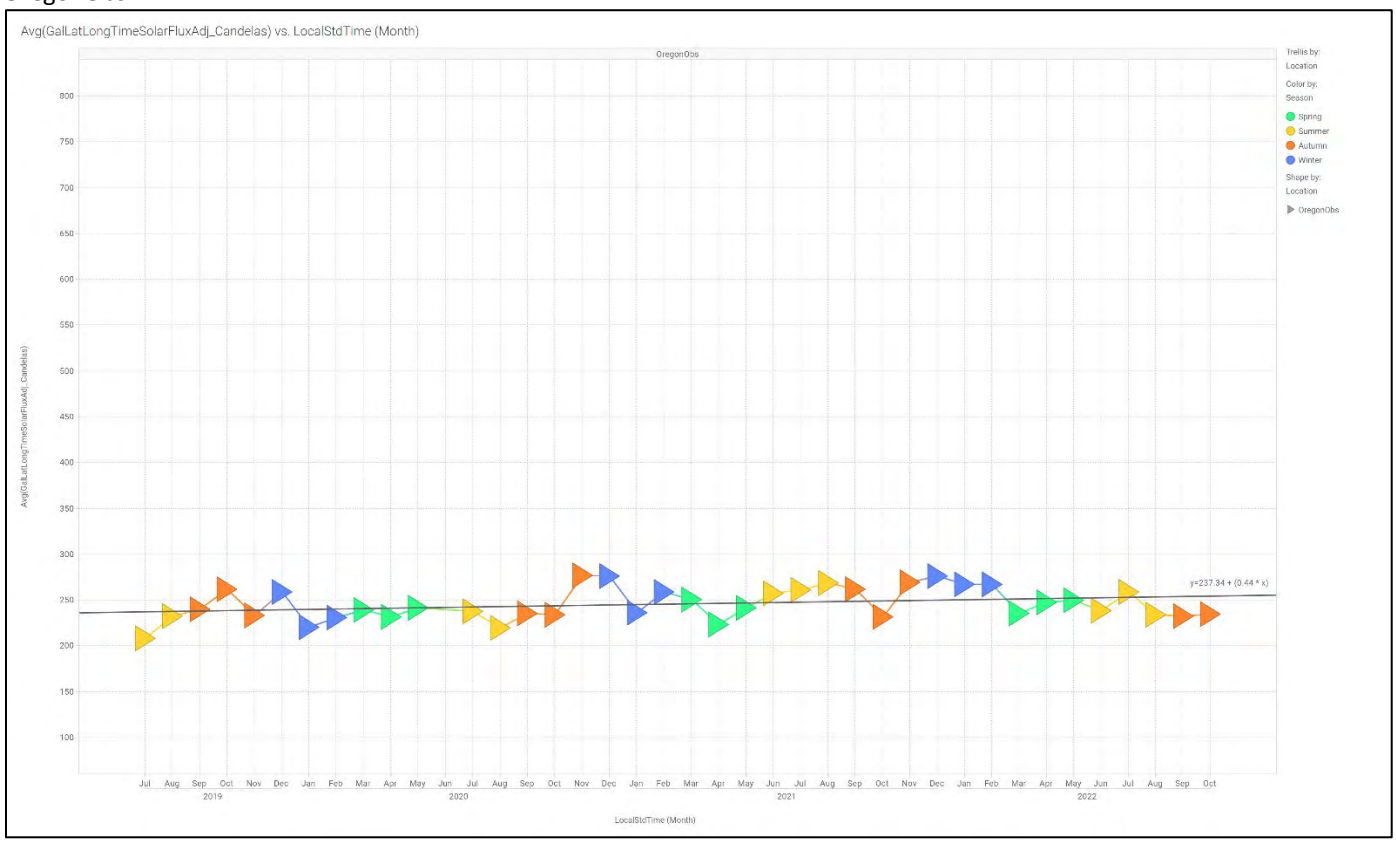

RimrockRanch

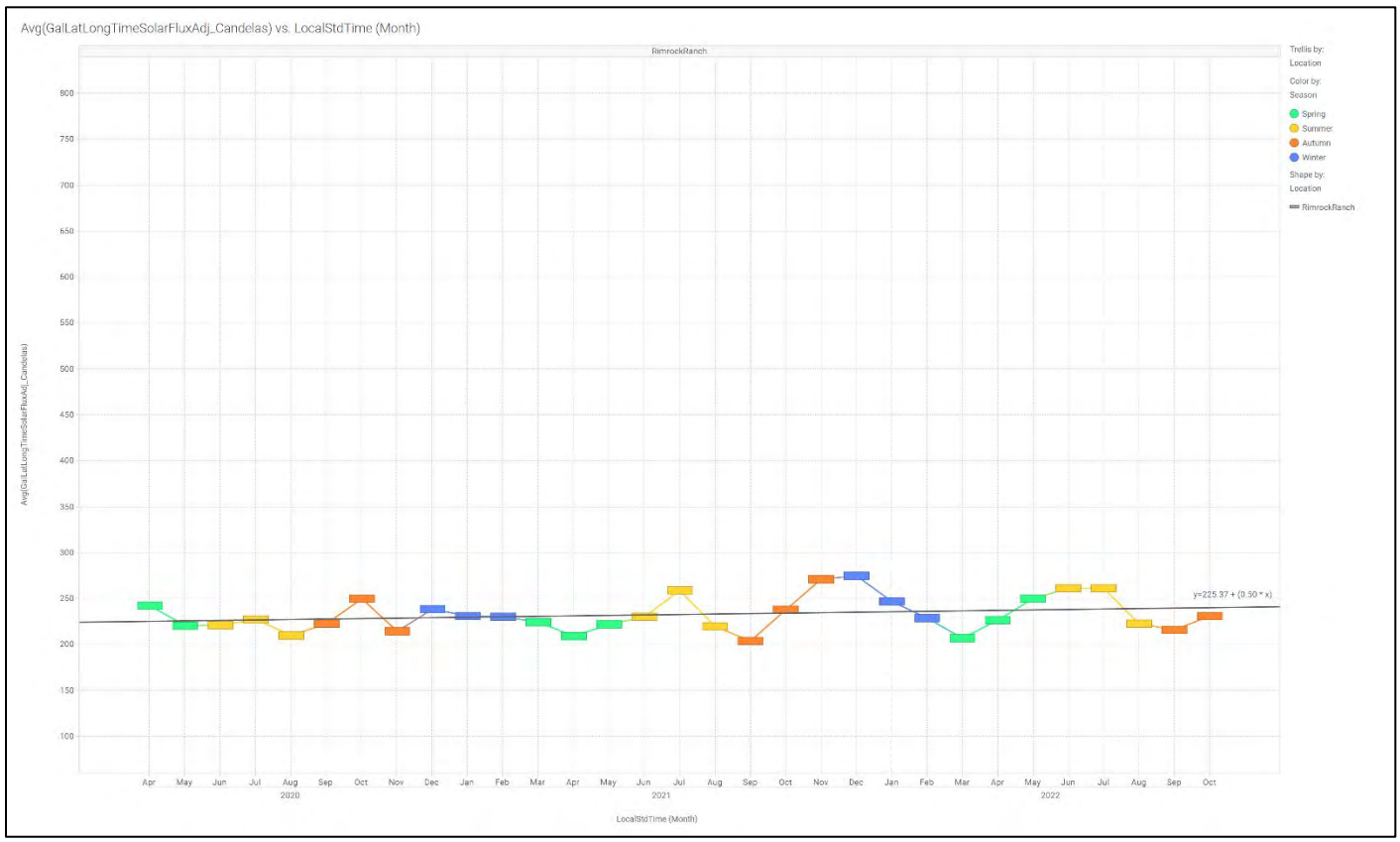

ShootingStar

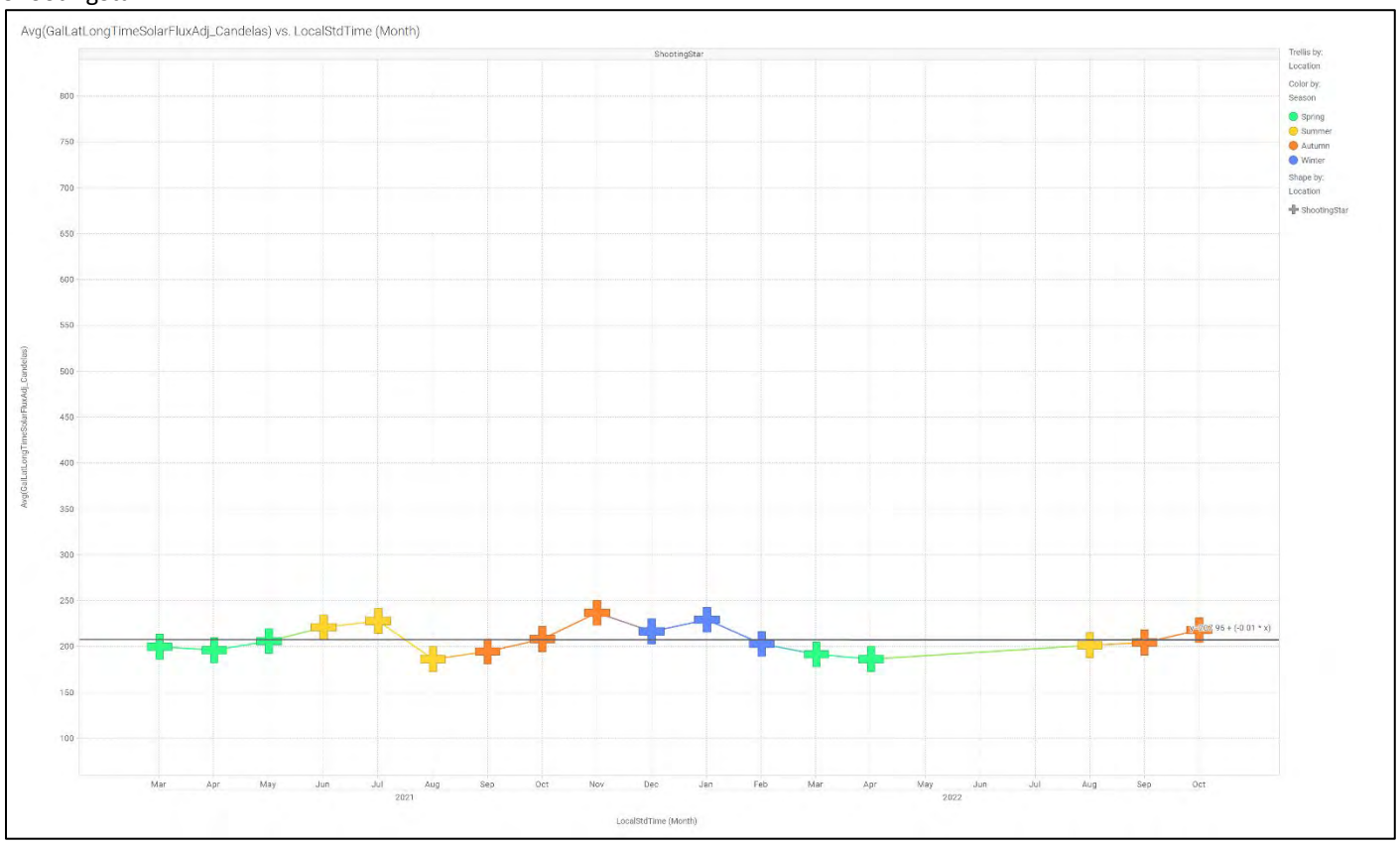

RavenRidge

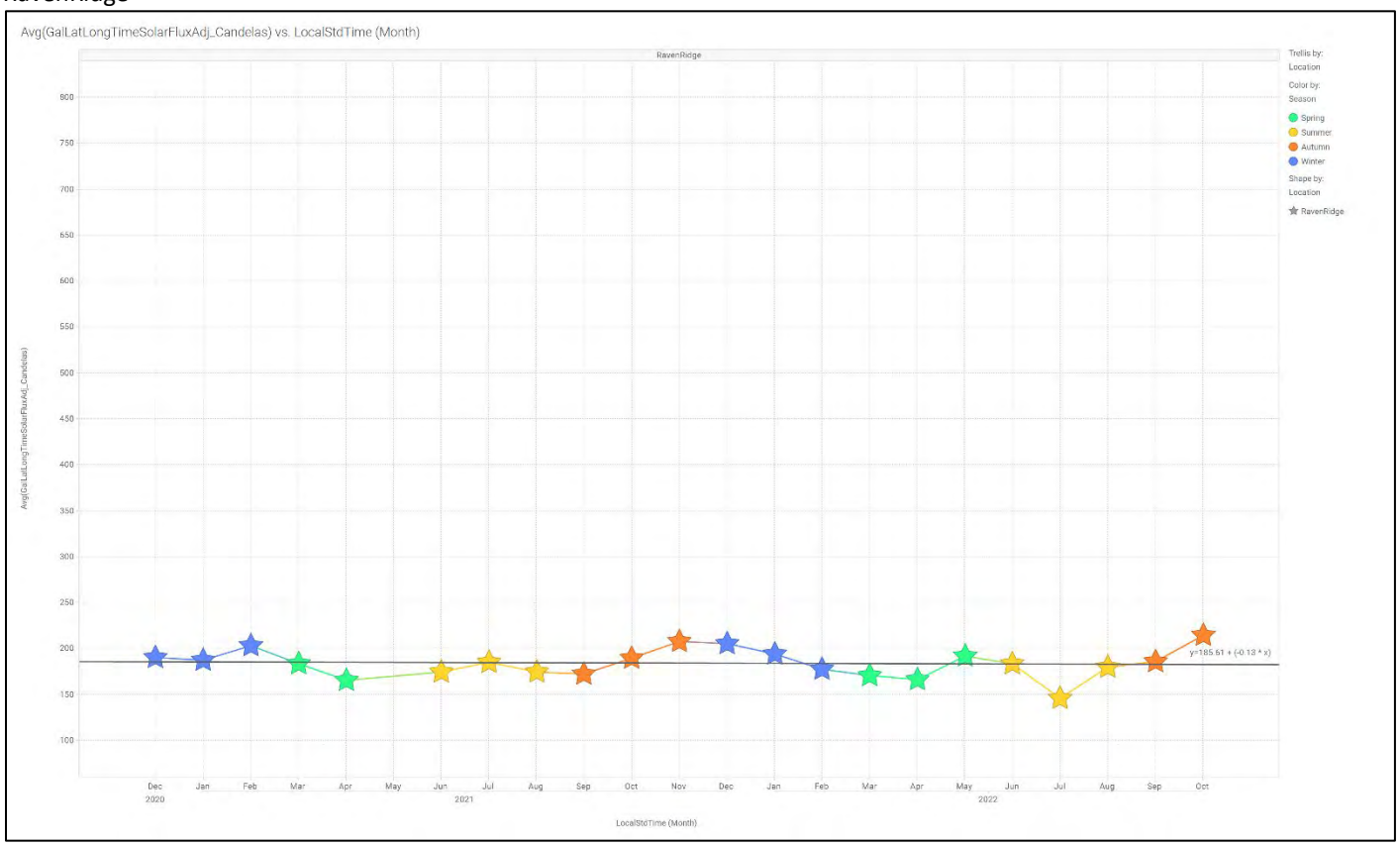

BlackButteRanch

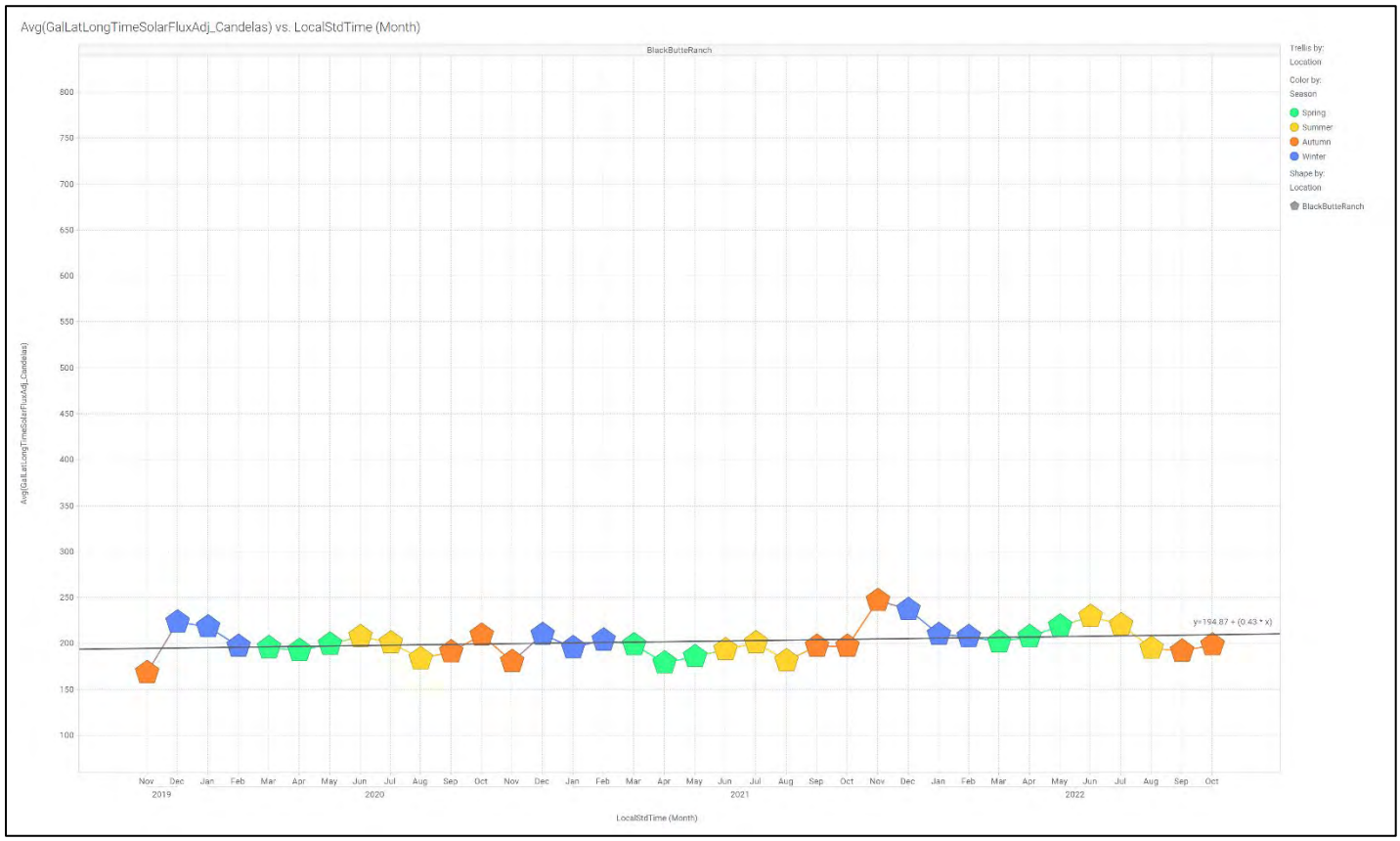

PineMtnObs

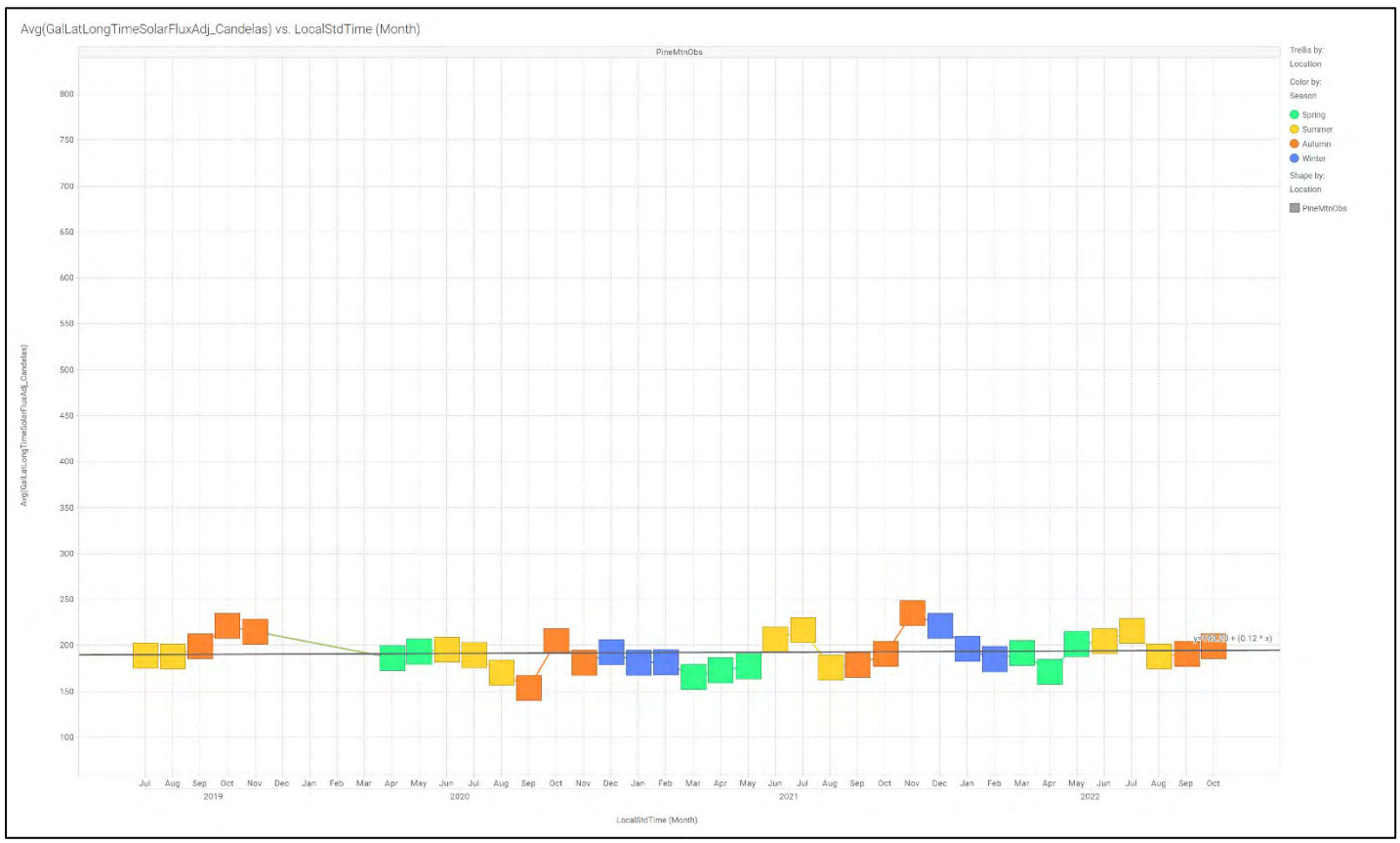

SummerLake

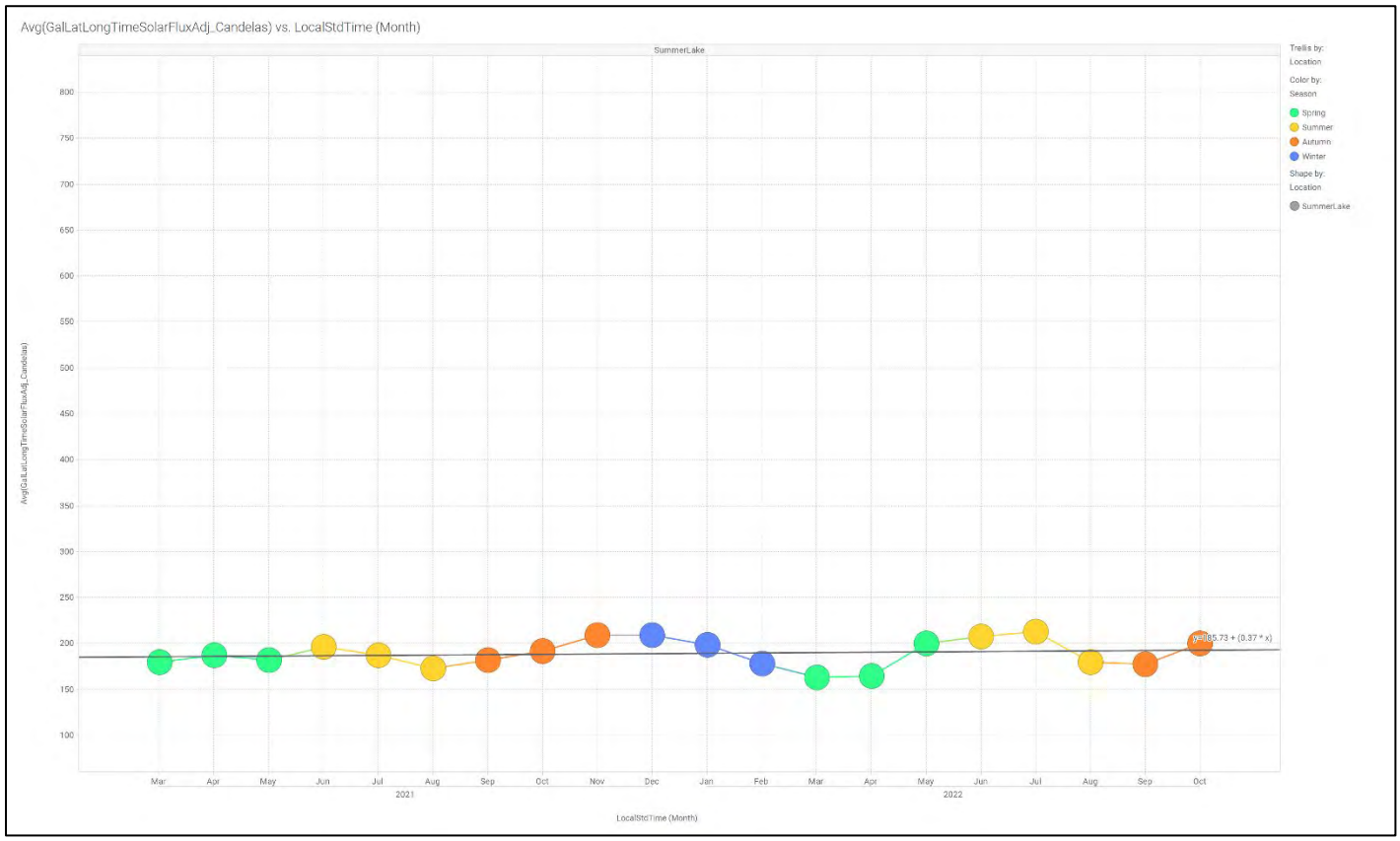

MalheurFS

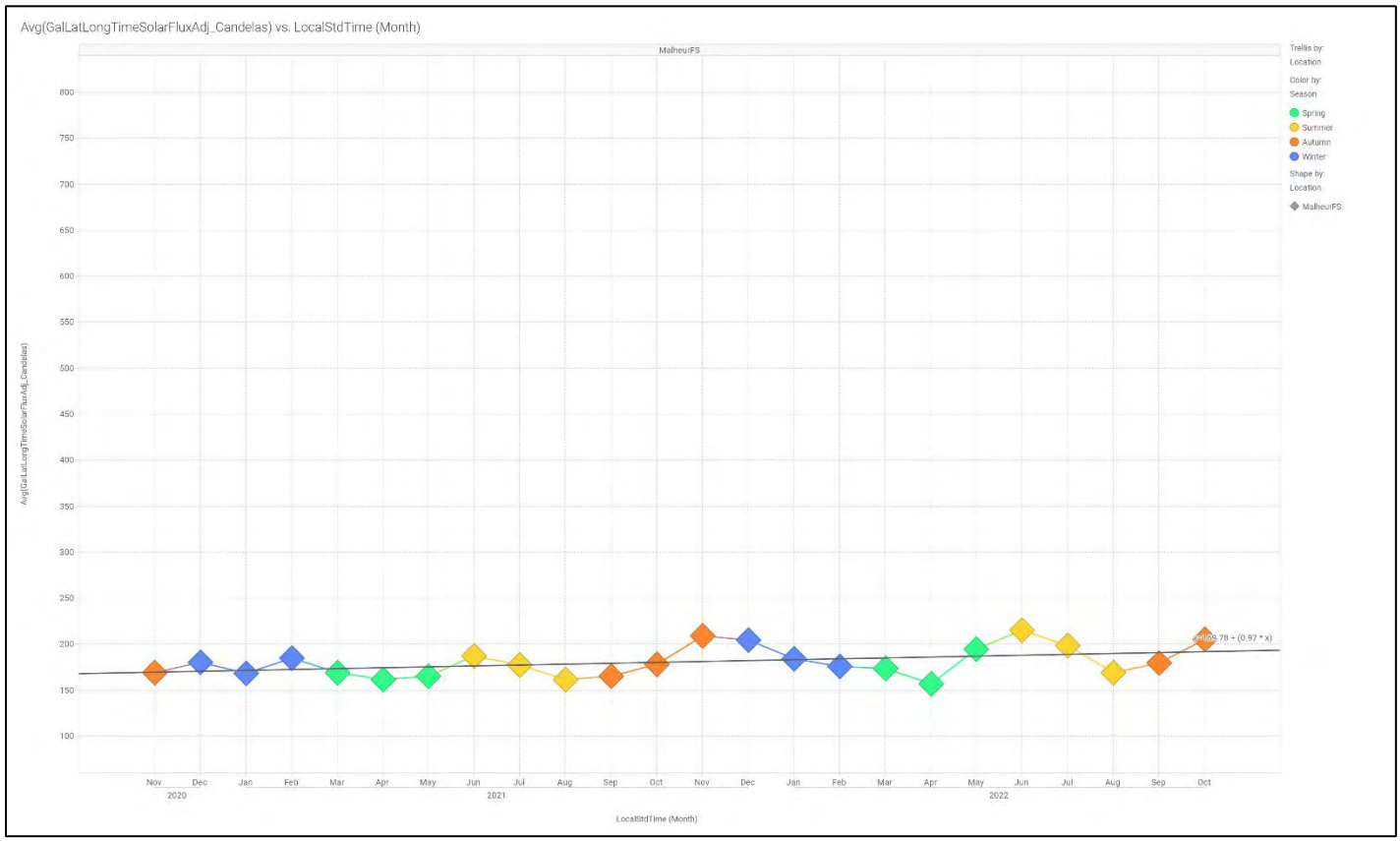

CampHancock

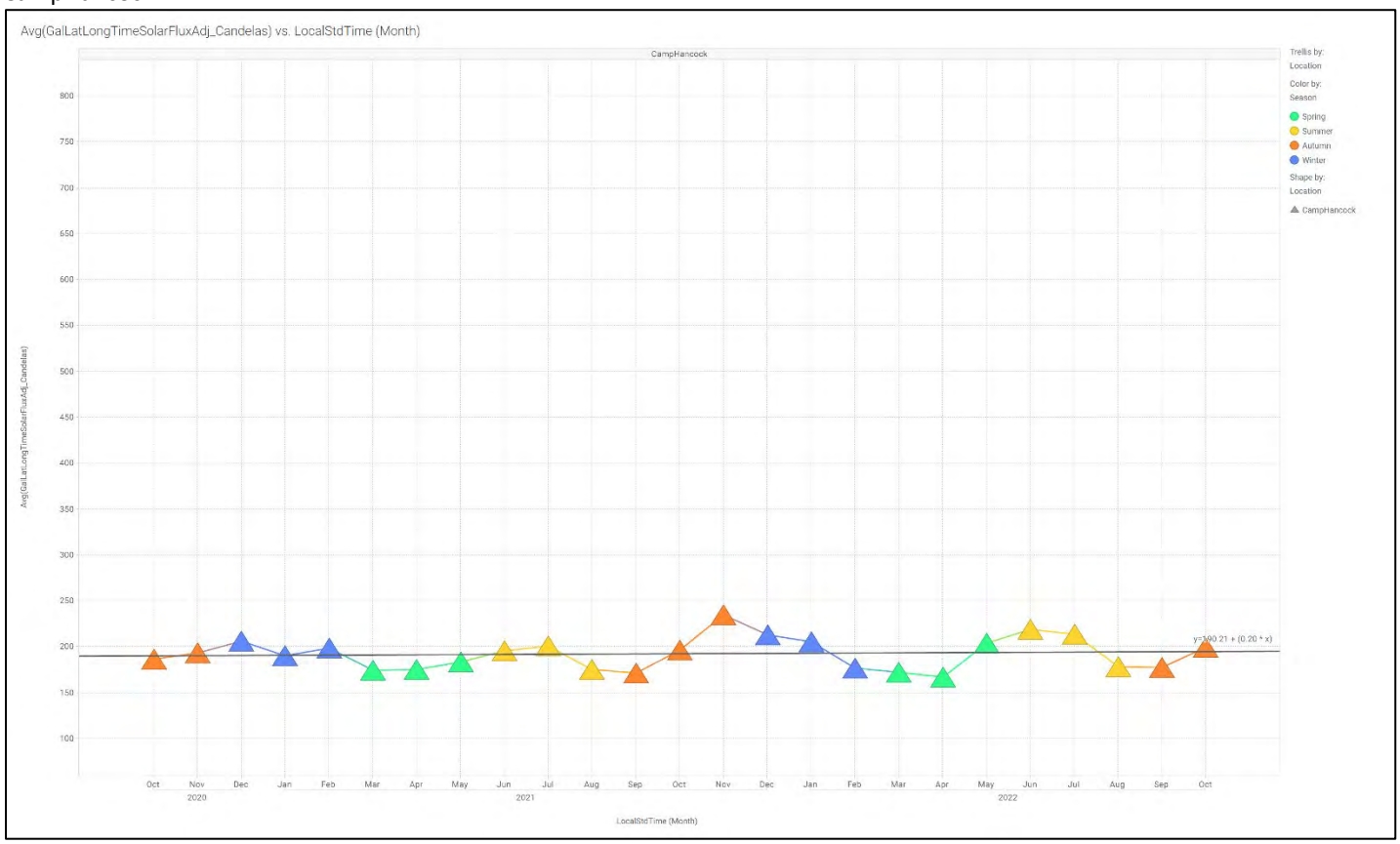

PrineResStPk

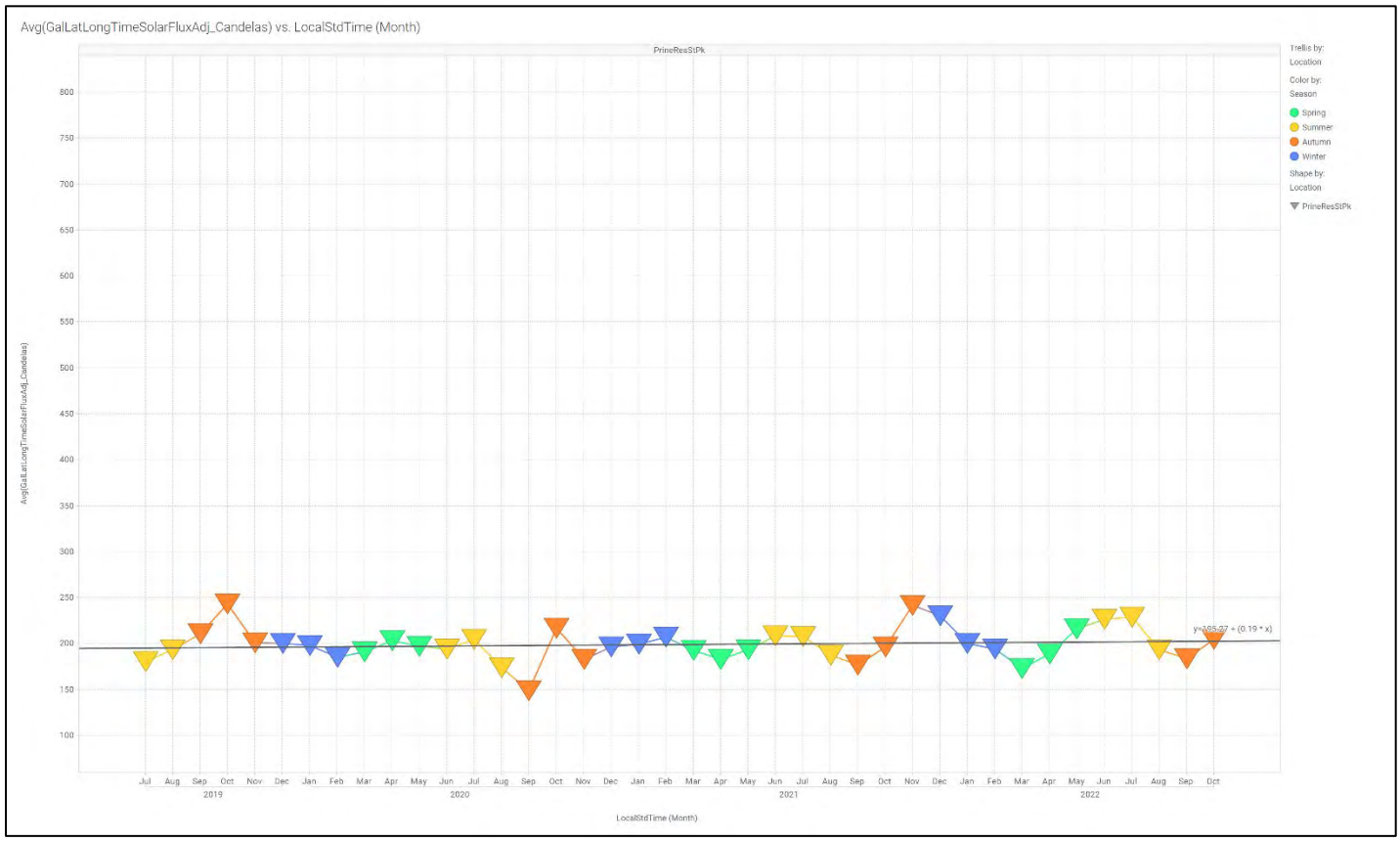

CamasSnoPark

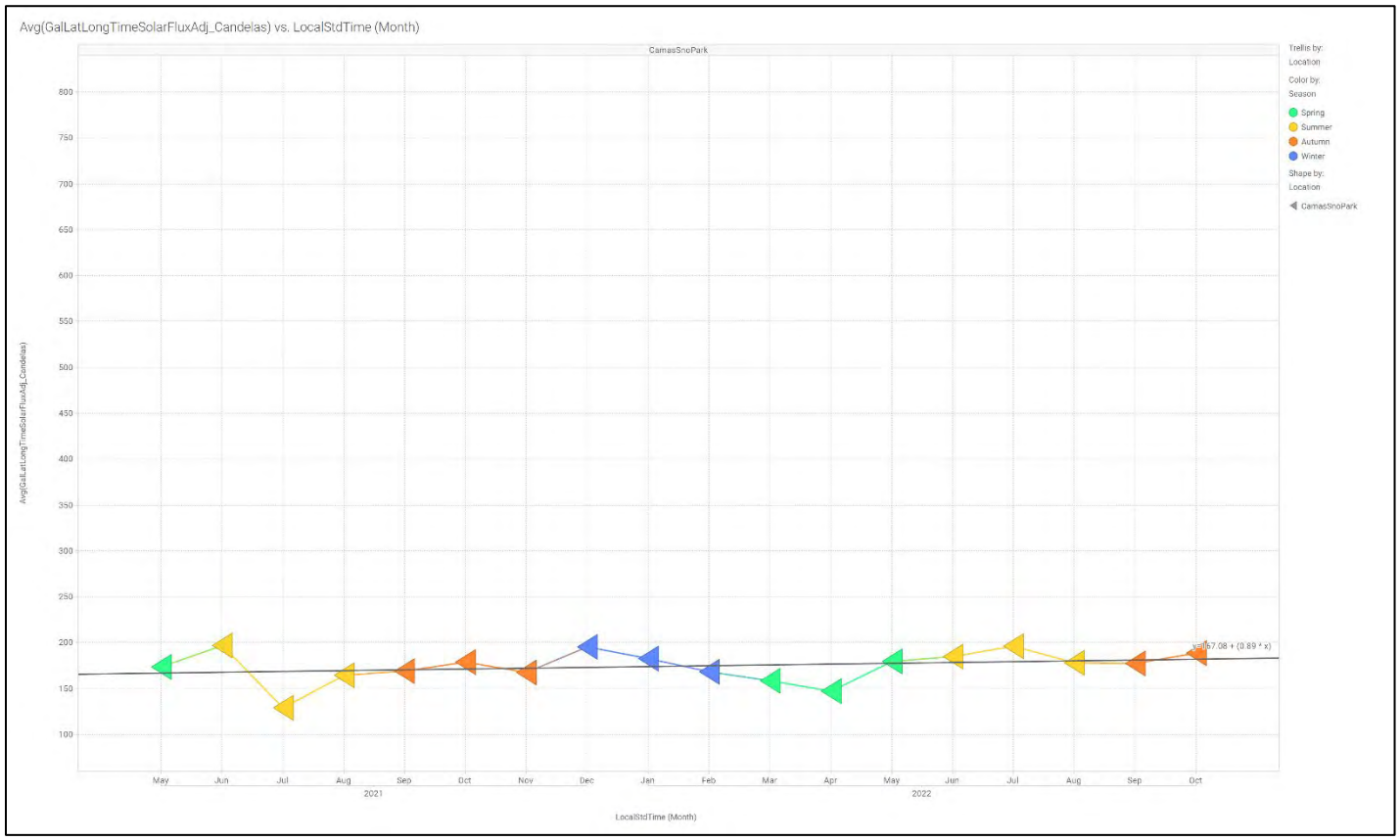

Cottonwood

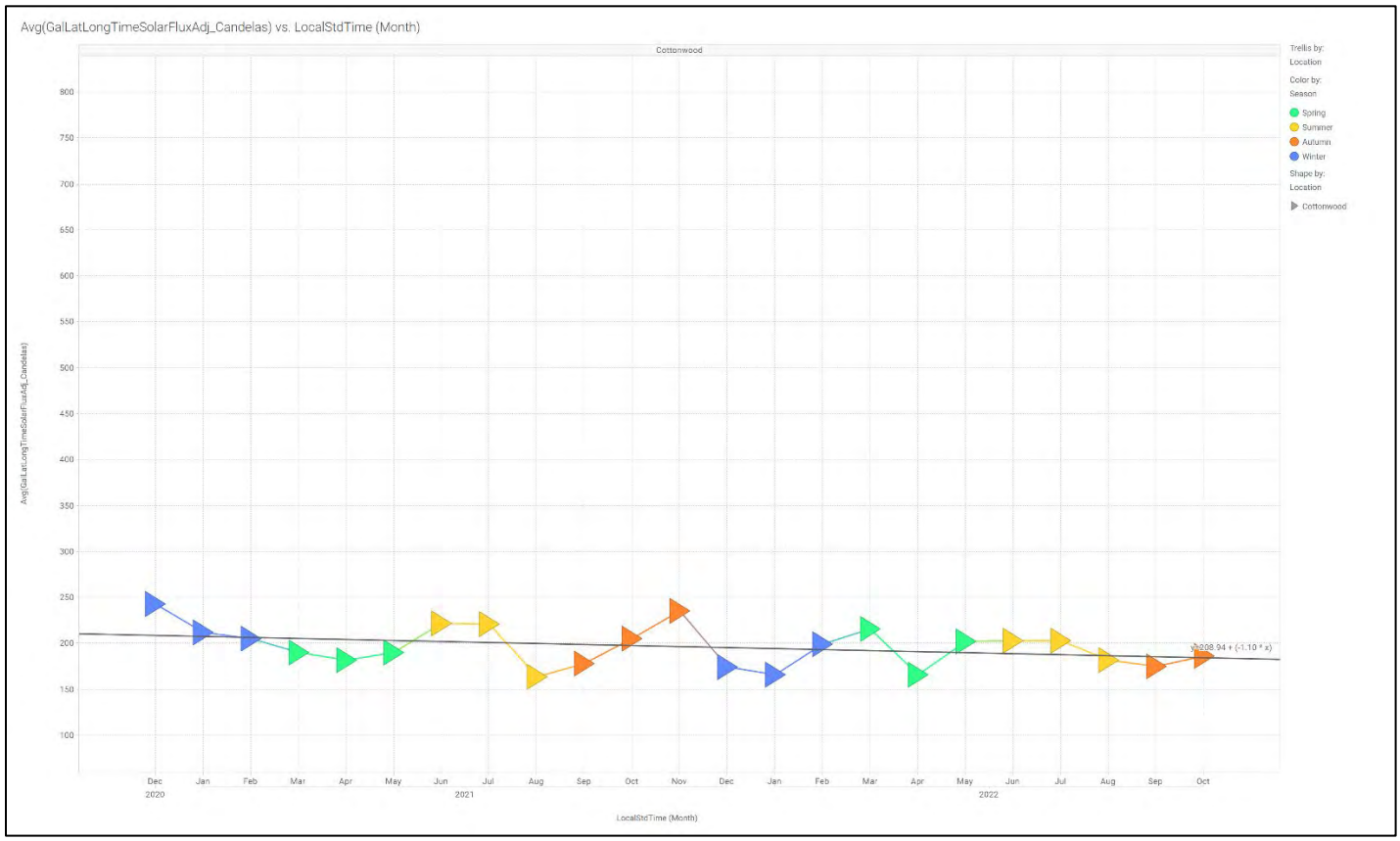

AlvordDesert

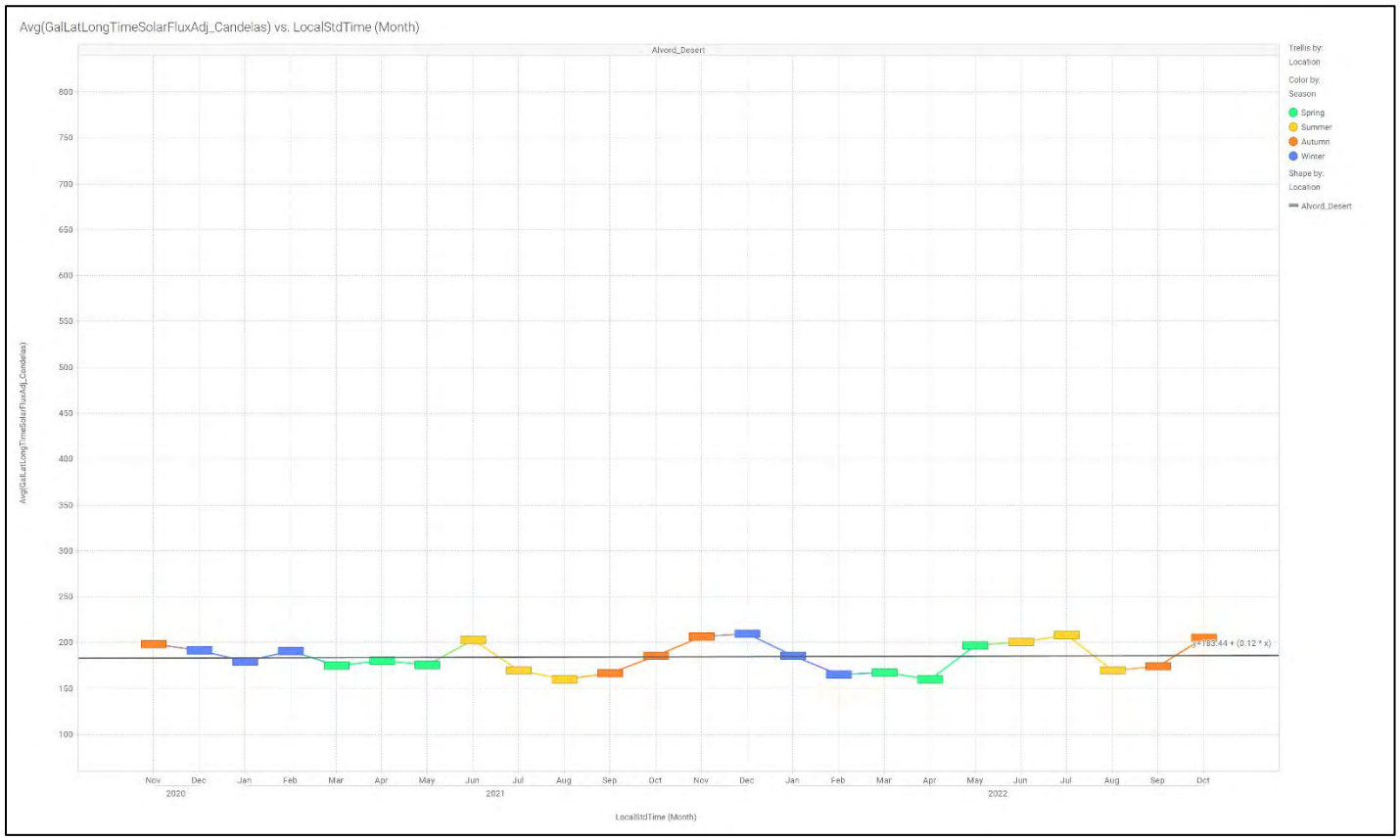

HartMountain